https://ntrs.nasa.gov/search.jsp?R=19680006318 2020-03-12T12:00:59+00:00Z

SPACECRAFT DEPARTMENT

MISSILE AND SPACE DIVISION

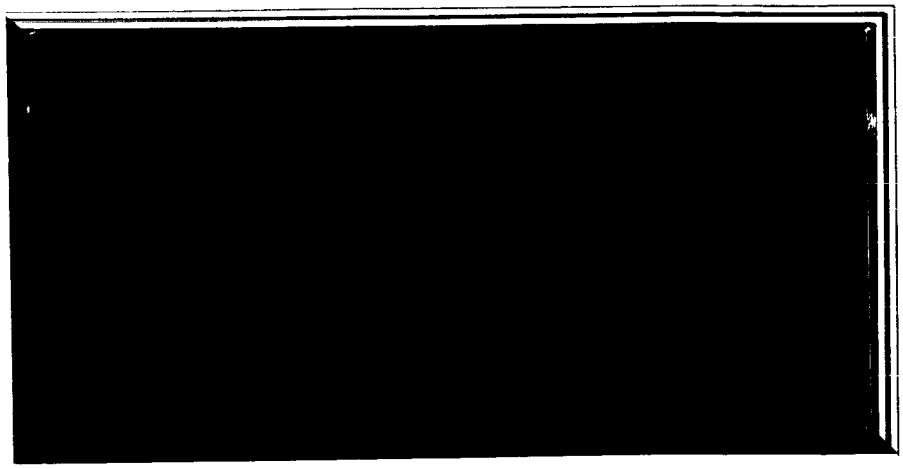

GPO PRICE $ _____

CFSTI PRICE(S) $ _____

Hard copy (HC) 3.00

Microfiche (MF) .65

ff 653 July 65

N68-15787
(ACCESSION NUMBER) (THRU)

114 1
(PAGES) (CODE)

CR-92530 03
(NASA CR OR TMX OR AD NUMBER) (CATEGORY)

FACILITY FORM 602

GENERAL ELECTRIC

REPORT NO. 68SD4208
24 JANUARY 1968

FEASIBILITY STUDY-30 WATT PER POUND ROLL-UP SOLAR ARRAY QUARTERLY TECHNICAL REPORT NO. 2 30 SEPTEMBER 1967 TO 31 DECEMBER 1967

PREPARED FOR

JET PROPULSION LABORATORY
CALIFORNIA INSTITUTE OF TECHNOLOGY
4800 OAK GROVE DRIVE
PASADENA, CALIFORNIA

PREPARED UNDER
CONTRACT NO. 951970
CONTRACTING OFFICER C.E. PRICE
PROJECT MANAGER W.A. HASBACH

PREPARED BY:

N.F. SHEPARD
F.A. BLAKE
W.S. BUSCH
A. LATOUR
P.J. DEMARTINO
D.N. MATTEO
W.C. YOUNG

APPROVED BY:

K.L. HANSON,
PROGRAM MANAGER

This work was performed for the Jet Propulsion Laboratory, California Institute of Technology, as sponsored by the National Aeronautics and Space Administration under Contract NAS 7-100.

GENERAL ELECTRIC
SPACECRAFT DEPARTMENT
A Department of the Missile and Space Division
Valley Forge Space Technology Center
P.O. Box 8555 • Philadelphia, Penna. 19101

"This report contains information prepared by the General Electric Co., Spacecraft Department under JPL Subcontract. Its content is not necessarily endorsed by the Jet Propulsion Laboratory, California Institute of Technology, or the National Aeronautics and Space Administration."

TABLE OF CONTENTS

LIST OF ILLUSTRATIONS

LIST OF TABLES

1.0 INTRODUCTION AND SUMMARY

This report covers the second quarter of the Feasibility Study - 30 Watt Per Pound Roll-up Solar Array Program being performed by the Spacecraft Department of the General Electric Company under Contract No. 951970 for Jet Propulsion Laboratory of the California Institute of Technology. It is organized to complement the midterm briefing to be presented to JPL. The objective of the program is to perform a preliminary design and design analysis of a 250-square-foot deployable (roll-up) solar panel which shall have a specific power capability of 30 watts per pound or greater and which shall be capable of meeting the environmental requirements of JPL Specification No. SS 501407.

The power capability of the array is to be based on cells having an efficiency such that an electrical output of 10 watts/square foot will be achieved at air mass zero, 55°C, and 1.00 AU. Cells to be considered in the design are 0.008-inch-thick, N/P, 10 ohm-cm protected by a 0.003-inch-thick filtered microsheet shield.

The initial section of the program consisted of studies of candidate arrangements and deployment concepts to sufficient depth that a basis for the selection of the system configuration was established. These system tasks were supported by two additional detailed studies, one involving deployment boom and deployment mechanism preliminary design, and the other involving conversion of empirical solar cell data into forms required by general array design computer program. These tasks were essentially completed during the first quarter and are reported in Quarterly Technical Report No. 1 (Reference 1-1, which also contains the dynamic analyses of the deployed panel).

The second major segment of the program involves the preliminary detailed design of the components making up the 30 watt per pound roll-up solar array panel. During this second quarter, the preliminary design of all major components has been started and, in some cases, virtually completed. Design tradeoff studies were completed which led to the selection of the baseline configuration. A component specification for the solar panel actuator (deployable boom) has been prepared and issued. Based on this specification, the SPAR Aerospace Products* BI-STEM has been selected as the solar panel actuator.

*Formerly SPAR Division of deHavilland Aircraft of Canada

In an effort to establish basic engineering information which was previously lacking, several tests have been run on the Hunter STACER and SPAR Aerospace Products BI-STEM deployable boom.

The specific power capability of the proposed roll-up solar array is 33.1 watts per pound, based on calculated component weights.

2.0 TECHNICAL DISCUSSION

This section consists of a general description of the selected system and a summary of the system tradeoff studies which were completed during the second quarter. These studies included: (1) the tradeoff of a single boom versus a double boom system, (2) the selection of the drum bearing arrangement, (3) the selection of the optimum power take-off arrangement, and (4) the deployable boom analysis.

A detailed description of each major system component is included. Experimental data are published on several tests which were conducted on the Hunter STACER and SPAR Aerospace BI-STEM deplayable booms. The thermal analysis which supports the selected design is presented along with a detailed weight breakdown of the proposed system. A description of the Engineering Demonstration Model is included.

2.1 GENERAL DESCRIPTION OF DESIGN CONCEPT

THE CONFIGURATION OF THE SOLAR ARRAY PANEL, ESTABLISHED ON THE BASIS OF TRADE STUDIES TO MINIMIZE WEIGHT, FEATURES:

A. TWO SUBPANELS AND THEIR ASSOCIATED STORAGE DRUMS

B. A SINGLE SOLAR PANEL DEPLOYMENT ACTUATOR

C. SOLAR PANEL NATURAL FREQUENCY REQUIREMENT (I.E., STRUCTURAL STIFFNESS) IS PROVIDED BY TENSION IN THE ARRAY SUBSTRATE.

D. A SINGLE POINT ATTACHMENT TO THE VEHICLE IN THE DEPLOYED STATE

E. MULTIPOINT ATTACHMENT TO THE VEHICLE IN THE STOWED STATE

F. BERYLLIUM STRUCTURAL ELEMENTS

G. SLIP RINGS TO TRANSFER THE ELECTRICAL POWER ACROSS THE INTERFACE BETWEEN FIXED AND MOVING PARTS

H. THE USE OF AN "OFF-THE-SHELF" ACTUATOR (DEPLOYABLE BOOM)

I. AN ARRAY MAXIMUM POWER VOLTAGE OF 91 VOLTS AT 1.000 AU AND 55 $^{\circ}$C

The array panel consists of the following major components:

a. Array blanket (2)

b. Storage drum (2)

c. Leading edge member

d. Outboard end support (2)

e. Center support

f. Solar panel actuator

The array blanket is attached to and rolled up on the storage drum in the stowed state. Interlayer cushioning is provided by foamed RTV580 buttons which are deposited on the rear of the array blanket. The leading edge member is attached to the solar panel actuator (deployable boom) at the center, and the leading edge of each array blanket is attached to

this tubular member on either side of the central boom attachment point. The attachment of the boom tip to the leading edge member is through the ball bearing joint which allows the boom to have torsional freedom as it is deployed.

Both storage drums are mounted to a center support structure through a shaft which is mounted to the center support. This center support structure is the only attachment of the array to the vehicle in the deployed condition. Each storage drum is mounted to the shaft with a preloaded pair of ball bearings.* Thus, in the deployed condition, each drum is cantilevered from the center support structure.

In the stowed (launch) position, the outboard end of each drum is supported by an arm which is mounted to the vehicle structure. This outboard end support serves two additional functions: (1) that of preventing the drum from rotating about its own axis, and (2) that of supporting the outboard ends of the leading edge member. The array deployment sequence is initiated by firing electro-explosive devices which release each of the outboard end supports. These supports then swing clear of the drums and leading edge member. In addition to the end support, the leading edge member is resting in a cradle on either side of the boom attachment point. This arrangement relieves the launch loads from the retracted boom.

In order to maintain the first mode resonant frequency of the entire deployed array above 0.04 Hz, it is necessary to maintain a minimum preload of 2 pounds in each array blanket. This is accomplished by mounting a Neg'ator constant torque spring motor in each drum. Those springs are matched at final assembly to provide nearly equal forces on each blanket. The storage drum must rotate approximately 15 times to fully deploy the array. The array power is transferred from the movable drum to the stationary structure by slip rings which are housed in each drum.

*This method of support is used for the Nimbus solar array paddles. Bearings similar to the Nimbus design have been selected.

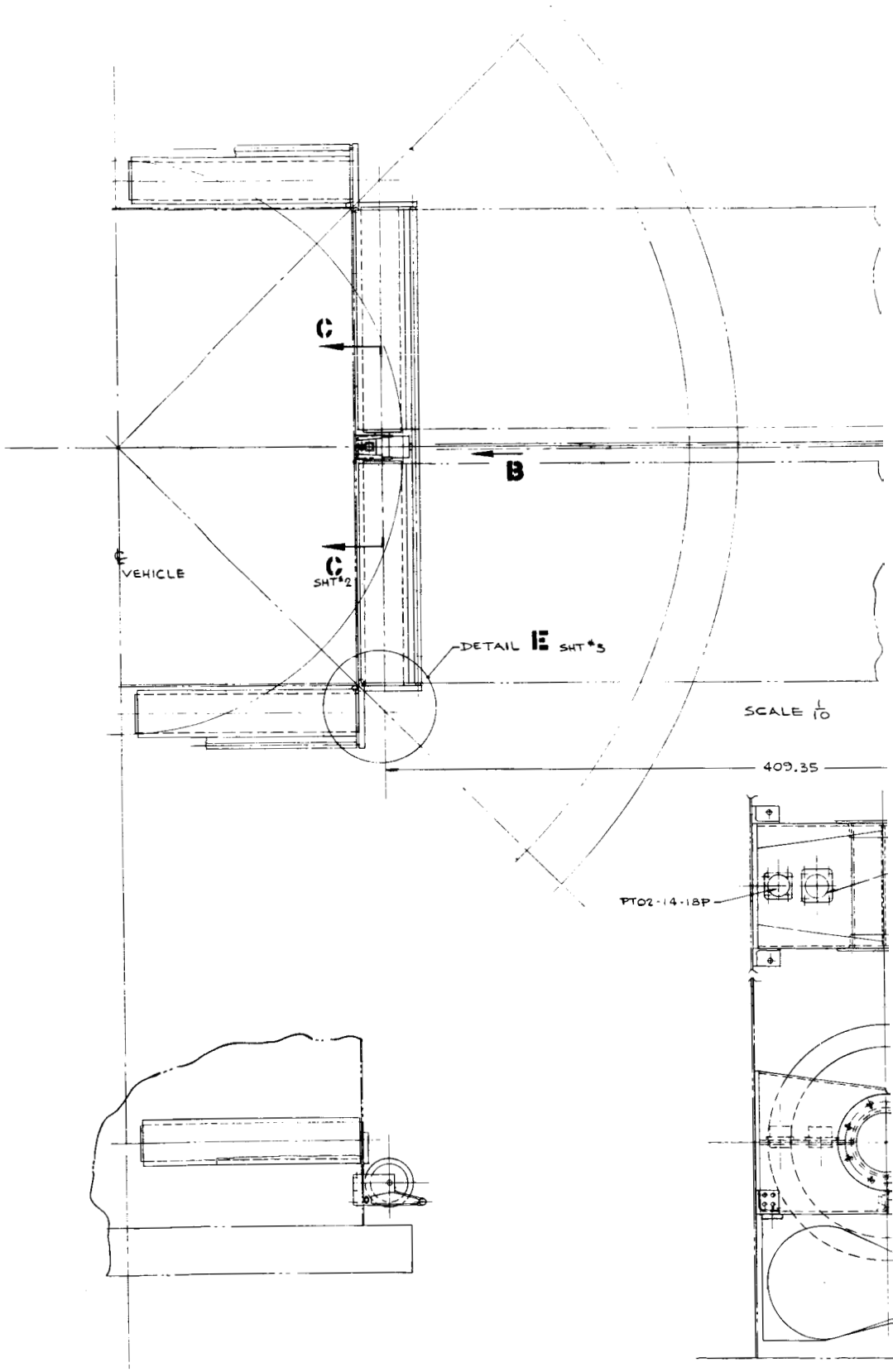

SECTION A - A
SCALE 1/2

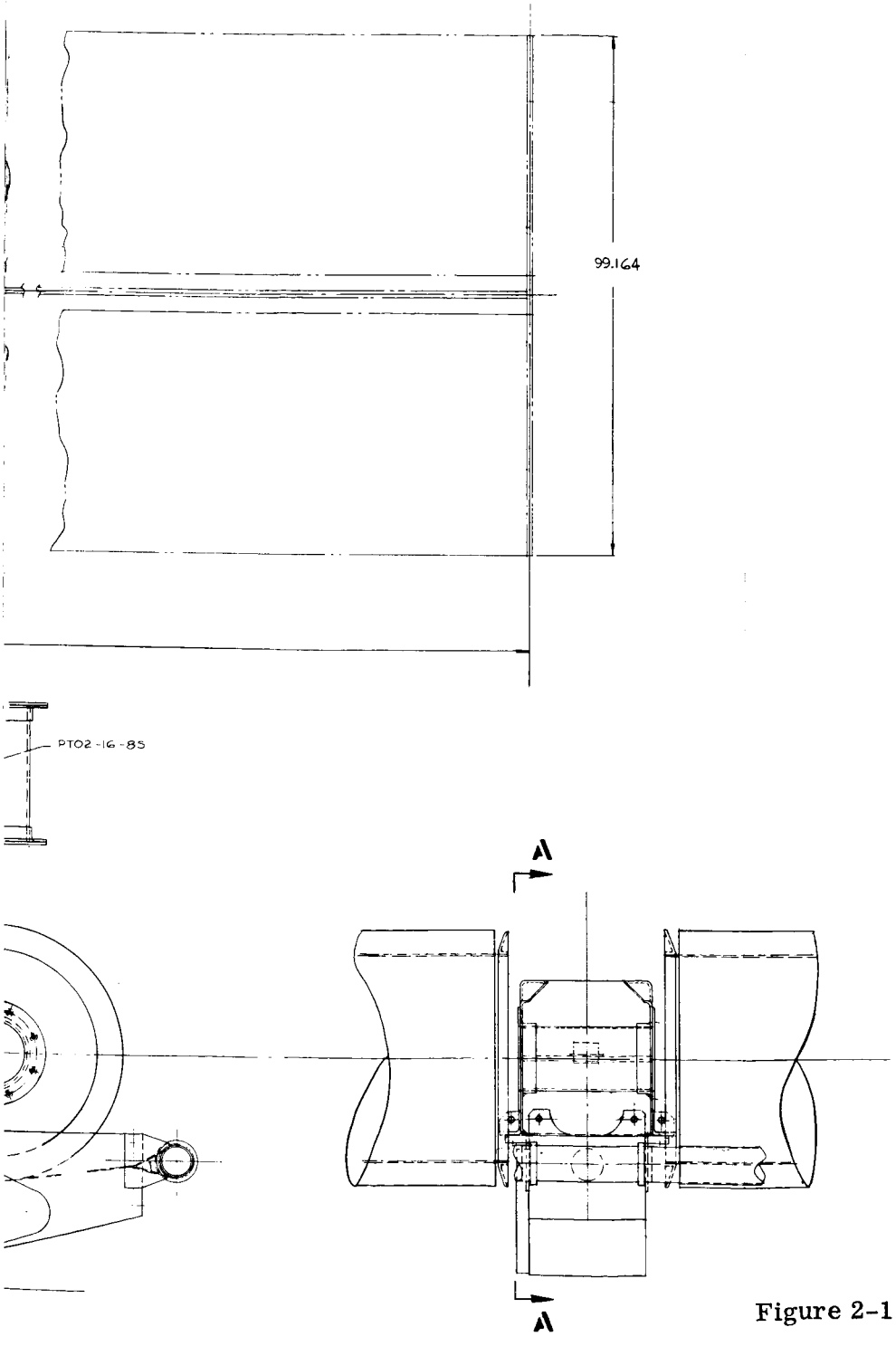

Figure 2-1. Roll-up Solar Array Configuration (Sheet 1 of 2)

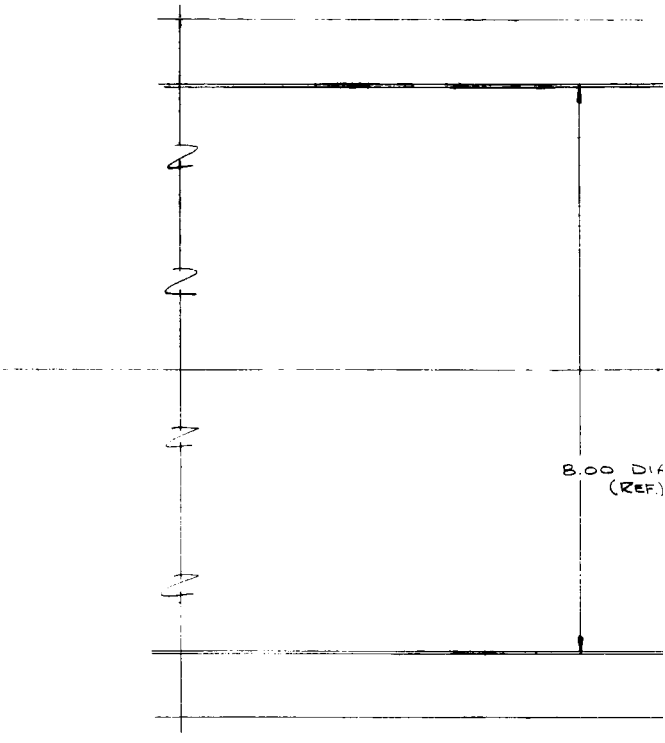

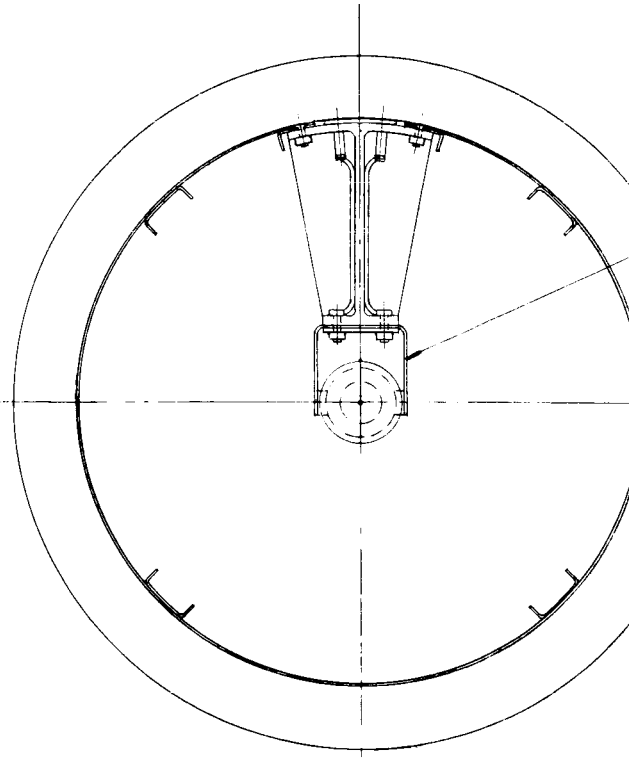

SECTION

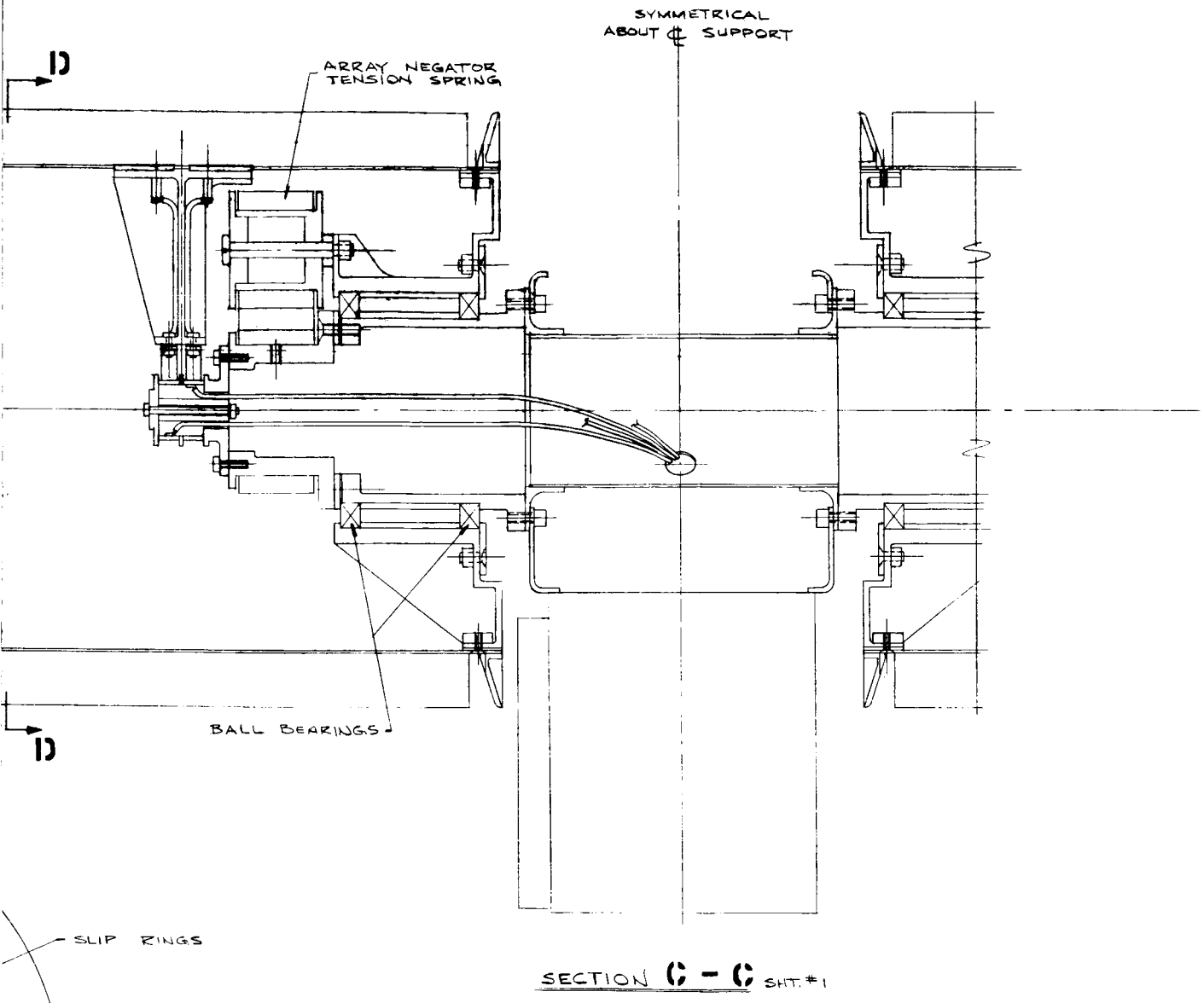

Figure 2-1. Roll-up Solar Array Configuration
(Sheet 2 of 2)

2.2 SYSTEM TRADEOFF STUDIES

2.2.1 Tradeoff of Single Boom Versus Double Boom

THE SINGLE-BOOM CONCEPT HAS BEEN CHOSEN AS THE PREFERRED SYSTEM BECAUSE IT RESULTS IN THE LOWEST SYSTEM WEIGHT AND IS THE LEAST COMPLEX SYSTEM. IN ADDITION, THE SHORTER DRUM ASSOCIATED WITH THE SINGLE BOOM PERMITS MORE OPTIONS IN DRUM DESIGN AND ATTACHMENT TO THE VEHICLE.

The purpose of this task was to define the deployment concept and select the optimum configuration for the roll-up solar array. Previously in the first quarter, the various array concepts or arrangements had been evaluated, and the configuration selected consisted of a single assembly in each spacecraft quadrant, mounted in a fixed position with the drum axis normal to the spacecraft vertical axis. This study was continued to determine the optimum configuration of the drum-boom system, and the results are presented in this section. No attempt was made to select a boom and deployment system or to fix a drum design.

Early system sizing work utilizing parametric representations of the Hunter STACER rods and aluminum drum weights were performed yielding the results shown in Table 2-1.

It is seen that the optimums are not sharp for either the single or double rod configuration. Subsequent analyses and configuration design studies were based on a double rod system 156 inches wide and a single rod system 102 inches wide (see Figure 2-2). Subsequent system weight studies with other types of rods (reported in first quarterly report) resulted in smaller weight differences between the single and double rod configuration than shown in Table 2-1.

The two candidates are compared in Table 2-2. The single rod system is clearly the preferred system and consists of a fixed (nondeployable) drum, mounted close to the vehicle support structure, with a single boom attached to the midpoint of the solar array panel leading edge. At the present time the BI-STEM rod has been selected and it would be appropriate to reiterate the aspect ratio optimization of the panel since the variation in BI-STEM weight with length is different than the Hunter STACER rod.

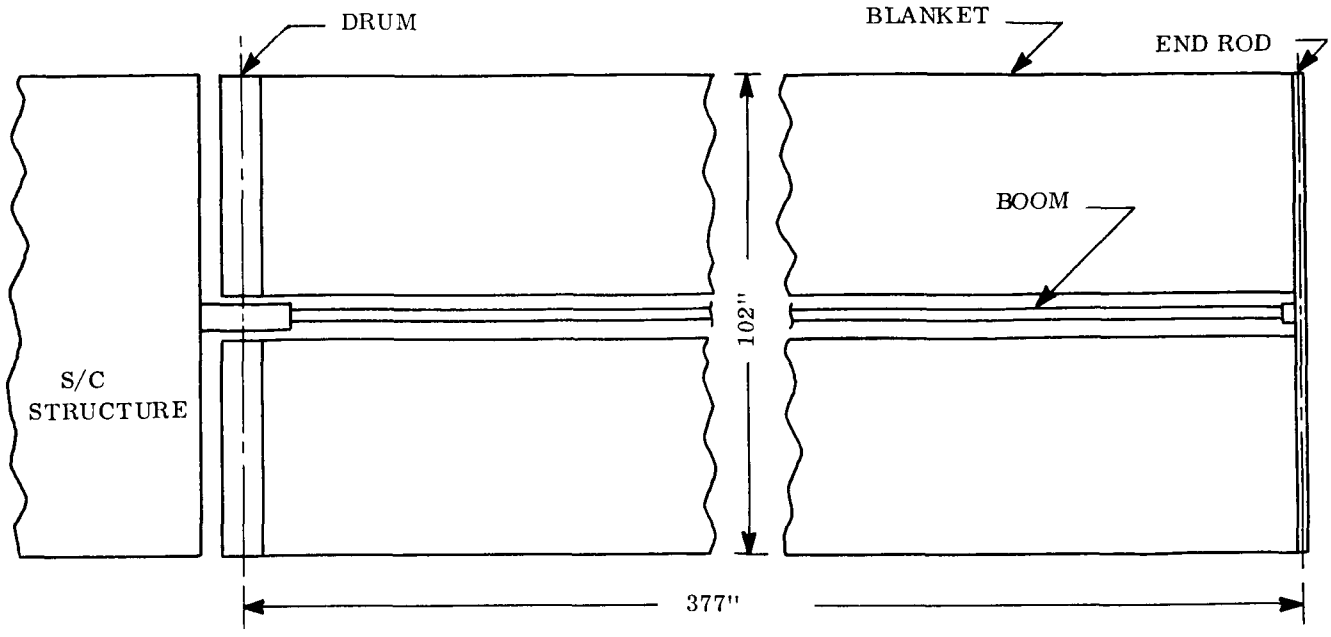

(A) SINGLE BOOM SYSTEM

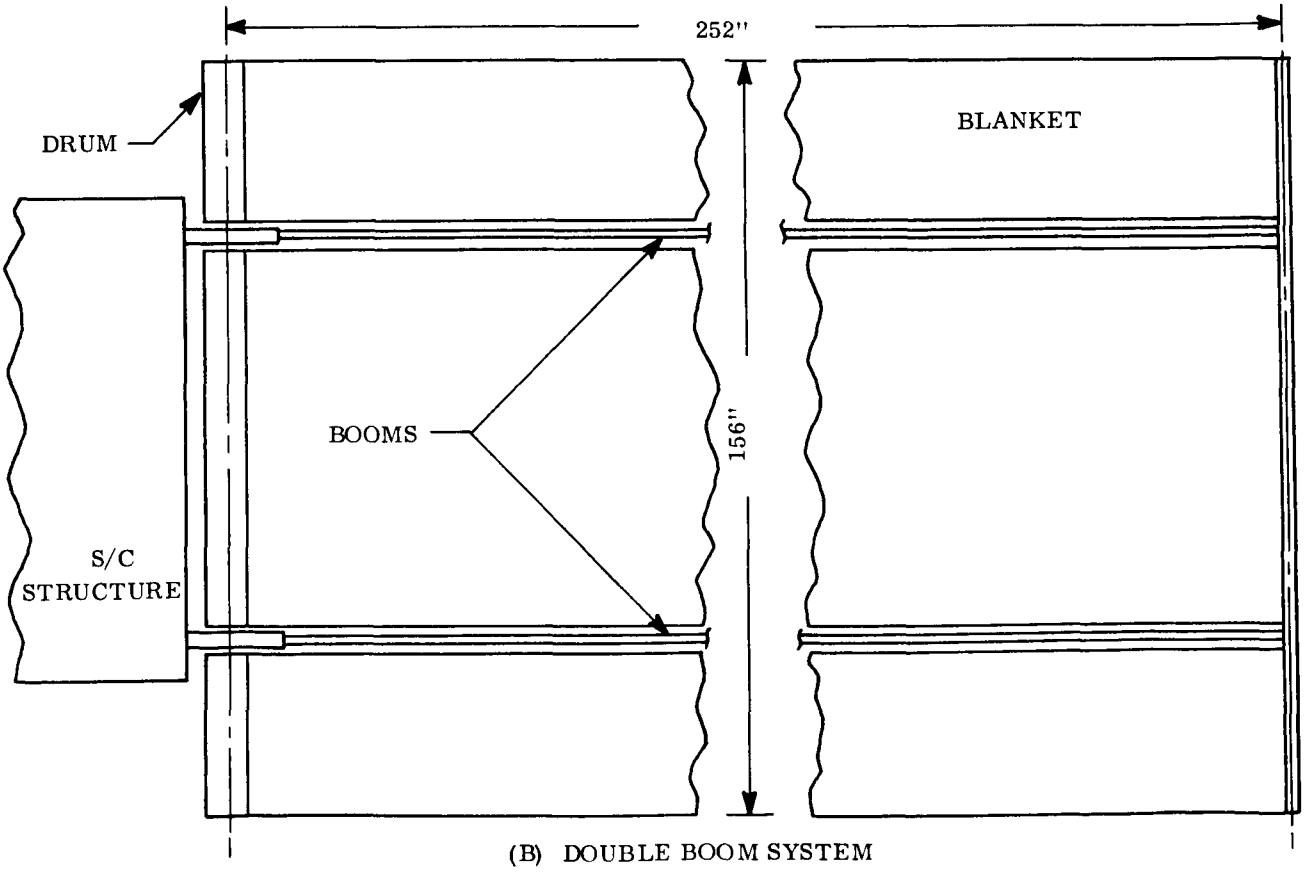

(B) DOUBLE BOOM SYSTEM

Figure 2-2. Typical Single and Double Boom Configurations

Table 2-1. System Weight Variations as a Function of Aspect Ratio

Drum Width (ft)	Array Length (ft, Rod Length)	Rod Tape Weight (lb)	Drum Weight (lb)	Total Weight (lb)	Specific Power (watts/lb)
Double Rod System Variations as Function of Drum Width					
13.0	19.228	7.737	16.384	90.439	27.643
12.0	20.830	8.744	15.430	90.246	27.702
11.0	22.723	10.007	14.476	90.307	27.683
Single Rod System Variation as Function of Drum Width					
12.0	20.833	4.372	15.430	77.279	32.351
11.0	22.723	5.003	14.476	76.709	32.591
10.0	24.996	5.812	13.522	76.316	32.758
9.0	27.773	6.877	12.567	76.180	32.817
8.0	31.245	8.327	11.613	76.428	32.710

Table 2-2. Comparison of Single and Double Rod Systems

Feature	Description
System Weight	Single boom system is lighter than double boom for all types of rods studied. Weight differences ranged from 5 pounds for Moly 180° overlap stem rods to 0.8 pound for BeCu BI-STEM rods.
Drum	Single rod system has shorter drum and is not wider than vehicle. The shorter drum provides more design options: a single drum, two drums cantilevered from a center support, two drums simply supported at ends, etc.
Complexity	The single rod system is preferable, since no rod deployment synchronization is required.
Flexibility and Stability	Single boom is at a disadvantage because of credibility of torsional stiffness and stability. Dynamics analysis in Reference 1-1 established the feasibility of utilizing substrate tension to provide structural stiffness for both torsion and bending.
Vehicle Mounting	The single rod system allows simple single-point vehicle mounting while the double rod system requires multipoint mounting.

2.2.2 Selection of Drum Bearing Arrangement

A TWO DRUM PER PANEL SYSTEM WAS SELECTED. EACH DRUM IS SUPPORTED AT THE INBOARD END BY A PAIR OF PRELOAD BEARINGS AND AT THE OUTBOARD END, DURING LAUNCH, WITH A TIE-DOWN SYSTEM. THE DEPENDENCE OF DRUM BEARING ALIGNMENT ON STRUCTURAL INTERACTIONS WITH THE VEHICLE WAS THE MAJOR DESIGN CONSIDERATION AFFECTING THIS SELECTION.

Table 2-3 shows the four basic bearing and support arrangements which were considered as candidate methods for mounting the drum. The weight of the drum and associated supporting brackets were calculated based on dynamic analysis and preliminary stress analysis. Magnesium was used as the drum material in this analysis. The total drum length is 94 inches in all cases.

Two major design considerations emerged from this tradeoff study:

a. The dependence of drum bearing alignment and preload on structural interactions with the vehicle.

b. Weight of drum and supports.

Approach II yields the minimum weight drum and supports, but the bearing alignment and preload is a function of the uncontrollable structural interactions with the vehicle. Approach I is slightly heavier than Approach II, but the bearing alignment is virtually independent of the vehicle structure.

Based on these considerations Approach I has been selected as the method of bearing arrangement and support.

Table 2-3. Drum Support Tradeoff Factors

APPROACH I	APPROACH II	APPROACH III	APPROACH IV
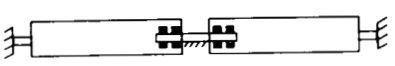	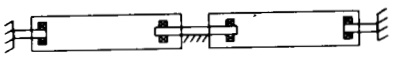	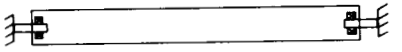	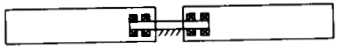
• Dual drum • Inboard bearings are preloaded pair • Outboard end of each drum is simply supported during launch phase; supports are released prior to array deployment • Drum and support weight = 18.6 lb • Maximum bending moment = 15,500 in-lb • Maximum shear load = 825 lb	• Dual drum • Single bearing inboard and outboard end of each drum • Drum and support weight = 17.4 lb • Maximum bending moment = 15,500 in-lb • Maximum shear load = 805 lb	• Single drum • Single bearing inboard and outboard end • Drum and support weight = 20.9 lb • Maximum bending moment = 58,000 in-lb • Maximum shear load = 1,860 lb	• Dual drum • Inboard bearings are preloaded pair • Outboard ends are not supported • Drum and support weight = 22.6 lb • Maximum bending moment = 70,800 in-lb • Maximum shear load = 2,850 lb
PROS • Bearing preload and starting torque is independent of vehicle structural interactions • Boom actuator can be mounted on center support • Shorter drums are easier to fabricate • Array wiring can be brought out of the center • Shorter width array panels are easier to assemble and wire • The outboard end of each drum can be open to allow access to the drum interior	PROS • Boom actuator can be mounted on center support • Shorter drums are easier to fabricate • Array wiring can be brought out of the center • Shorter width array panels are easier to assemble and wire • Lightest weight drum and supports	PROS • Shorter boom length	PROS • Bearing, preload and starting torque is independent of vehicle structural interactions • Boom actuator can be mounted on center support • Shorter drums are easier to fabricate • Array wiring can be brought out of the center • Shorter width array panels are easier to assemble and wire • The outboard end of each drum can be open to allow access to the drum interior
CONS • Slightly heavier than Approach II	CONS • Bearing alignment and preload is dependent on vehicle structural interactions	CONS • Bearing alignment and preload is dependent on vehicle structural interactions • Boom actuator must be mounted separately • Wiring from the array must exit through the ends of the drum • Long drum is more difficult to fabricate • Heavier than Approach II	CONS • Much heavier than Approach II

2.2.3 Selection of Optimum Power Takeoff Arrangement

INTERNAL SLIP RINGS HAVE BEEN SELECTED FOR THE POWER TAKEOFFS. THIS SELECTION WAS MADE BASED ON MINIMIZING THE TOTAL SYSTEM WEIGHT.

Preliminary tradeoff studies have been conducted to determine the optimum method for transferring the array power from the moving drum to the stationary support structure and for providing the necessary array blanket preload force. Four basic configurations have been considered:

a. Two Neg'ator constant torque spring motors to provide the blanket preload force and four separate spiral wrapped copper (OFHC102) bus strips which have an insignificant effect on the blanket preload.

b. Four separate beryllium copper (BERYLCO 10) spiral wound clock springs. These springs function as both the power takeoff leads and the blanket preload force springs.

c. Two sprial-wound clock springs. These springs act as both the power takeoff leads and the blanket preload force springs. Both power leads are carried on the same strip by laminating two BeCu (BERYLCO 10) conductor strips between polyimide film.

d. Two Neg'ator constant torque spring motors to provide the blanket preload force and two internal slip ring assemblies for the power transfer.

2.2.3.1 Analysis of Spiral Wound Configurations

For the analysis of the first three configurations, all power takeoff leads were assumed to be wound as spiral power springs. Figures 2-3 and 2-4 show the wound and unwound configurations, respectively. The number of turns on the arbor (n_2) in the wound conditions is given by (Reference 2-1):

$$n_2 = \frac{\sqrt{\left(\frac{4}{\pi}\right) \ell h + d_1^2} - d_1}{2h}$$

where:

h = thickness of the strip

ℓ = active length of the spring strip

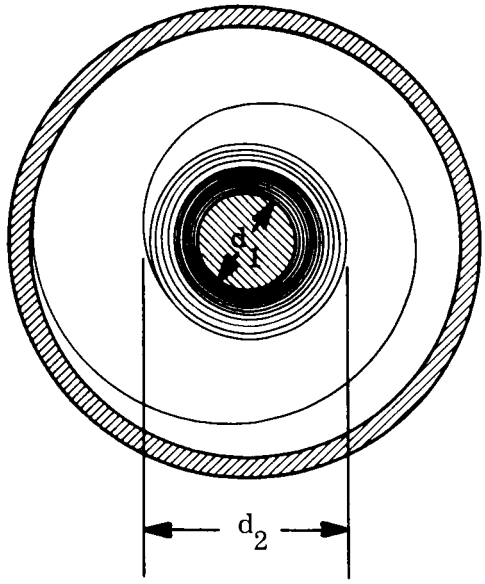

Figure 2-3. Power Spring Wound on Arbor

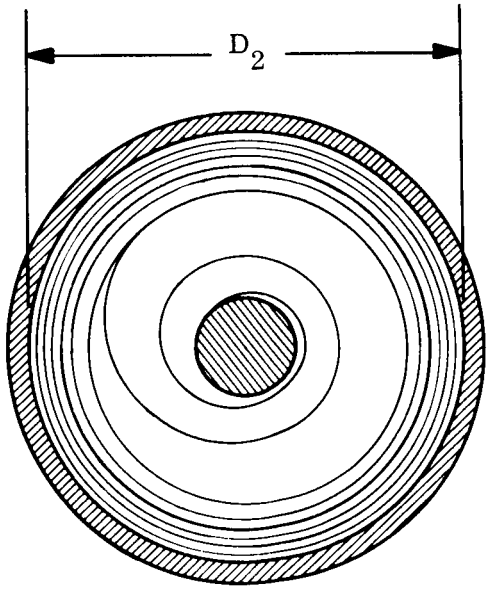

Figure 2-4. Power Spring Unwound and Resting Inside Case

The number of turns on the inside of the case in the unwound condition (n_1) is given by (Reference 2-1):

$$n_1 = \frac{D_2^2 - \sqrt{D_2^2 - \left(\frac{4}{\pi}\right) h \ell}}{2h}$$

The total number of turns (N) delivered by the spring is:

$$N = n_2 - n_1$$

The moment in the fully wound condition (M) is given by (Reference 2-2):

$$M = \frac{2\pi I E N'}{\ell + \pi (d_1 + h)}$$

where

$$N' = n_2 - n_o$$

$$n_o = \frac{\sqrt{\left(\frac{4}{\pi}\right) h \ell + d_1^2}\,(n_2)}{2 (D_2 - h)}$$

I = moment of inertia of strip

E = modulus of elasticity of strip

The bending stress in the strip is:

$$S = \frac{Me}{I}$$

where e = distance from neutral axis to outer most fiber

The first three basic configurations were analysed for the condition that 8 in.-lb is required per drum in the fully deployed state to provide the required array blanket preload. The measure of performance used to compare the various approaches was effective weight. Effective weight is defined as follows:

$$\text{Effective Weight} = \text{Total Spiral (or slip ring) Weight} + \text{Total Neg'ator Weight (if any)} + \frac{\text{Total Power Loss in Spiral}}{30}$$

The last term has been included to account for the fact that a power loss in the array subsystem must be, from the systems viewpoint, compensated for by an increase in array power (and weight). The specific array power as a goal in this contract is 30 watts/lb.

Figure 2-5 is a plot of effective weight versus strip width for Configuration 1. The copper strip thickness has been varied to show the effect of this parameter. A thickness of 1 mil has been allowed on each side of the copper for a high emittance coating. For each strip thickness there is an optimum strip width. Strip thicknesses greater than 0.002 inch result in increased stress in the copper and strip thickness less than 0.002 inch result in increased spiral weight. The torque developed by the 2.00-inch-wide strip when fully wound is 0.02 in.-lb per spiral.

Figure 2-6 is a plot of effective weight and stress versus strip thickness for configuration 2. The minimum effective weight occurs for a thickness of 0.02 inch. The stress at this thickness is 126,000 psi. A design of this configuration would have to utilize a strip thickness which is less than the optimum to reduce the stress in the spiral.

Figure 2-7 is a plot of effective weight and stress versus strip thickness for Configuration 3. Note in this case there is only one spiral per drum and it must develop 8 in.-lb when fully wound. The thickness of the center polyimide film is 0.010 inch in this plot. Center film thicknesses greater than 0.010 inch result in excessive stress and thicknesses less than 0.010 inch result in higher effective weights. A BeCu thickness of 0.008 inch results in the minimum effective weight, but this thickness would have to be reduced to reduce the stress in the strip.

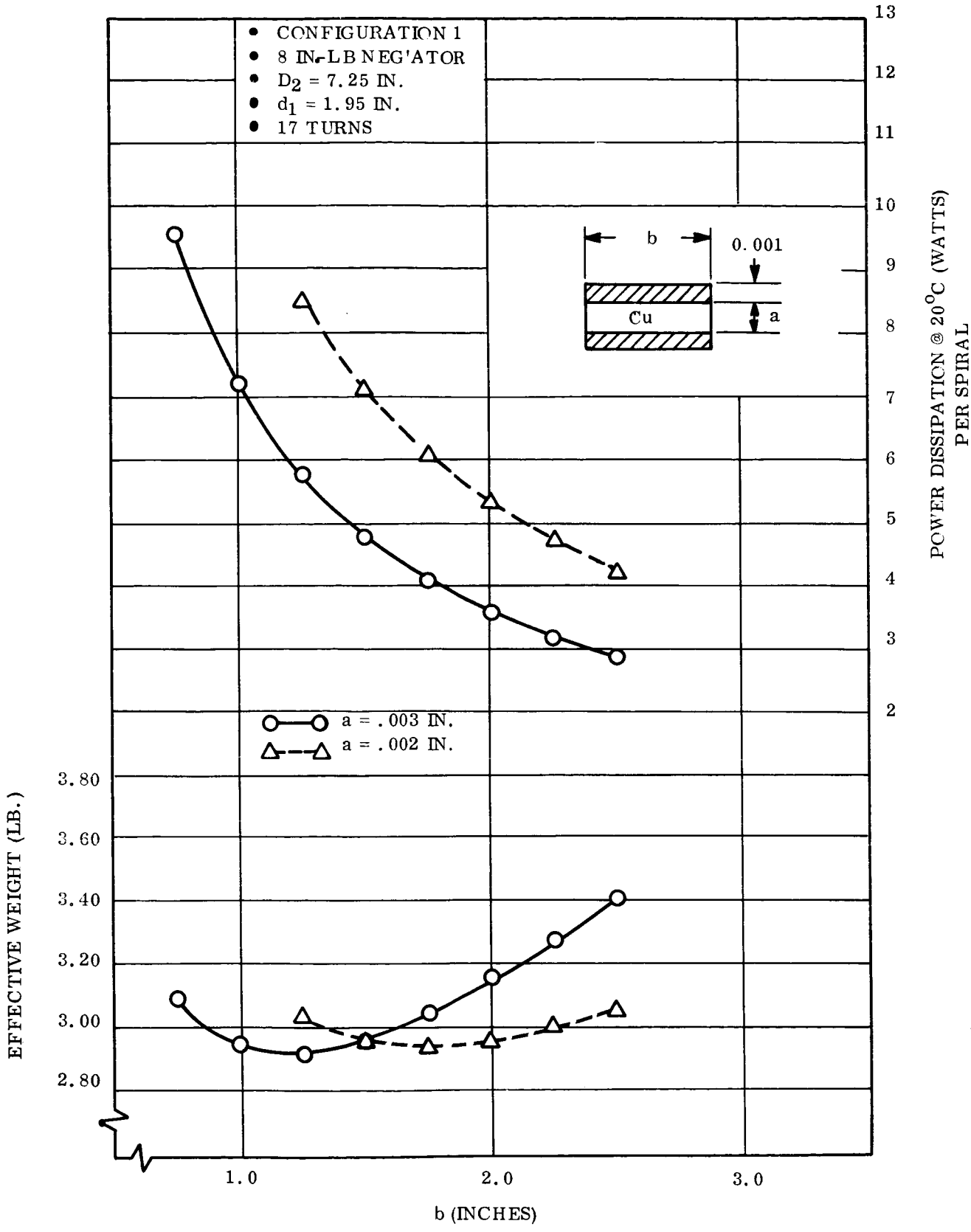

Figure 2-5. Effective Weight of Configuration 1

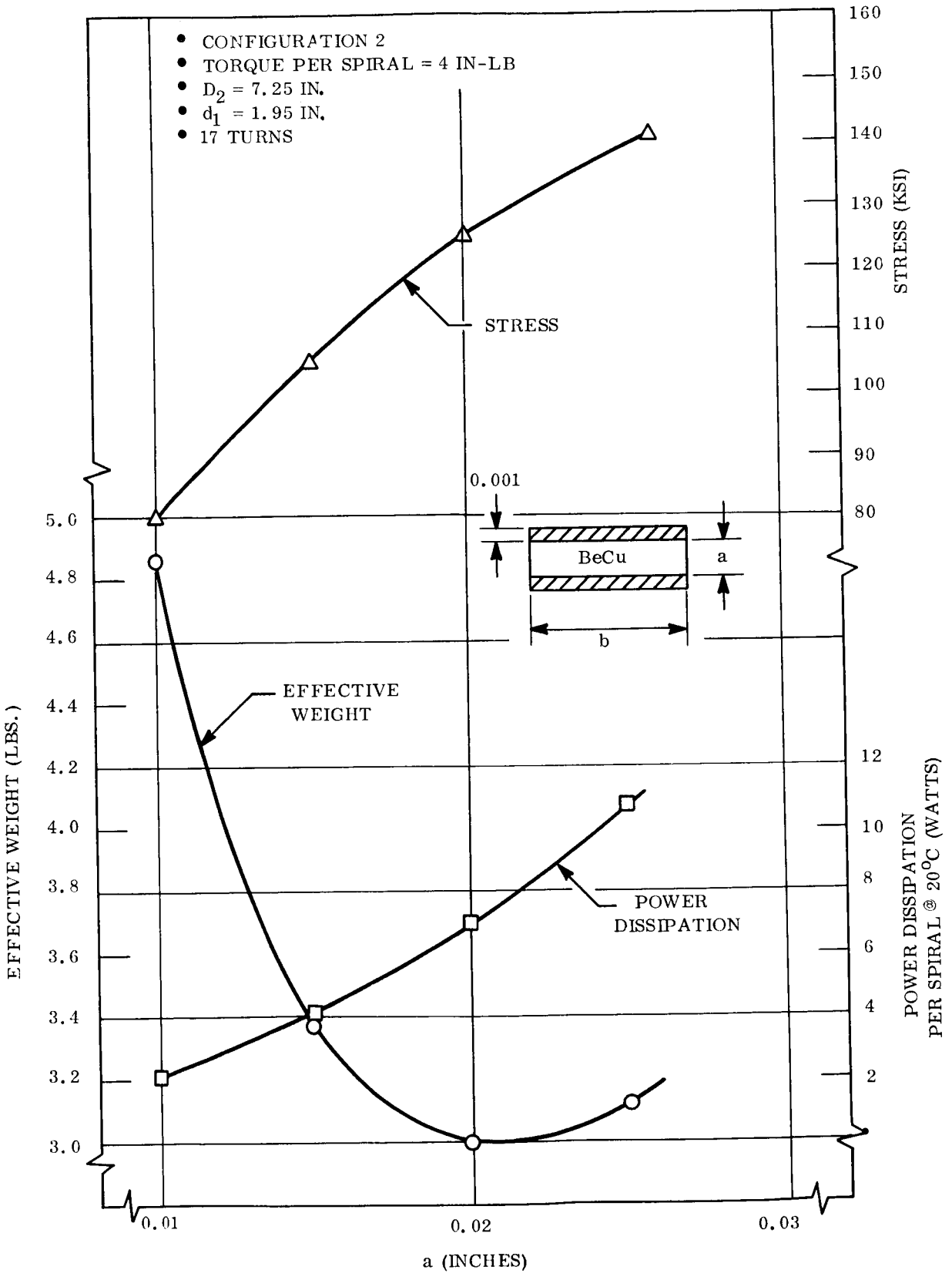

Figure 2-6. Effective Weight of Configuration 2

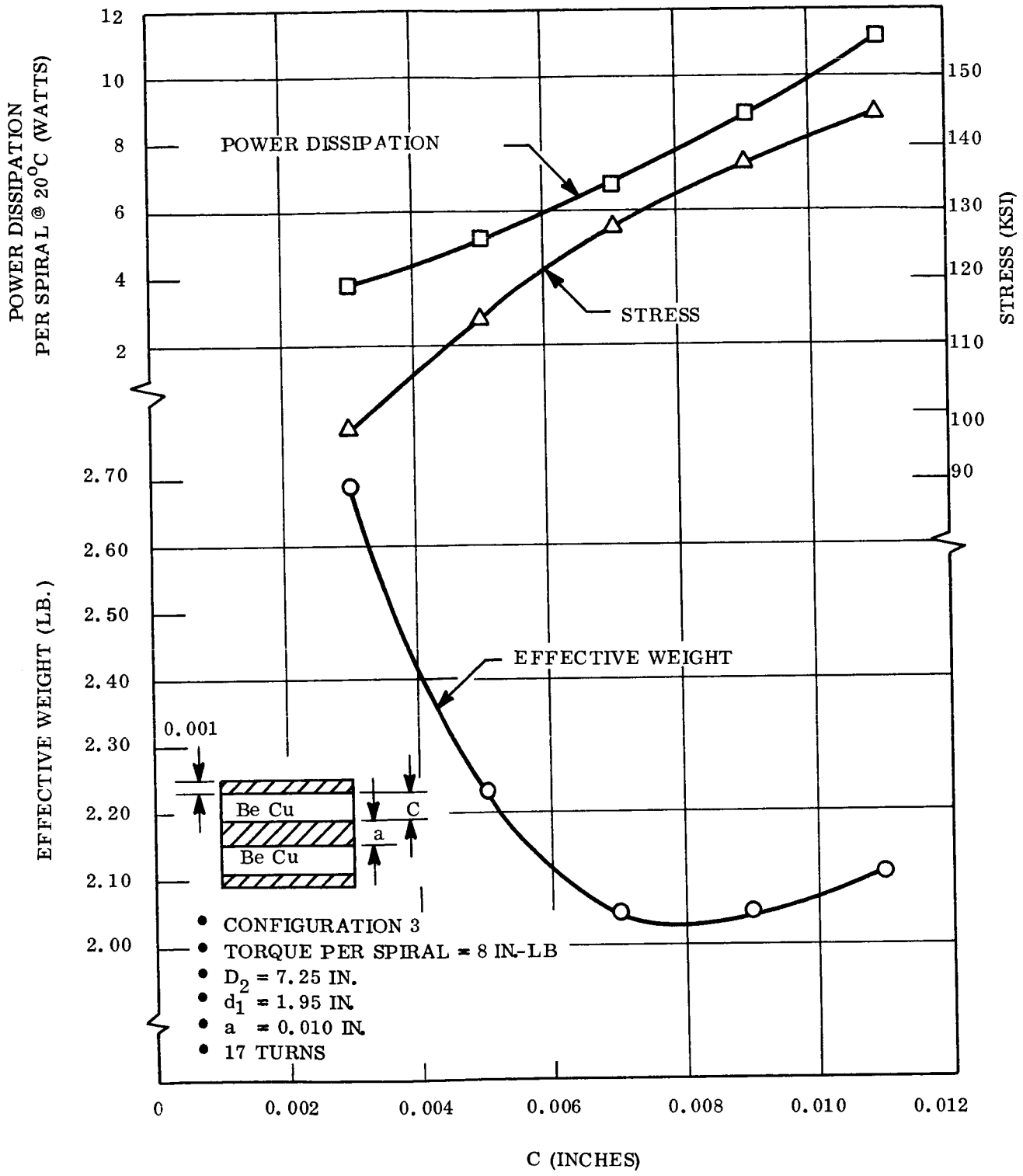

Figure 2-7. Effective Weight of Configuration 3

2.2.3.2 Analysis of Slip Ring Configuration

A design analysis of a slip ring assembly to accomplish the power transfer from the movable drum to the stationary support structure was performed for comparison with the spiral wound flat strip configurations. This assembly consists of two silver rings mounted on a Texolite shaft (see Figure 2-1). These rings are 1.00 inch in diameter, and there are two wipers per ring. The wiper material is silver/niobium diselenide. Graphite should be added to the wipers if much testing is to be done in the earth's atmosphere.

The pertinent design characteristics for the proposed assembly are summarized in Table 2-4. From these data, the effective weight of the slip ring configuration is given by:

$$\text{Effective Weight} = 0.8 + 1.3 + \frac{3.5}{30.} = 2.2 \text{ lb.}$$

2.2.3.3 Conclusions

The parameter used for this evaluation is the effective weight of the system as previously defined in Section 2.2.3.1. If the effective weight of each configuration is compared, the slip ring approach is superior in performance and was therefore selected as the method of power transfer from the movable drum to the stationary support structure. It is expected that the development cost of the slip ring assembly will be more than a spiral wound copper strip.

Table 2-4. Slip Ring Design Characteristics

Item	Characteristics
No. of rings	2
Wipers per ring	2
Wiper material	Silver/niobium diselenide
Ring material	Silver
Ring diameter	1.00 in.
Area per wiper	0.092 $in.^2$
Current per ring	13.8 amp
Wiper force	340 grams
Starting torque	0.3 in.-lb (vacuum) 0.6 in.-lb (air)
Contact resistance	0.003 ohm
Power dissipation/assembly	1.75 watts
Weight/assembly	0.4 lb

2.2.4 Deployable Boom Analysis

THE 1.34 IN. DIAMETER "OFF-THE-SHELF" BI-STEM IS MORE THAN ADEQUATE FOR THE ORBITAL LOADING CONDITIONS. IT WILL MEET THE 1G VERTICAL DEPLOYMENT REQUIREMENT WITH, AT MOST, SIMPLE AIDS.

2.2.4.1 Introduction

This section contains the structural analysis for the storable extendible boom element of the roll-up solar array. The member is subjected to deployed condition environment as sited in Reference 2-3 and must deploy in a 1g field to demonstrate the operating function of the arrays release, deployment, and locking mechanisms, with suitable test equipment. The 1g demonstration will be accomplished by an engineering demonstration model as described in Section 2.8.

The deployed condition environment is schematically represented in Figure 2-8. The blanket preload, required to keep the array surface plane and to provide a minimum natural frequency of 0.04 Hz, is the primary structural load. This loading is coupled with the thermal bending of the rod due to the temperature gradients associated with a solar illumination at 260 mw/cm^2 intensity. A pitch angle acceleration of 2×10^{-5} radians/sec^2 may also be applied to the array in combination with the above loading conditions; however, the magnitude of the resultant force is so small as to render this condition negligible.

The structural requirements associated with the aforementioned deployed condition are:

a. The boom element shall have a positive margin of safety for both ultimate and limit design loads as defined in Reference 2-3.

b. Under the above loading, with the exception of dynamic load inputs, the solar array surface shall maintain a plane normal to the sun within $\pm 10^{\circ}$. Thus the angle α, shown in Figure 2-8 shall be such as to limit the resultant tip deflection of the rod end to be less than $\ell \sin 10^{\circ}$.

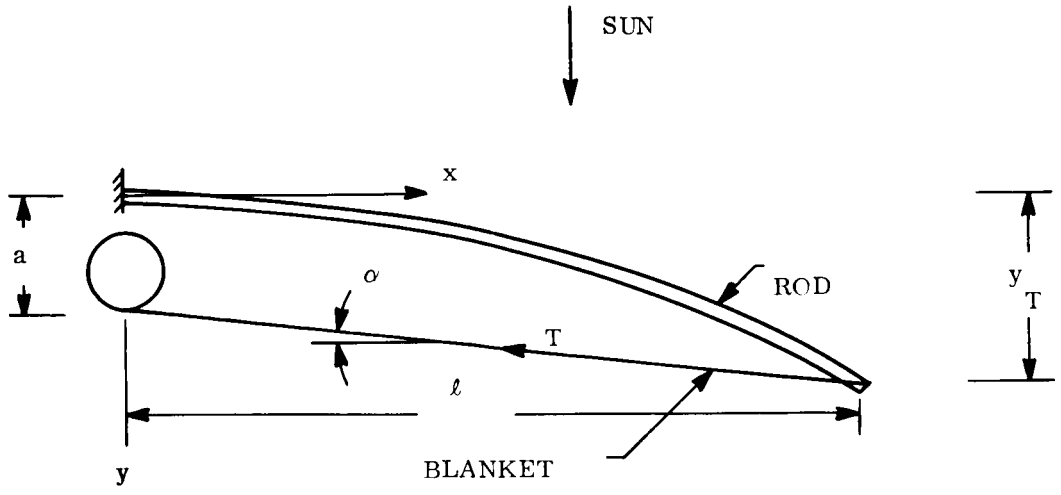

a. SYSTEM SKETCH

P AND Q ARE COMPONENTS OF
BLANKET TENSION T

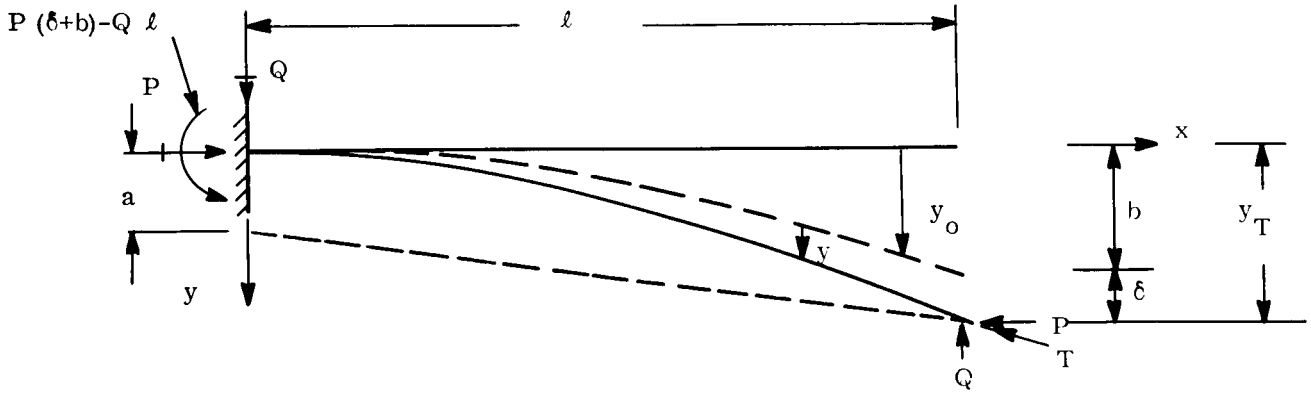

b. FREE-BODY DIAGRAM OF DEPLOYMENT ROD

Figure 2-8. Deployment Rod Orbital Thermostructural Loading

The extension rod for the 1g demonstration model will be loaded as shown in Figure 2-9. In addition to the blanket preload, a vertically deployed array will apply forces to the rod at its end directed parallel to the local vertical. The forces applied at the rod tip will be the gravity forces associated with blanket and end rod weights. The weight of the boom element will also be significant. For this loading condition, the boom element must maintain structural integrity or else deployments aids are needed.

2.2.4.2 Analysis

Deployed Condition

The details of the analysis of the extension rod for the deployed condition are shown in Appendix A. As mentioned, the rod is subjected to a temperature gradient and the solar panel blanket tension. The analysis contained herein is for the geometry of Figure 2-8, which shows an offset or eccentricity between the extension rod and the blanket at the drum end (i.e., distance a in Figure 2-8), as was the case in the early stages of this study. At present, there is no such offset. However, to obtain results for the present configuration, it is only necessary to set a = 0 in the solution obtained. Thus, the effect of such an offset can be assessed and the solution of the problem is more general.

In order to facilitate the integration of the beam-column equation the unloaded rod deflection curve under a linear temperature gradient across the rod section has been assumed to be parabolic that is (see Figure 2-8)

$$y_o = k x^2 = \frac{b}{\ell^2} x^2 \qquad (2\text{-}1)$$

where b is the tip deflection of a rod of length ℓ for a given temperature gradient ΔT. Although the actual rod curvature due to such a gradient would be constant, it is felt that this assumption will give sufficiently accurate results. For a perfectly straight rod to which is applied a gradient ΔT, the tip deflection will be:

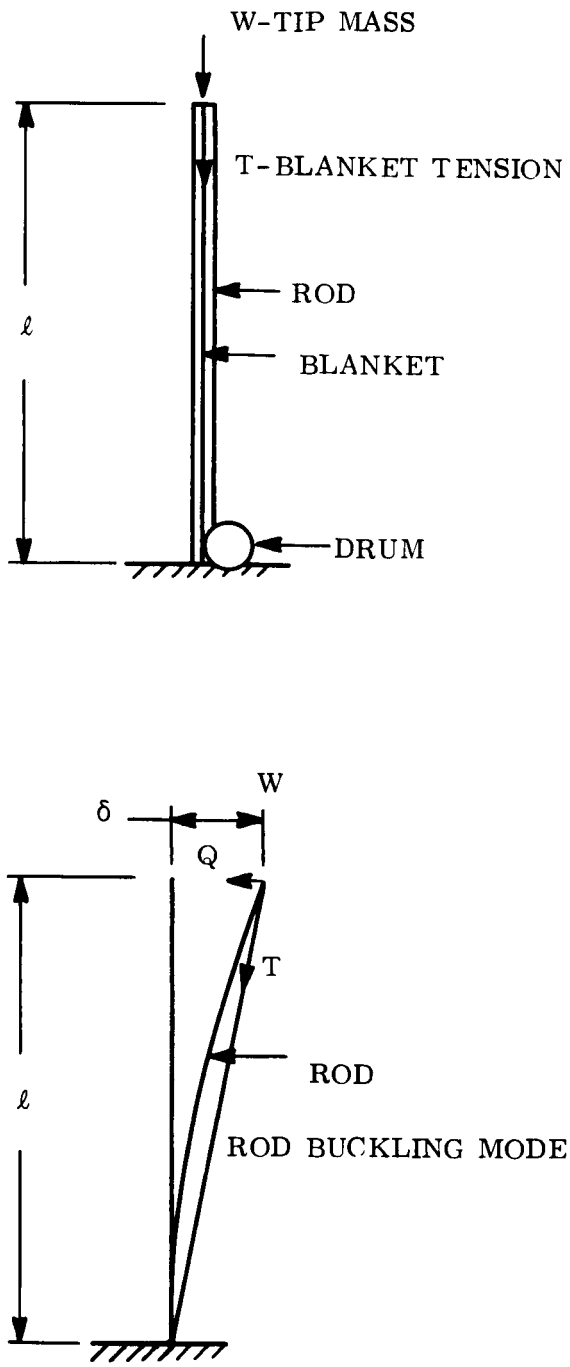

Figure 2-9. Rod Loading - 1g Demonstration Model

$$b = \frac{\alpha \Delta T \ell^2}{4 r} \tag{2-2}$$

where α - coefficient of thermal expansion

r - rod radius

At this point, the differential equation of the elastic curve can be solved. We have

$$EI \frac{d^2y}{dx^2} = -M = - \left\{ P (y+y_o) + Q\ell - P (\delta+b) - Qx \right\} \tag{2-3}$$

where P and Q are the components of the blanket preload T and y and δ are as shown in Figure 2-8. The solution of the above for the resultant deflection curve for the boundary conditions of a cantilever beam is:

$$y = -\frac{Q}{kP} \sin kx + \left\{ \frac{Q\ell}{P} - \delta - b - \frac{2b}{k^2\ell^2} \right\} \cos kx$$

$$- \frac{b}{\ell^2} x^2 + \frac{Q}{P} x + \delta + b + \frac{2b}{k^2\ell^2} - \frac{Q\ell}{P} \tag{2-4}$$

where

$$k = \sqrt{\frac{P}{EI}}$$

E - Modulus of elasticity

I - Rod Moment of inertia

At this point δ must be determined. At $x = \ell$, $y = \delta$ and using $\frac{Q}{P} = \frac{b+\delta-a}{\ell}$,

$$\delta = b \left\{ \frac{2 (1-\cos k\ell) - k\ell \sin k\ell}{k\ell \sin k\ell} \right\} + a \left\{ \frac{\tan k\ell - k\ell}{\tan k\ell} \right\} \tag{2-5}$$

or

$$\delta = \delta_1 + \delta_2 \tag{2-5a}$$

$$\delta = \frac{b\left\{2\,(1-\cos k\ell) - k\ell \sin k\ell\right\} + a\left\{k\ell \cos k\ell\,(\tan k\ell - k\ell)\right\}}{k\ell \sin k\ell} \qquad (2\text{-}5b)$$

Equation 2-5 is arranged such that the contribution of the deflection δ due the thermal gradient (δ_1) and the blanket offset (δ_2) can be obtained separately. We can see from Equation 2-5b that at $\sin k\ell = 0$, δ is infinite, and the critical load corresponds to $k\ell = \pi$ and

$$P_{CR} = \frac{\pi^2 EI}{\ell^2} \qquad (2\text{-}6)$$

Thus the critical load is the same as a pin-ended column. Also, by making "a" negative, we can decrease the deflection when ΔT is applied as shown in Figure 2-8.

To obtain the bending moments on the rod substitute Equations 2-4 and 2-5 into 2-3. To obtain the location of the maximum bending moment we have:

$$\frac{dM}{dx} = 0 \qquad (2\text{-}7)$$

Solution of Equation 2-7 for x yields:

$$x = \frac{1}{k} \tan^{-1} \left\{ \frac{2b\,(1-\cos k\ell) - a\,k^2\ell^2 \cos k\ell}{\left[a\,k^2\ell^2 + 2b\right] \sin k\ell} \right\} \qquad (2\text{-}8)$$

Substituting Equations 2-8, 2-4, and 2-5 into 2-3 gives the magnitude of the maximum bending moment. At $x = 0$ we can obtain the root bending mount which is:

$$M_R = T\,a \qquad (2\text{-}9)$$

The total deflection of the rod tip is:

$$y_T = b + \delta \qquad (2\text{-}10)$$

In order to satisfy the requirements of Reference 2-3 it is necessary that:

$$y_T < \ell \sin 10^o \qquad (2\text{-}11)$$

and that the stresses induced in the rod in this condition are of such a magnitude as to insure a positive margin of safety.

The solutions for Equations 2-2 and 2-5a have been programmed on the GE deskside time-shared computer system. The program also gives the permissible deflection, the maximum bending moment on the rod and its location and the root-bending moment.

Stress-free rod curvature developed during fabrication can be included in the above analysis, if it is again assumed that the associated rod deflection is parabolic, merely by modifying b such that

$$b = b' + b'' \qquad (2\text{-}12)$$

where

b' - rod tip deflection due to a temperature gradient

b'' - rod tip deflection due to initial rod curvature.

2.2.4.3 1g Demonstration Model

The forces applied to the extendible boom in the 1g field are as shown in Figure 2-9. In addition to the blanket tension (T), there will be additional forces (W) consisting of rod end fittings, edge member, and Kapton strips, and solar cells (see Section 2.8), which, unlike the force T, are directed along the local vertical. It has been shown in the previous paragraphs that such a member loaded at its tip by a force directed through a fixed point at or near its base (i.e., such as the rod in the deployed condition) has a critical buckling load equal to the Euler buckling load for a pin-ended column. However, it is well known that a column loaded by a force, such as W in Figure 2-9 directed as shown is a fixed-free Euler column and fails at a value of load equal to $(\pi^2 EI)/4\ell^2$ which is one-quarter of the pin-end critical load. The column shown in Figure 2-9 has a critical load which is within a range bounded by the fixed-free and the pined-pined Euler buckling loads.

The analysis for the extension rod loaded by tip forces Q and P is shown in Appendix A. It should be noted that the deflection is opposed by the lateral force, Q, which is a component of the blanket tension force T. The result obtained solving for a tip deflection δ is:

$$\delta = - \frac{Q}{Pk} (\tan k\ell - k\ell) \tag{2-13}$$

For the demonstration model of Figure 2-9 we have:

$$a = 0$$

$$Q = T \frac{\delta}{\ell}$$

$$P = T + W$$

If the above relations are substituted into Equation 2-13, we have:

$$\delta \left[1 + \frac{T}{P k\ell} (\tan k\ell - k\ell)\right] = 0$$

For δ other than zero, the quantity in brackets must be zero, which is satisfied by:

$$\tan k\ell = - \frac{W}{T} k\ell \tag{2-14}$$

The solution for Equation 2-14 is shown graphically in Figure 2-10.

The preceding solution does not account for the distributed loading associated with the members weight which is significant in a 1g field. This effect would be more complicated to deal with in this manner; so an approximate critical load was assumed for this study by applying a percentage (i.e., 30 percent in this case) of the total rod weight to the tip. Thus W will include, in addition to the weight of the other items mentioned, three-tenths of the weight of the rod.

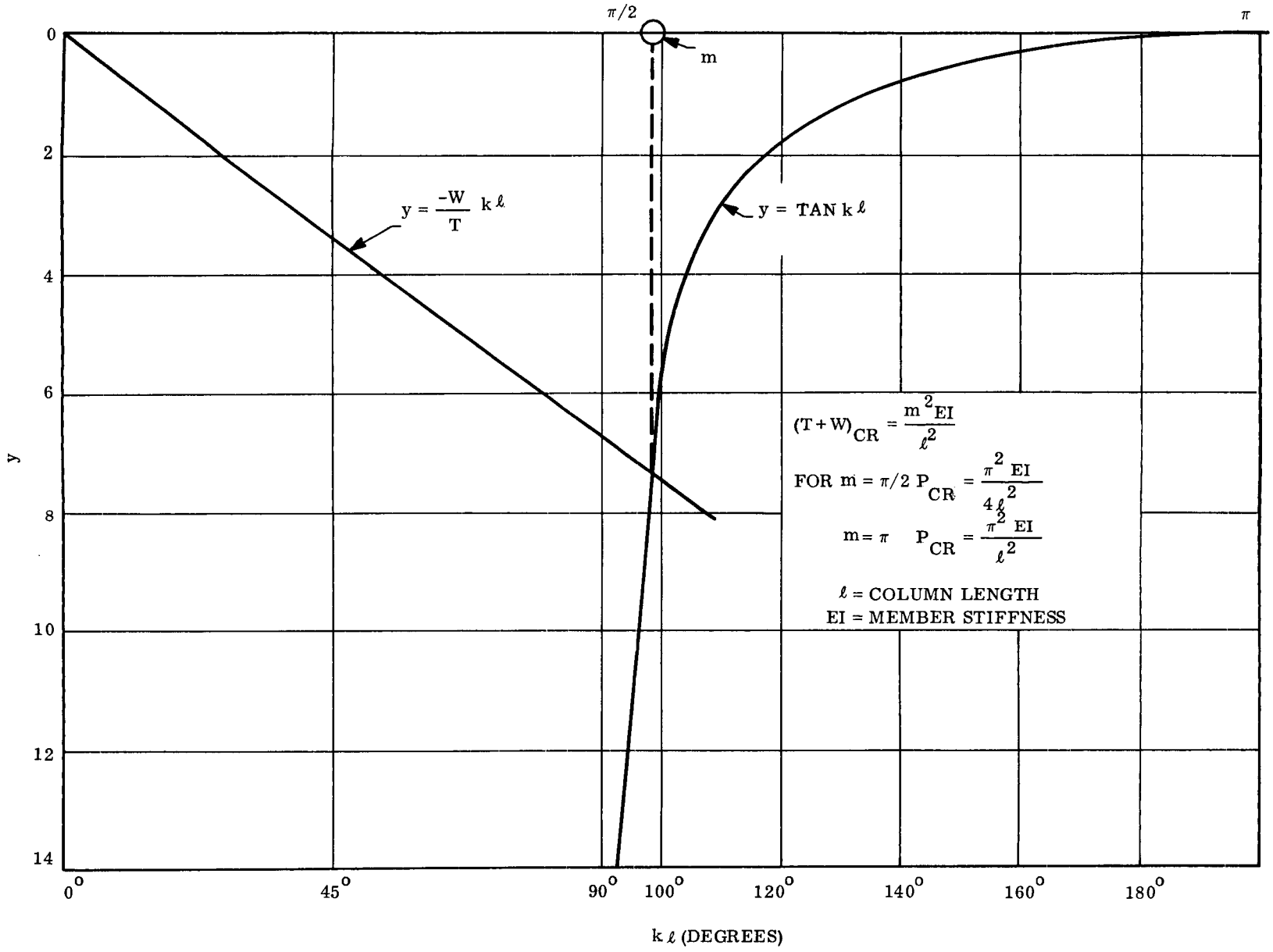

Figure 2-10. Critical Buckling Load for 1g Model Rod

Therefore, the critical load for the rod-loaded as in Figure 2-9 will be:

$$(T+W)_{CR} = \frac{m^2 EI}{\ell^2} \qquad (2\text{-}15)$$

where m is that value of $k\ell$ for which the equality of Equation 2-14 is obtained (see Figure 2-10).

Accounting for the effect of the weight in this manner is probably somewhat conservative; however, it should be mentioned that rods are not manufactured straight. Thus in actuality the loading would be applied to an initially curved member which, of course, would fail at a load less than the critical load predicted for a straight member.

2.2.4.4 Results

Deployed Condition -

The analysis was performed using the following rod characteristics:

Rod	-	BI-STEM
Diameter	-	1.34 in.
Thickness	-	0.007 in.
Weight	-	6.37 lb
Material	-	Silver Coated Stainless Steel
Length	-	33.5 ft.
Youngs Modulus	-	29×10^6 Psi
Minimum Moment of Inertia	-	0.01185 $in.^4$
Coefficient of Thermal Expansion	-	9.3×10^{-6} in./in./^oF
Solar Absorbtance	-	0.12
Emittance	-	0.04

For a temperature gradient at 53.9°F based on the analysis of Reference 2-4 and a blanket tension of 4.0 pounds, the following results were obtained:

Rod Tip Deflection - 35.68 in.

Permissible Deflection - 69.81 in.

Maximum Bending Moment (at rod mid-length) - 46.44 in.-lb (ultimate)

Ultimate Bending Strength = 984 in.-lb (Reference 2-5)
M.S. = high

1g Demonstration Model -

$T = 4.0$ lb

$W = 1.2 + 0.3\ (6.37) = 3.11$ lb

From Figure 2-10 at $\frac{W}{T} = 0.778$ $m = 1.71$

$$(T+W)_{CR} = \frac{m^2 EI}{\ell^2} = 6.25 \text{ lb}$$

$(T+W)_{CR} = 7.11$ lb (limit

$$MS = \frac{6.25}{1.25\ (7.11)} - 1 = -0.30$$

2.2.4.5 Discussion

The preceding results indicate that the structural safety margin for the off-the-shelf BI-STEM rod is high when subjected to the deployed condition environment but is negative if extended vertically to its full length in 1g for the demonstrated model. Therefore, it can be concluded that:

a. A smaller BI-STEM unit could be considered for use in a flight system.

b. The present demonstration model can not be extended to its full length without experimental determination of the load carrying capability for the 1g vertical deployment. Such an experimental determination has been made and is described in Section 2.5.3.

The deflection calculated for the BI-STEM rod is within that allowed to satisfy the requirements in Reference 2-3. However, uncoated BeCu would deflect considerably less in the same environment and would do so with a positive margin of safety for the deployed condition. Of course, in a 1g field, a BeCu rod would fail at a column load some 50 percent lower than a stainless steel member.

2.3 COMPONENT DESIGN STATUS

2.3.1 Solar Panel Actuator

THE SOLAR PANEL ACTUATOR (DEPLOYABLE BOOM) IS THE **BI-STEM** MANUFACTURED BY **SPAR** AEROSPACE PRODUCTS (FORMERLY DEHAVILLAND AIRCRAFT)

The SPAR Aerospace BI-STEM is considered the best technical approach for the boom actuator. The 1.34-inch diameter was selected because it is an available design which is more than adequate for the orbital load requirements. As shown in Quarterly Technical Report No. 1 (Reference 1-1), the use of the BI-STEM actuator results in the minimum weight system when compared to the 180-degree overlapped STEM and the interlocked rod.

Figure 2-11 is a photograph of a unit which is similar to the one proposed for the 30 Watt Per Pound Roll-up Solar Array. The outline drawing for the actuator which is proposed is shown in Figure 2-12. The unit will be equipped with an extension limit switch which stops the motor when the array has deployed to its full length. A retraction limit switch will stop the motor when the array has retracted to within approximately 1 foot of its initial launch stowed position.

The pertinent design characteristics for the BI-STEM actuator are shown in Table 2-5.

A component specification for the solar panel actuator has been prepared and is included as Appendix B of this report.

Table 2-5. BI-STEM Design Characteristics

Extended Boom Length	33.5 ft $\pm$ 2.0 in.
Boom Diameter	1.34 in. nominal
Boom Material	301 stainless steel (silver plated)
Boom Material Thickness	0.007 in.
Boom Material Width	4.000 in.
Motor Voltage	27 vdc
Current	2.00 amperes (approx)
Extension/Retraction Rate	1.5 in/sec

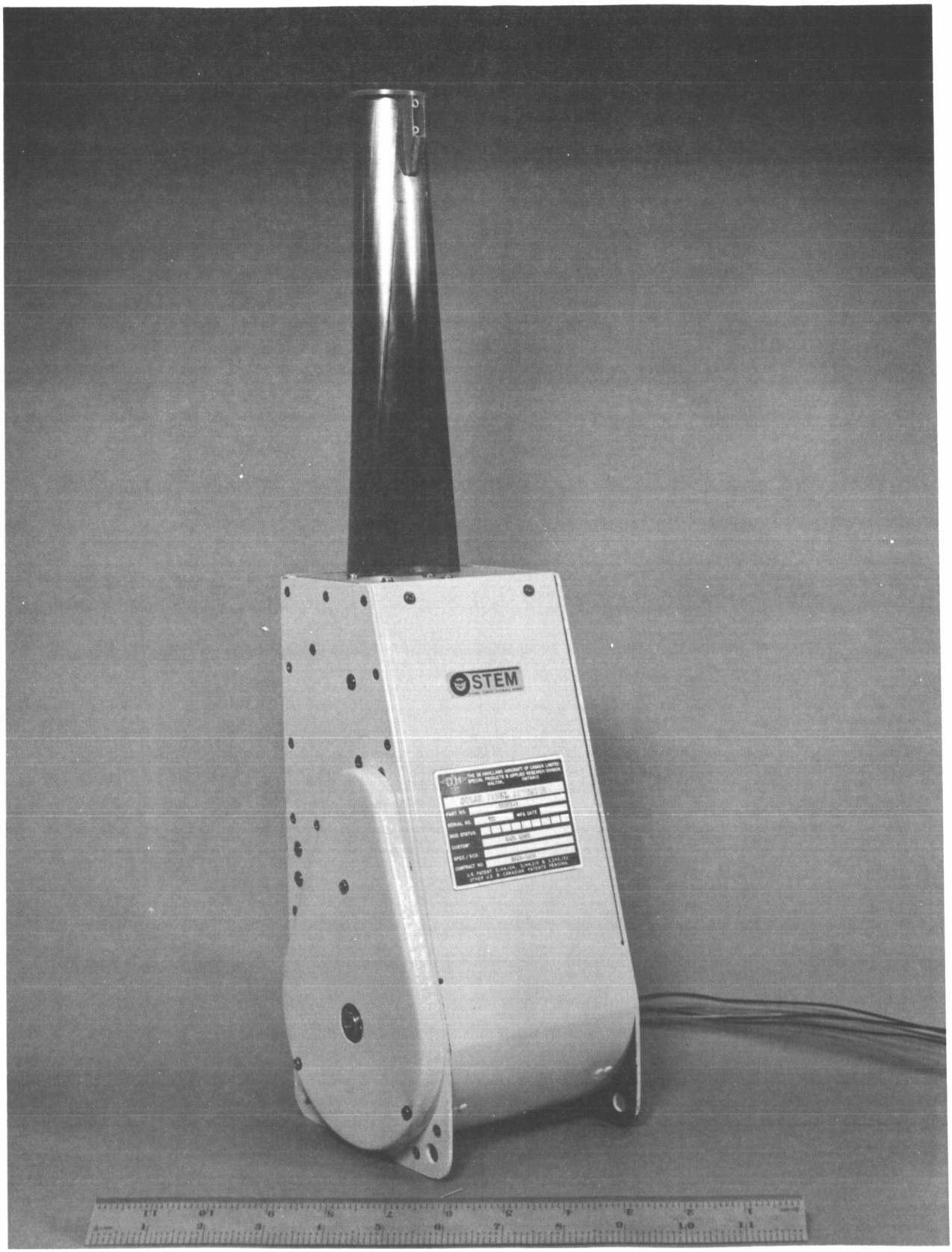

Figure 2-11. Photograph of a BI-STEM Actuator

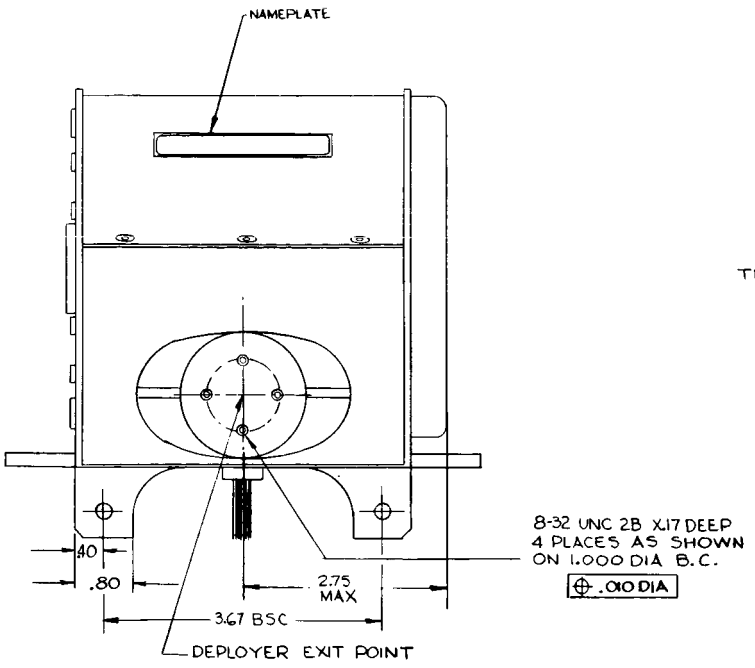

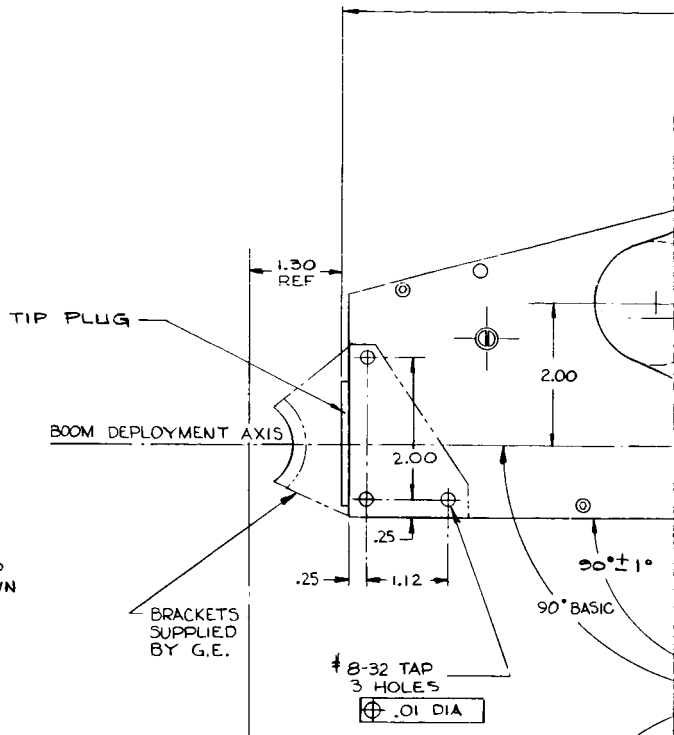

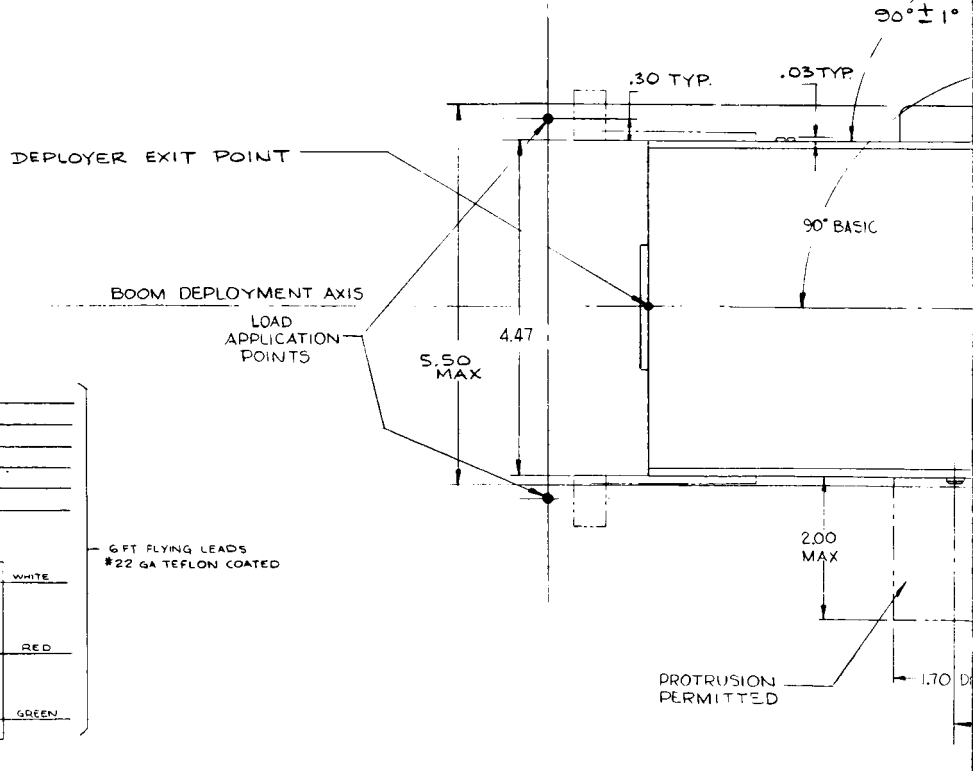

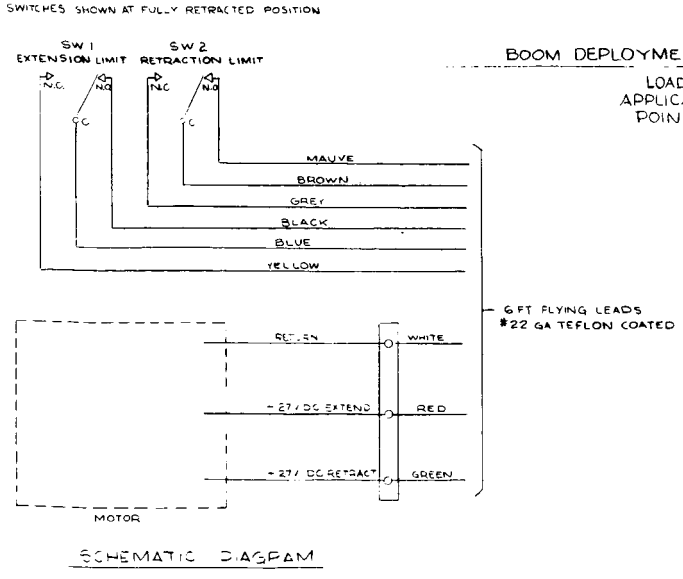

SCHEMATIC DIAGRAM

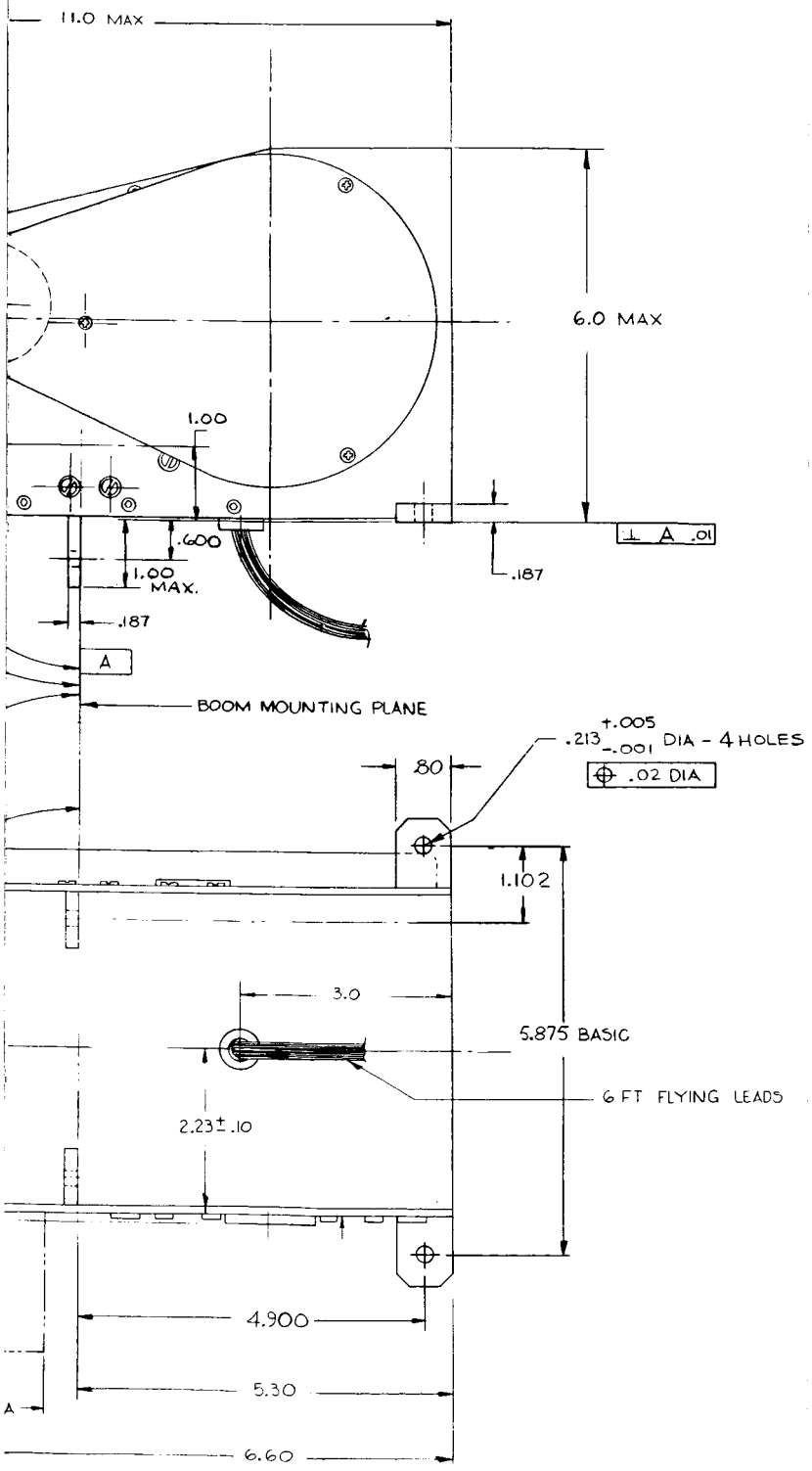

NOTES

1. INTERPRETATION OF DRAWING TERMS AND TOLERANCES PER 118A1664.
2. PART TO BE MARKED WITH MANUFACTURERS IDENT, AND MARK "GE 47E214524P1 PER 118A1526 CLASS 2 ON VENDOR NAMEPLATE APPROVED BY GE.
3. PARTS MUST CONFORM TO REQUIREMENTS OF SVS 7534

SOURCE CONTROL DRAWING

ONLY THE ITEMS LISTED ON THIS DRAWING IN THE "SOURCE OF SUPPLY" TABULATION HAVE BEEN TESTED AND APPROVED BY M.S.D. FOR USE ON SOLAR ARRAY EQUIPMENT. A SUBSTITUTE ITEM SHALL NOT BE USED WITHOUT PRIOR WRITTEN APPROVAL BY M.S.D.

NO CHANGES SHALL BE MADE TO THE DESIGN, CONFIGURATION, MATERIAL, PARTS OR MANUFACTURING PROCESSES WITHOUT PRIOR WRITTEN APPROVAL OF PURCHASING.

Figure 2-12. Outline Drawing of BI-STEM Actuator for Array

2.3.2 Array Blanket

THE ARRAY BLANKETS PRODUCE 2500 WATTS MAXIMUM POWER AT 1.000 AU AND 55°C AND WEIGH A TOTAL OF 42.5 POUNDS.

The array blanket assembly drawing is shown as Figure 2-13. Note that two array blanket assemblies are required for each array.

A distance of 0.800 inch in the parallel direction and 0.818 inch in the series direction has been allowed for each 2 x 2 cm solar cell. The submodule is composed of 19 parallel connected solar cells with an overall width of 15.188 inches. A string consists of 242 series connected submodules. The basic building block within the string is a module consisting of 20 or 22 series connected submodules. There are 12 modules per string, 11 with 20 series submodules and one with 22 series submodules. A spacing of 0.250 inch is allowed between modules. Therefore, the total length of a string is 200.346 inches. There are three adjacent strings in the parallel direction on each blanket, with 0.125 inches allowed between strings and at the edges. Therefore, the total width of each blanket is 46.064 inches. There are two adjacent strings in the series direction on each blanket with 1.000 inches allowed between strings and 7.00 inches allowed at the outboard end as a leader. The total length of the deployed array is 409 inches (measured from the center line of the leading edge member to the centerline of the drum.)

The V-I curve for the selected configuration is shown in Figure 2-14 for earth's distance from the sun at a temperature of 55°C. The maximum power voltage under these conditions is 91 volts. If 8-mil cells of 10 ohm-cm base resistivity are utilized, the required AMO efficiency @ 28°C is 10.55 percent; this includes an allowance of 6 percent for cover glass loss. This value of 6 percent is based on measured data on a carbon arc simulator with blue cut-on filters. This efficiency is necessary to obtain 10 watts/ft^2, the contract requirement, with these assumptions.

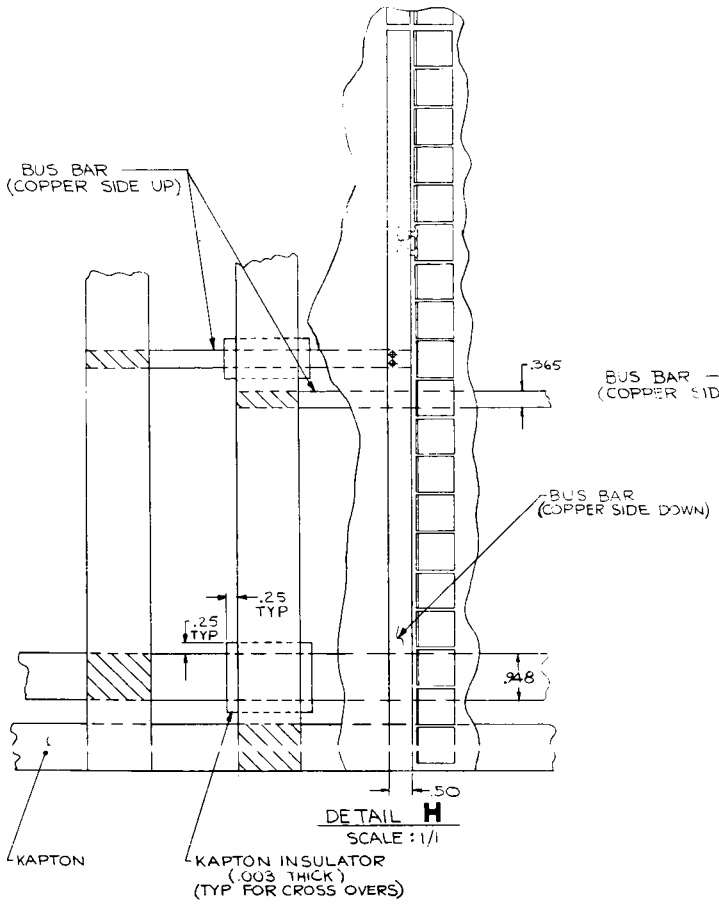

DETAIL **H**
SCALE : 1/1

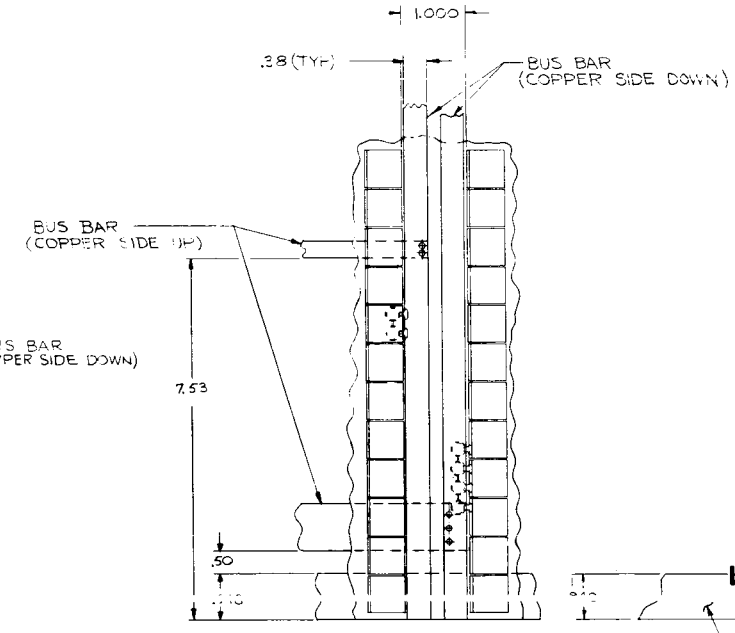

DETAIL **G**
SCALE : 1/1

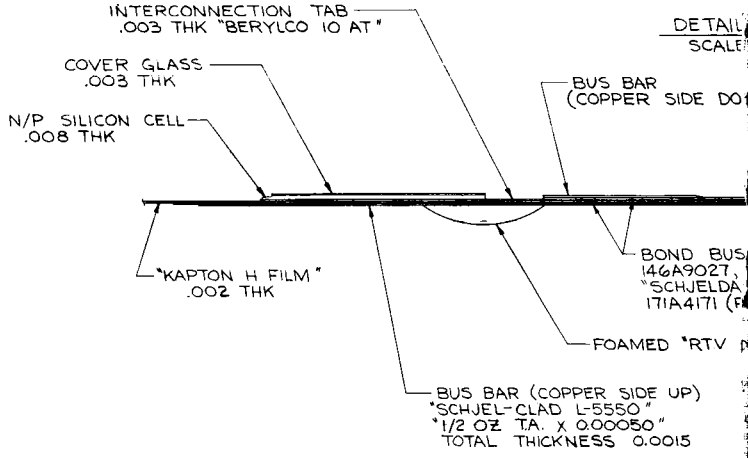

SECTION **F - F**
SCALE : 10/1

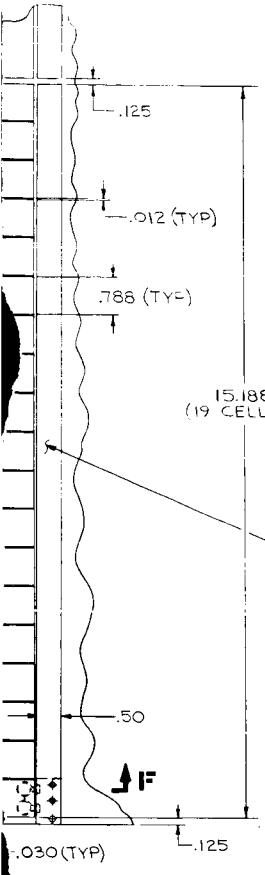

.030 (TYP)

DE UP)

AR TO FILM USING
PE 1 (.002 TO .003 THK
GT-100" TAPE PER
CESS).

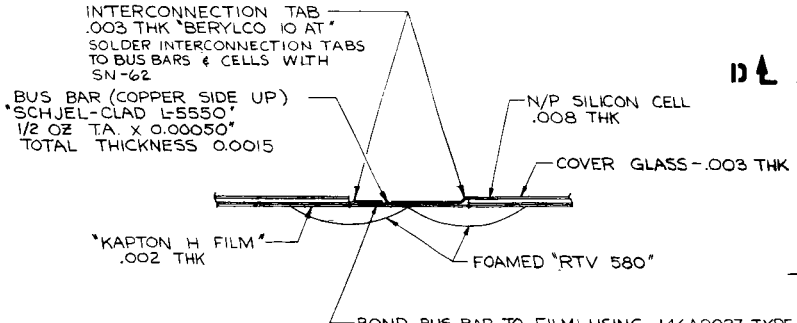

SECTION D-D
SCALE : 10/1

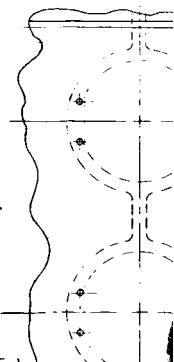

"SCHJEL-CLAD GT-5600"
2 OZ Cu x 3 MIL POLYESTER

.948 TY
.50
43.66
40.20
37.2
46.064
REF

241-2

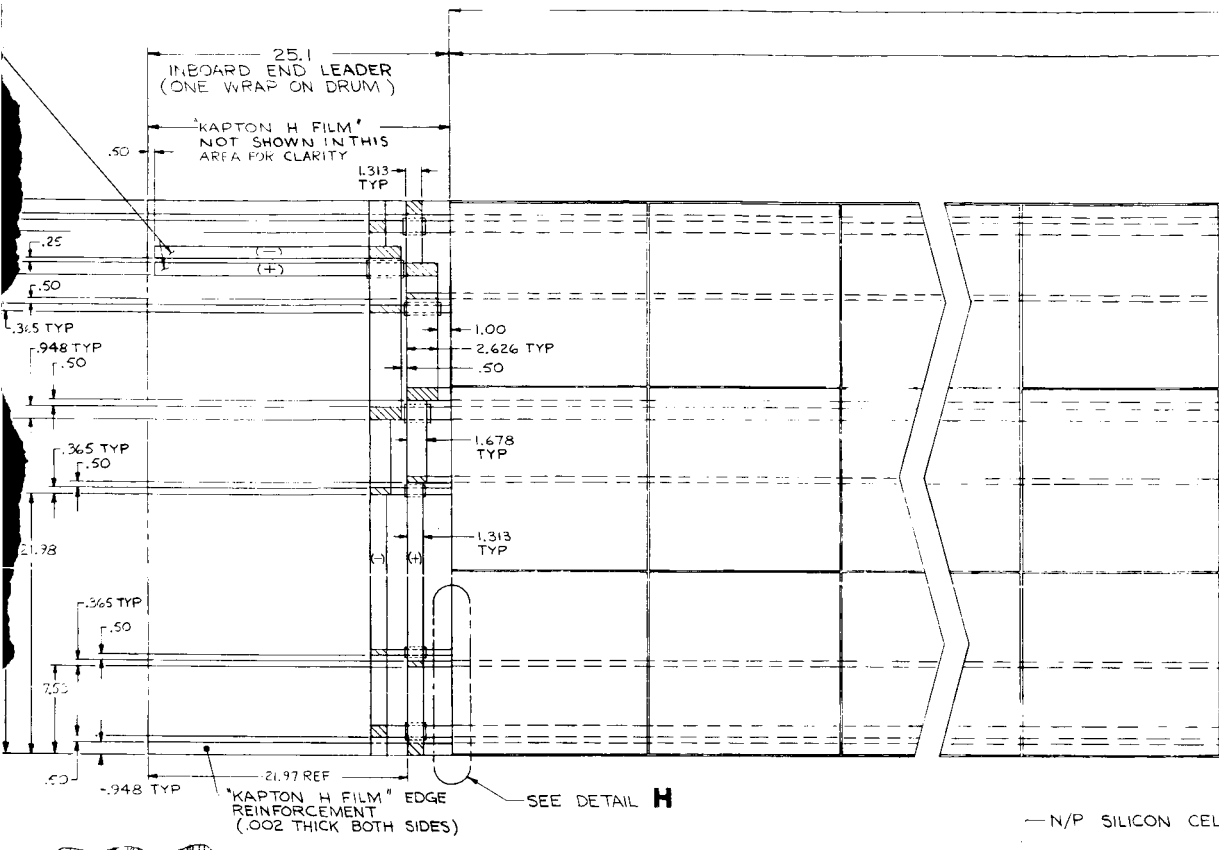

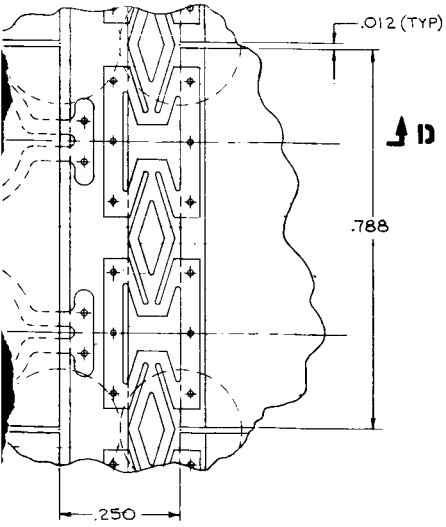

DETAIL C
SCALE: 10/1

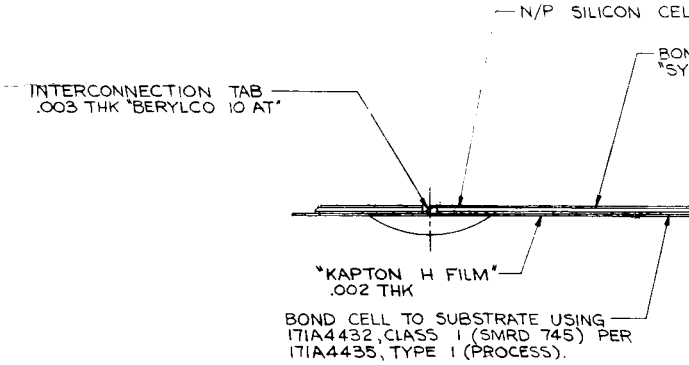

SECTION B-
SCALE: 10/1

2-41-3

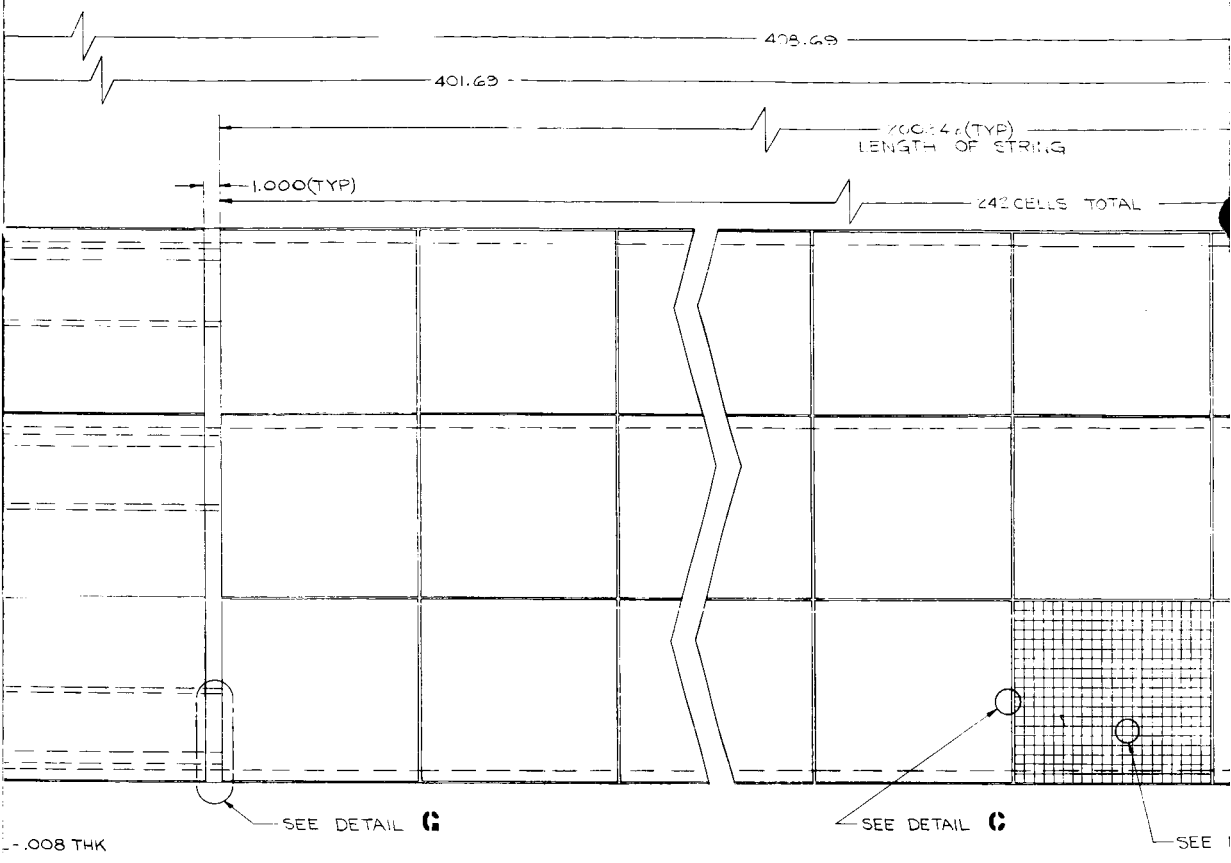

-.008 THK

D GLASS TO CELL USING
GARD 182" BOND GAP TO BE .0005.

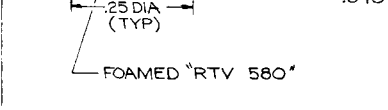

B

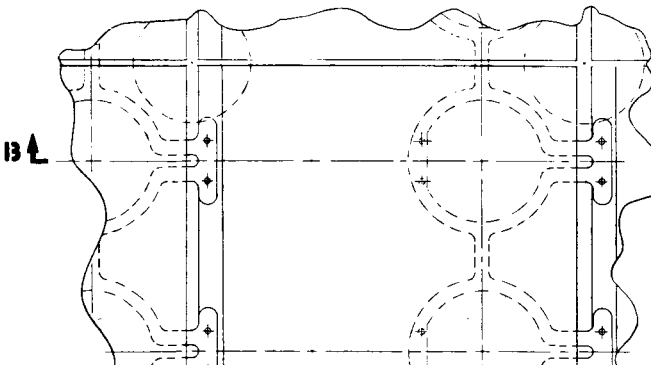

DETAIL A
SCALE: 10/1

2.42.1

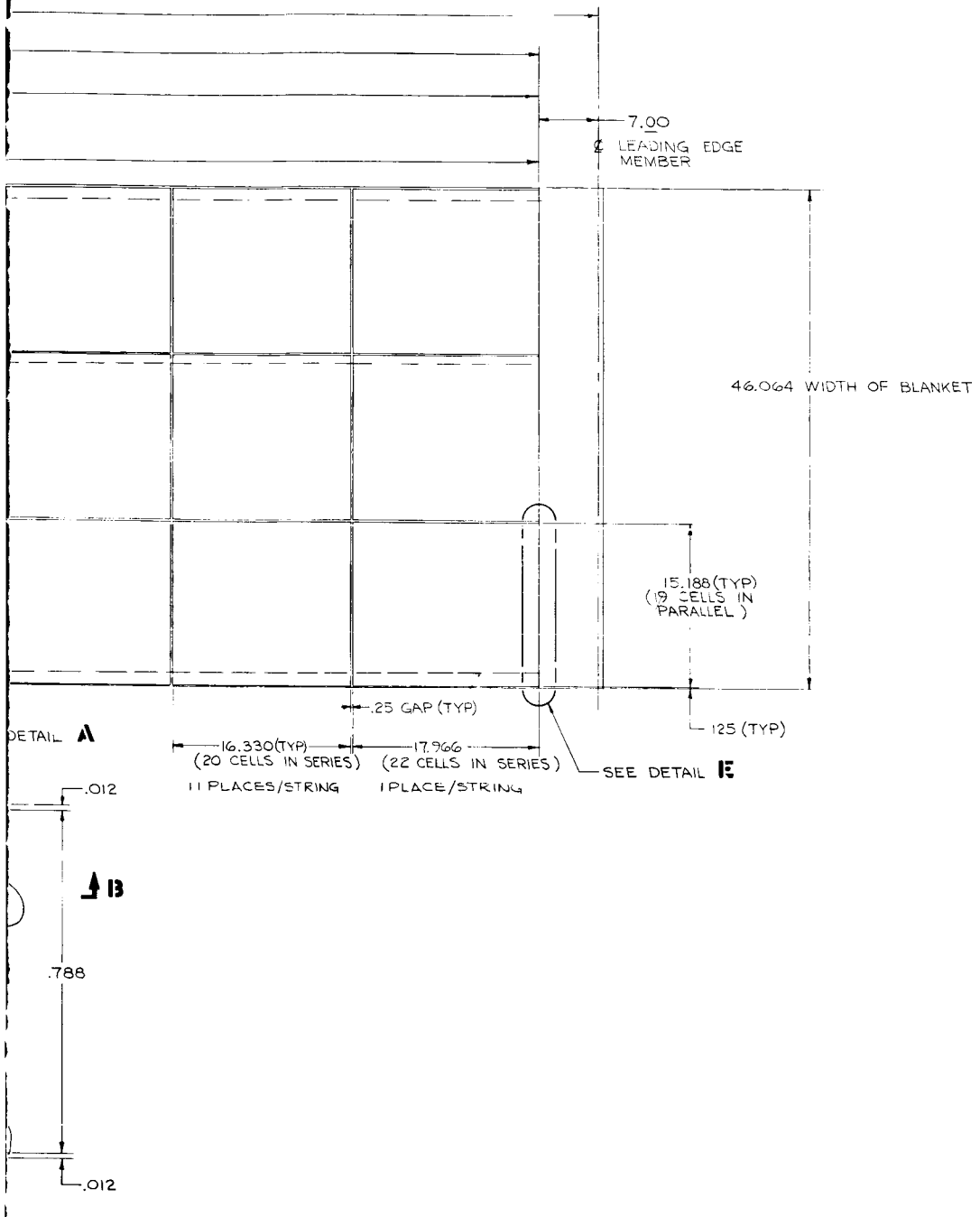

Figure 2-13. Array Blanket

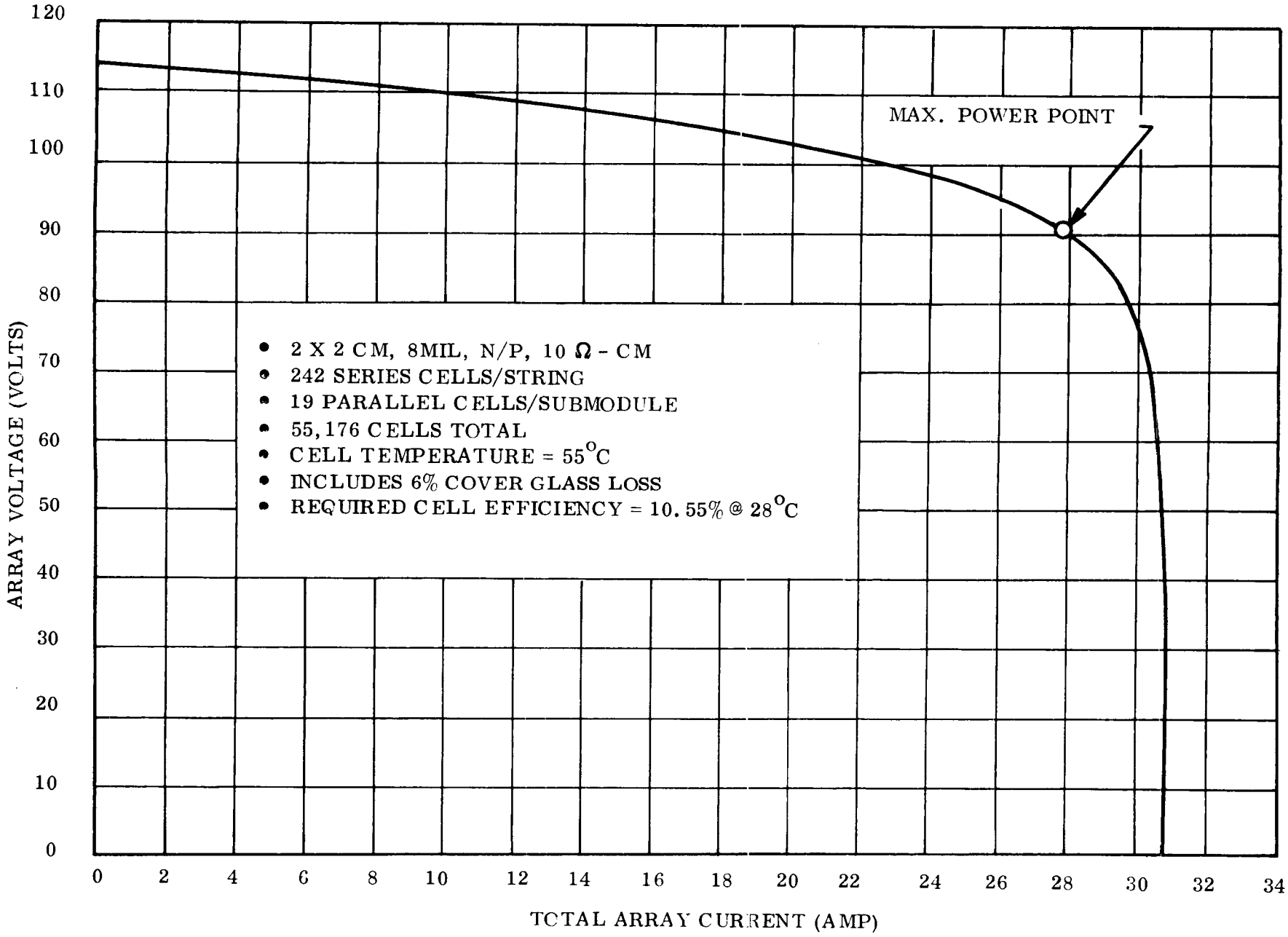

Figure 2-14. Array V-I Curve at 1.000 AU

All bus strips which carry current to the drum are bonded to the rear side of the array blanket. This design minimizes the magnetic fields produced by the array, since the effects of current flow in a series string of solar cells is nullified by the same current flowing beneath the string on the rear side of the array in the reverse direction. In addition, opposite polarity bus strips run adjacent to each other on the rear side of the array blanket.

The following is a description of some of the critical design areas of the array blanket assembly:

a. Substrate Sheet - Dupont "Kapton" 0.002 inch Thick. Kapton fulfills the requirements of a lightweight, (0.0148 lb/ft^2), high-strength (25,000 psi at 25^{o}C to 17,000 psi at 200^{o}C), temperature resistant (525^{o}C cut through) film suitable for use as the array substrate and has demonstrated its suitability on previous engineering models built by General Electric. Its major drawback, low resistance to tear propagation (8 gm/mil), is circumvented by reinforcement of its edges by bus bars and by the reinforcement over the entire area of the cell-to-substrate bonds which limit the travel through which a puncture initiated tear could propagate. Clean-cut holes do not behave as initiated tears and may be used as needed for electrical interconnection between the cell face and the underside bus bars.

b. Cell to Substrate Bond - General Electric SMRD745. SMRD745 compound has been used in earlier models to perform both cell-to-Kapton and Kapton-to-Kapton bonds. Recent tests with this material bonding gold-plated copper tabs to Kapton have consistently reached or exceeded 98 psi in shear before a peeling was encountered. Stress in the Kapton at this load was 15,330 psi suggesting that yield of the base material was the probable initiator of separation.

c. Bus Bars - Schjel Clad L5550. This material is a lamination of 1/2 oz/ft^2 copper on 1/2-mil mylar. This material has been qualified on another program which involved physically cycling over a 1-inch radius while loaded at 8.9 lb/in. Under tensile loading, values of 98 and 115 lb/in. were carried. All of these loading conditions are well beyond the loads required by the 30 watt/lb configuration.

d. Bus Bar-Kapton Bond - Schjeldahl GT 100. GT 100 is one of the family of polyester resin thermoplastic adhesives. Recent tests have shown it to be capable of 9.8 lb/in.^{2} in shear and 3.7 lb/in. of linear edge before peeling. Although not as strong a bond as the SMRD745, it is more than adequate for the 30 watt/lb loading conditions, and is a good handling material due to practically instantaneous curing.

e. Interlayer Cushioning - Foamed RTV 580 Pads. Foamed buttons 0.250 in. dia x 0.040 in. thick were experimentally evaluated for their ability to provide sufficient radial and axial damping of vibration and acoustic test excitations with regard to prevention of cell or interconnection damage. This system which adds only 0.0048 lb/ft^2 to the solar cell blanket did provide adequate protection for the array tested (1 ft wide, 0.012 in. cells, 0.006 in. glass). It needs to be reevaluated for the lighter cells and glass of the 30 watt/lb configuration as soon as possible.

A weight breakdown for the proposed array blanket is shown in Table 2-6 and a summary of the key design characteristics is shown in Table 2-7.

Table 2-6. Array Weight Breakdown

Item	Weight	
	Lbs	Lbs/Ft^2 Module Area
Cover Glass	8.73	0.0349
Cover Glass Adhesive	0.98	0.0039
Cells	19.46	0.0779
Interconnections	4.07	0.0163
Solder	0.19	0.0008
Substrate Adhesive	2.00	0.0080
Substrate	4.14	0.0166
Buttons	1.20	0.0048
Bus Strip	1.20	0.0048
Bus Strip Adhesive	0.53	0.0021
Total	42.50	0.1701

Table 2-7. Array Design Characteristics

Number of Cells	55,176.
Number of Parallel Cells/Submodule	19.
Number of Series Cells/String	242.
Number of Parallel Strings/Array	12.
Maximum Power Voltage @ + 55^{o}C	91. VDC
Maximum Power @ + 55^{o}C, 10.55% EFF. AMO (Includes 6% Cover Glass Loss)	2500.
Active Cell Area	226.03 ft^2
Gross Module Area	250.09 ft^2
Gross Array Area	261.67 ft^2

2.3.3 Storage Drum

A LIGHTWEIGHT STORAGE DRUM OF BRAZED BERYLLIUM SHEET HAS BEEN DESIGNED. STUDIES OF ALTERNATE FABRICATION METHODS AND DESIGN REFINEMENTS TO IMPROVE PRODUCIBILITY ARE UNDER WAY.

The basic drum is made in two identical sections, each cantilevered from a single, center support (see Figure 2-1). Each drum section is 8.0 inches in diameter by 47.1 inches long and is provided with a removable end cap on each end. The inboard end cap acts as a bearing housing and provides the primary load path from the drum skin to the center support. The outboard end cap provides a load path from the drum to the movable outboard end support. Both end caps are attached to the drum by fastening flathead screws through holes in the drum into nut plates in the end cap flanges. The caps are made removable to provide access to the interior of the drum for installing the internal slip rings, the constant torque spring motor, and the preloaded drumbearings.

The drum is essentially a thin-walled cylinder and is fabricated from cross rolled beryllium sheet (see Figure 2-15). The preliminary design drawings for the storage drum assembly have been sent to vendors qualified to fabricate with beryllium. Feedback has been received regarding cost and design changes which would improve the producibility of these parts. All beryllium fabricated parts utilize state-of-the-art joining techniques.

The use of beryllium in the drum has resulted in a lighter-weight structure with a slightly more complicated method of fabrication than a conventional aluminum or magnesium unit. A weight increase of 2.4 pounds would result if the drum were fabricated from magnesium. The beryllium drum skin is 0.025-inch thick and is made in four quadrants to simplify the forming tooling. The four circular quadrants can be joined by furnace brazing with silver or aluminum based braze alloy, or adhesive bonded with epoxy. Channel-shaped doublers are used inside the tube to back up the longitudinal joints, and a circular, ring doubler is used inside the tube at each end to provide additional material thickness for the countersunk, endcap-mounting holes.

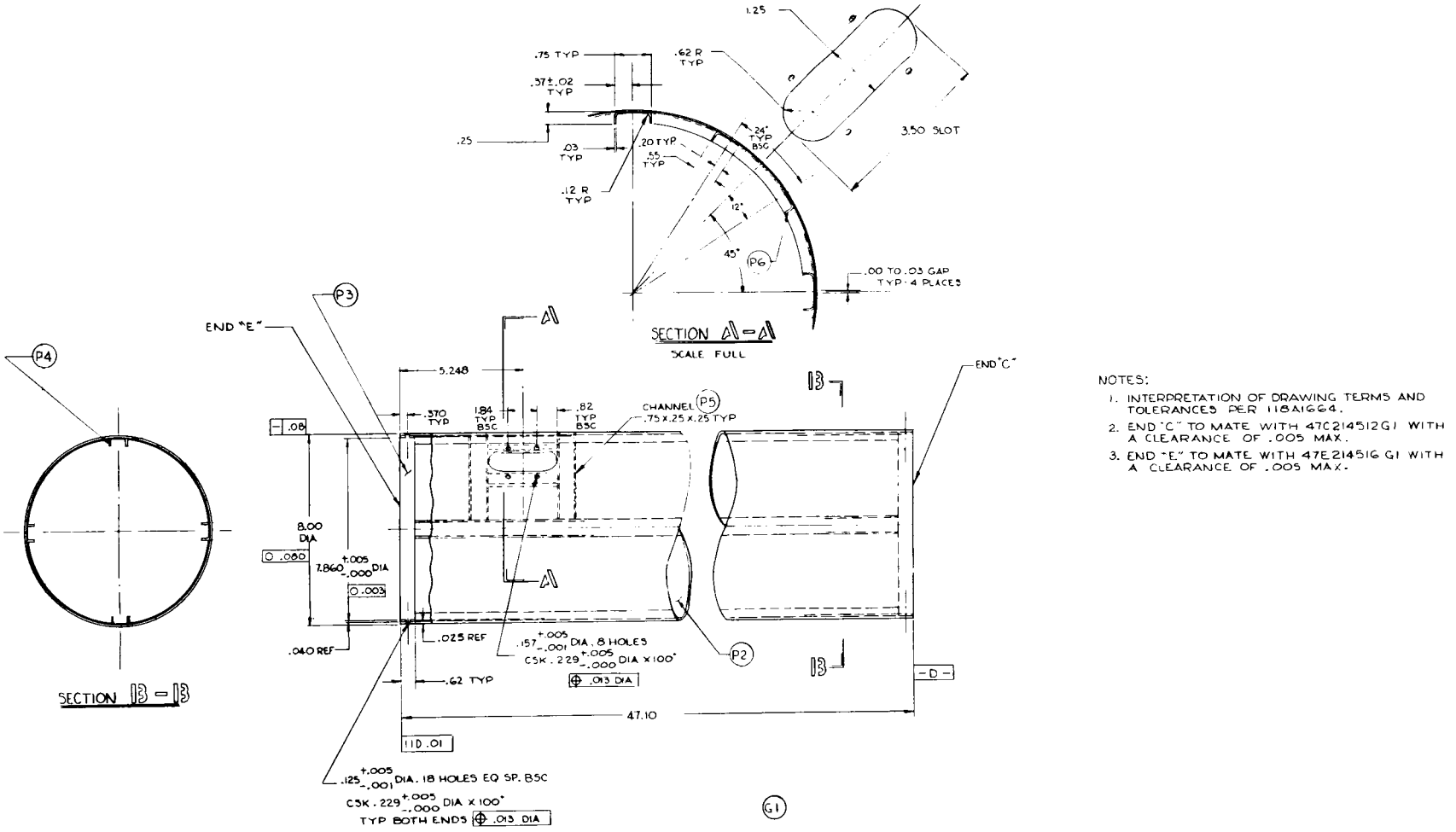

NOTES:

1. INTERPRETATION OF DRAWING TERMS AND TOLERANCES PER 118A1664.
2. END "C" TO MATE WITH 47C214512G1 WITH A CLEARANCE OF .005 MAX.
3. END "E" TO MATE WITH 47E214516 G1 WITH A CLEARANCE OF .005 MAX.

Figure 2-15. Storage Drum Shell

One hole is provided in the skin, near the inboard end to permit the electrical connections to be made between the solar array bus bars and the internal drum power takeoff. The hole is reinforced with channel and angle-shaped doublers.

Machining for fastener holes, etc., will be performed on the completed assembly and will be followed by a light etch to remove surface flaws.

The end caps may be furnace-brazed with hot-formed cross-rolled sheet or machined from a beryllium forging. Each unit consists essentially of a circular, flat sheet, with an outer flange for attachment to the drum, and a center boss for attachment to the support structure. Both caps also contain six equally spaced, radial stiffeners leading from the outer flange to the center boss to strengthen the assembly for bending load.

The inboard end cap has a large center boss, machined to serve as a housing for the two preload bearings. In addition, this end cap also has provision for mounting the output drum of the constant torque spring motor.

Both end caps have nut plates riveted to the inside surface of the circular outer flange. These mate with the countersunk holes in the ends of the drum and provide a means of attaching the drum to the end caps.

The preliminary design drawing of the outboard end cap and inboard end cap are shown as Figures 2-16 and 2-17, respectively.

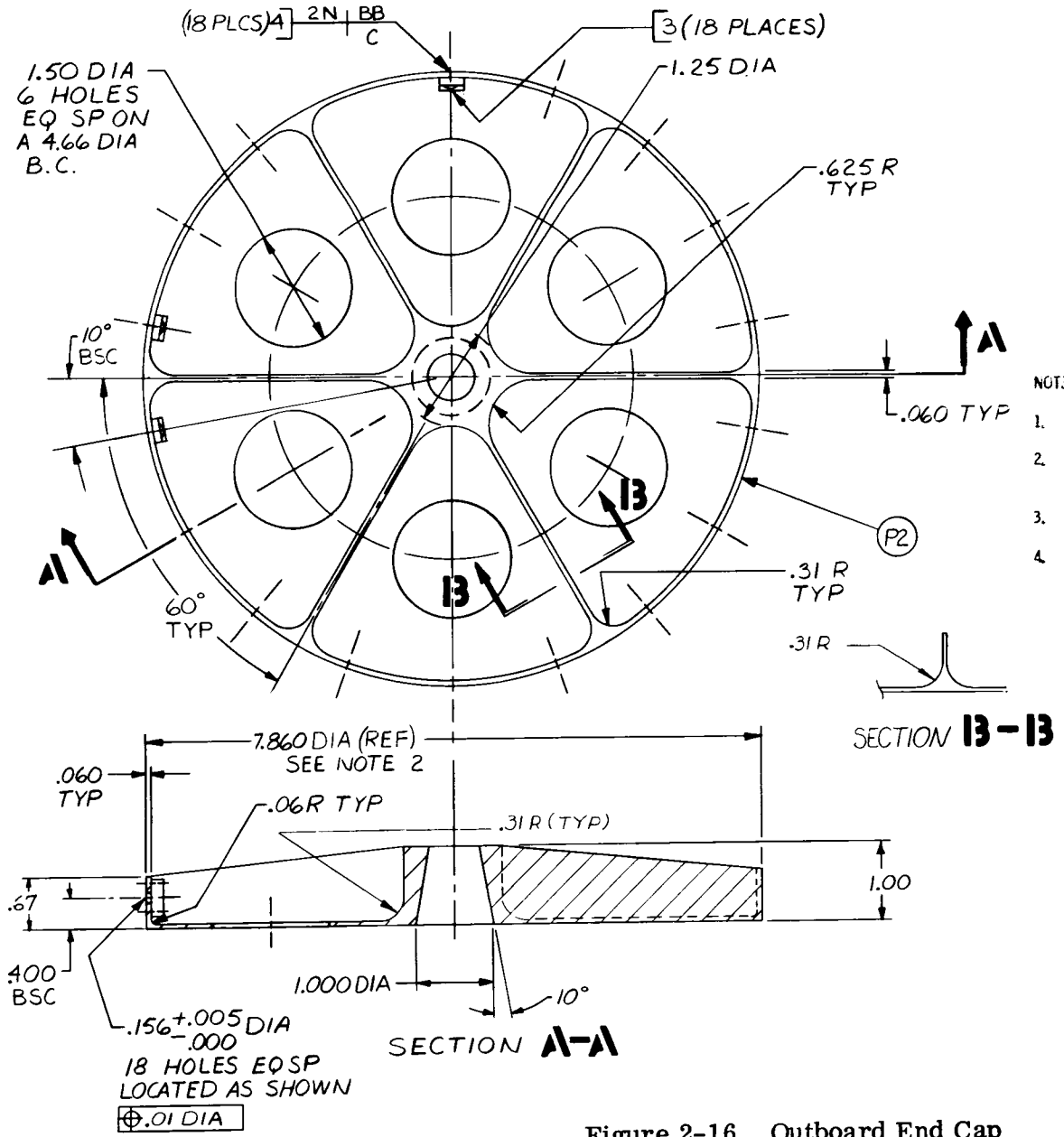

NOTES:

1. INTERPRETATION OF DWG. TERMS AND TOLERANCES PER 118A1664.
2. THIS DIAMETER TO MATE WITH END "C" OF 47D214514 WITH A CLEARANCE OF .005 MAX.
3. RIVET PER 171A4287.
4. MARK PART "GE47C214512 " G1 OR P1 AS APPLICABLE PER 118A1526 CL 17.

Figure 2-16. Outboard End Cap

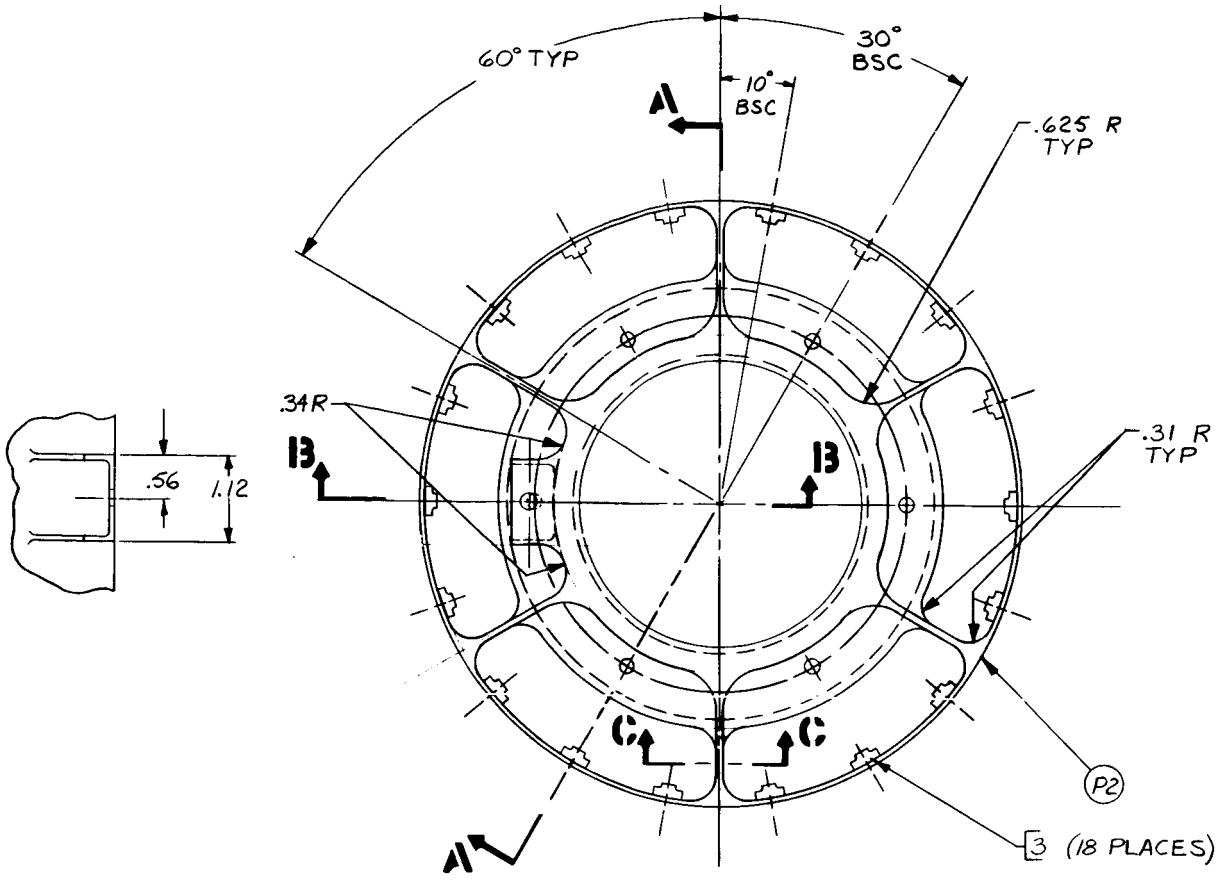

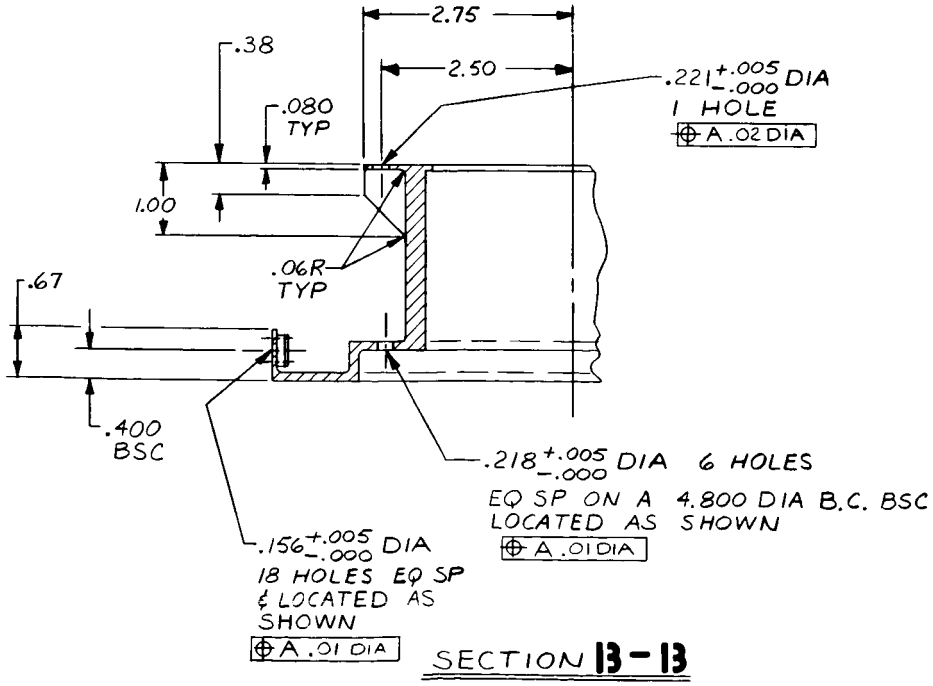

SECTION B-B

2.31

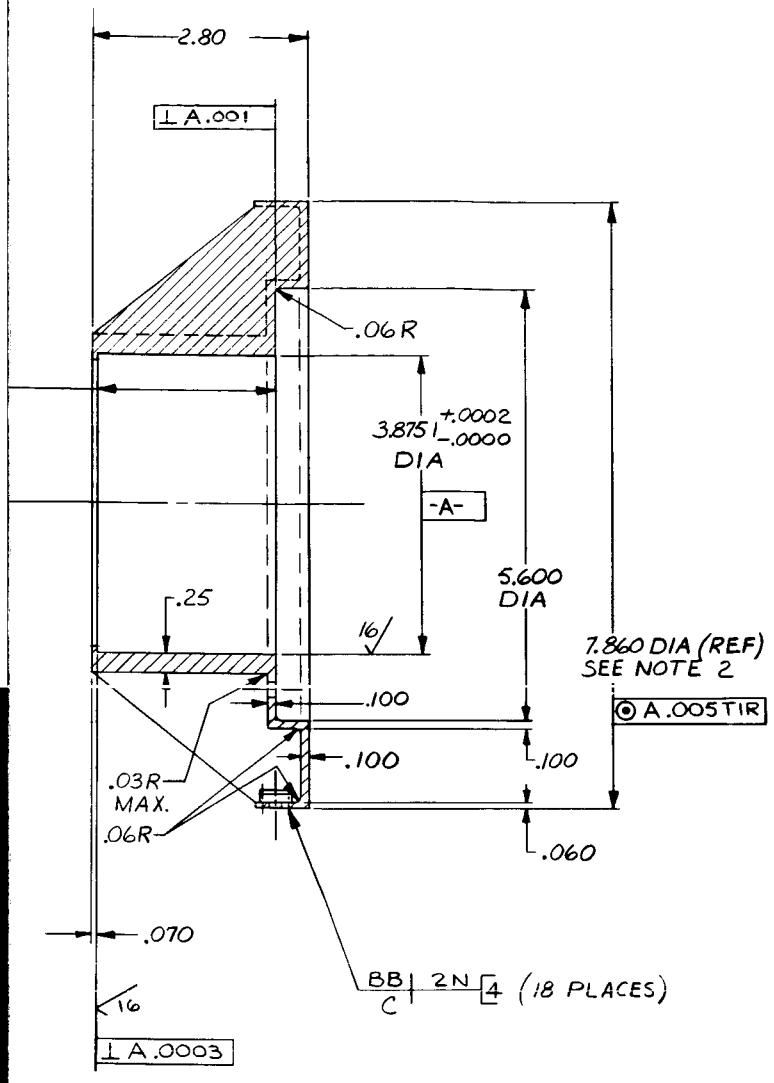

SECTION A-A

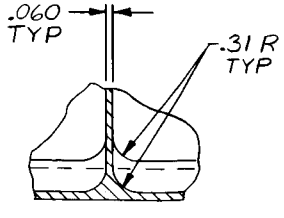

SECTION C-C

NOTES:

1. INTERPRETATION OF DWG TERM & TOLERANCES PER 118A1664.
2. THIS DIA TO MATE WITH END "E" OF 47D214514G1 WITH A CLEARANCE OF .005 MAX.
3. MARK PART GE47E214516_ G1 OR P1 AS APPLICABLE PER 118A1526 CL 17.
4. RIVET PER 171A4287.

Figure 2-17. Inboard End Cap

2.3.4 Leading Edge Member

THE LEADING EDGE MEMBER ACTS AS THE TRANSITION PIECE BETWEEN THE OUTER TIP OF THE DEPLOYABLE BOOM AND THE LEADING EDGE OF THE SOLAR ARRAY BLANKETS. IT WILL BE FABRICATED FROM CROSS-ROLLED BERYLLIUM SHEET.

The leading edge member (LEM) is directly attached to the array along its length, and is attached at its midpoint to the boom tip through a bearing which will permit the boom to rotate relative to the LEM.

In the stowed condition, the two movable outboard end supports also support the ends of the LEM through the use of tapered plugs which nest in the open ends of the LEM. When the end supports are released from the drum, theyalso release the ends of the LEM. The center of the LEM is supported by a yoke attached to the forward part of the boom actuator mechanism.

The LEM length is determined by the width of the solar array. The cross section is designed to provide the stiffness required to maintain the solar array preload.

The LEM is a thin-walled tube 100.0 inches long by 1.30 inches in diameter and is fabricated from 0.020-inch-thick cross-rolled sheet beryllium. The tube is fabricated from a flat sheet, rolled into a circular section and furnace-brazed or adhesive-bonded with a flat doubler reinforcing the longitudinal joint. A short section in the center (4.45 inches) is reinforced by the addition of a 0.020-inch thick sleeve and two 0.25-inch wide rings (see Figure 2-18). This is necessary because the boom is attached to the LEM at its center, and this region requires additional strengthening. The two rings mate with the support yoke on the boom housing and prevent lateral movement of the LEM in the stowed configuration.

In its final configuration, the two ends of the tube will be fitted with plugs containing tapered holes to receive the supporting tapered plugs of the movable end supports.

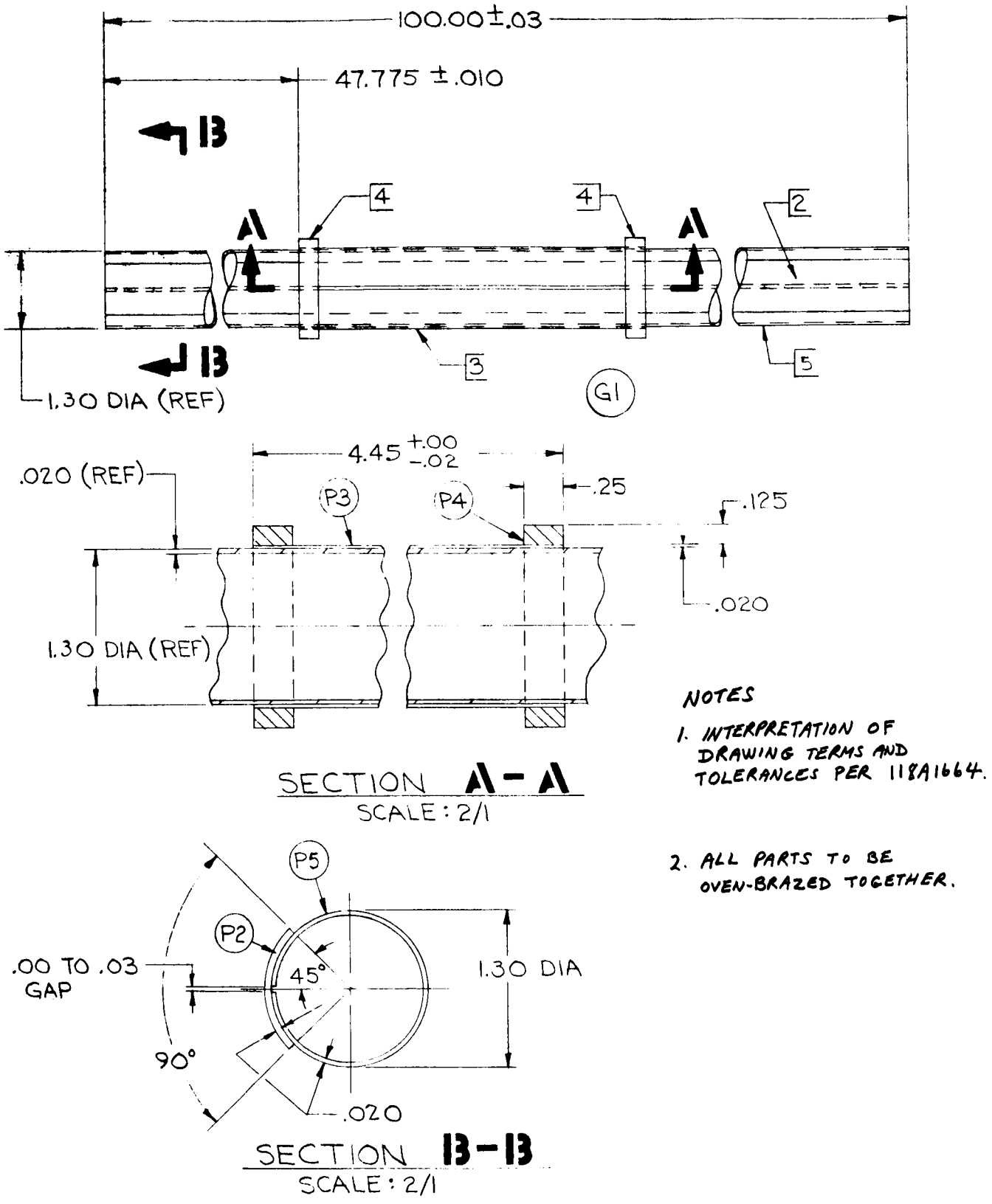

Figure 2-18. Leading Edge Member

2.3.5 Outboard End Support

THIS COMPONENT SUPPORTS THE OUTBOARD END OF THE STORAGE DRUM AND THE LEADING EDGE MEMBER DURING THE LAUNCH PHASE. IT WILL BE FABRICATED FROM ALUMINUM.

The outboard end support is a hinged arm, attached to the vehicle support structure to provide the following functions during ground handling activities and during launch and ascent: (1) support the outboard ends of the drum (2) support the outboard ends of the leading edge member, (3) prevent rotation of the drum about its longitudinal axis (see Figure 2-19). The fixed portion of the hinge is bolted directly to the vehicle mounting structure. The movable support is held in a fixed position relative to the drum and is prevented from rotating about its hinge during launch by a bolt and an electro-explosive separation nut. A tapered plug fixed in the movable support nests into a tapered hole in the drum end cap and provides the means of transferring the launch loads from the drum to the support.

When the separation nut is actuated, the hinged support arm rotates away from the drum and the leading edge member through the action of a torsion spring at the hinge point. A built-in stop limits the travel of the support, and the combined action of the spring and the stop will keep the support a fixed distance from the cantilevered drum. A bolt catcher will retain the released bolt, and there will be no debris or loose parts resulting from the release sequence. Once the support arm pivots out of the way, the drum is free to rotate about its own axis, and the leading edge member is free to move outward when the boom is deployed.

The end support has been designed to take all launch loads imposed on the outboard end of the drum except those loads which are along the longitudinal (or rotation) axis of the drum and the leading edge member. These loads will be in a direction which would tend to pivot the support about its hinge; consequently, the array has been designed to have the drum axial loads imposed only on the center support. The leading edge member longitudinal loads will be imposed upon the leading edge member center support attached to the boom actuator.

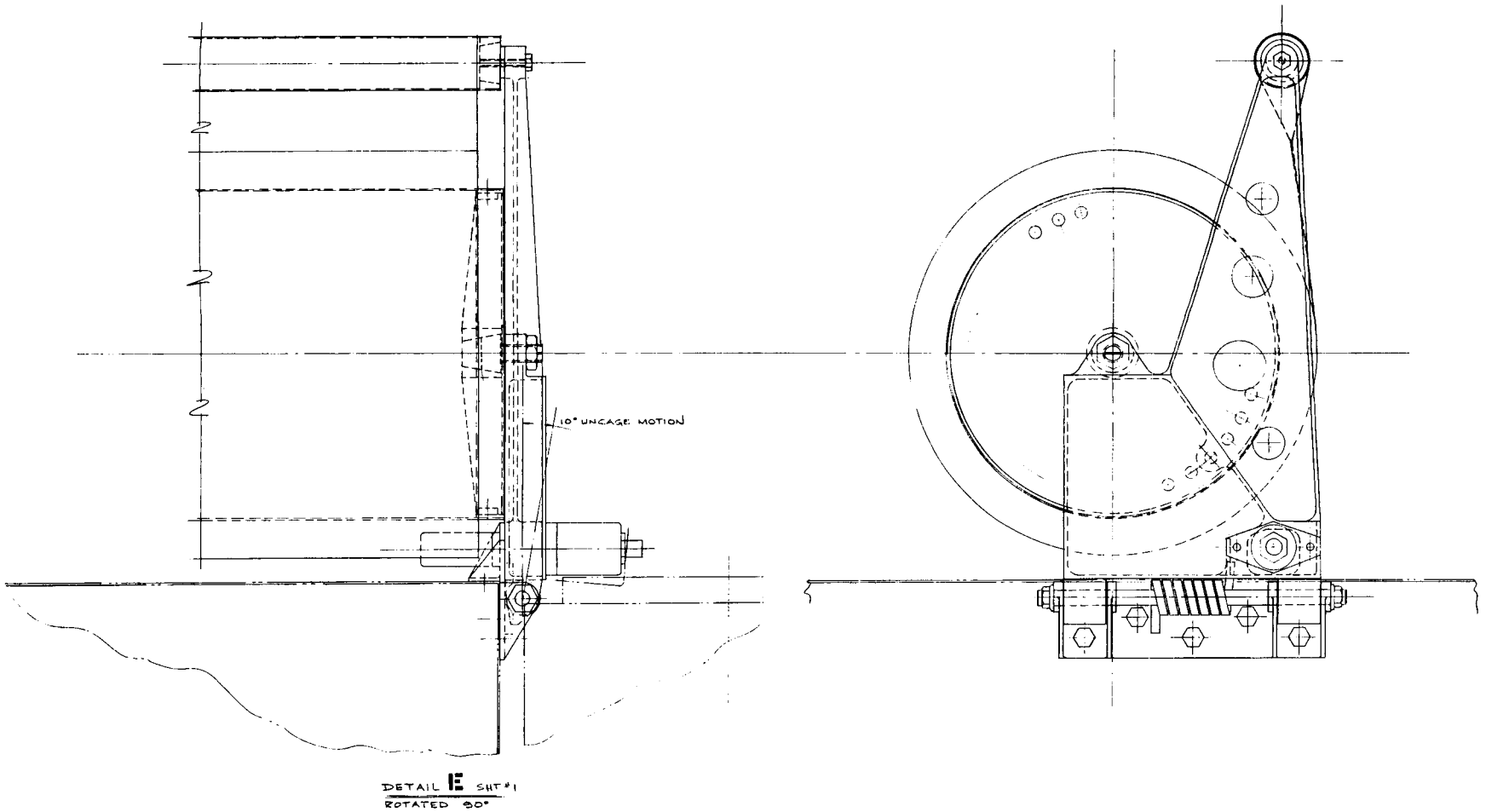

Figure 2-19. Outboard End Support

End Support Details

The basic end support structure is a two-piece hinged assembly. The fixed section is essentially a flat aluminum plate with four raised bosses machined to accept a hinge bolt and to nest into the mating hinge bosses of the movable support. The movable support is a hollow, welded aluminum, box construction, 1 inch thick, and tapering from 6 inches in depth at the hinge end to 5 inches at the drum support end. The support is approximately 6 inches long from the hinge point to the drum support point; however, a 7-inch extension continues beyond the drum support to pick up the support of the leading edge member. The box structure is reinforced at the hinge end, at the drum support point, and at the point of attachment to the separation nut, to provide for the higher local stresses expected in these areas.

The actual support of the outboard drum end is accomplished by a tapered pin in the support, nesting into a mating tapered hole in the outboard end cap of the drum. A 20-degree taper has been used in the design of the pin to ensure that it is self-releasing (industry standard for self-releasing tapers is 16 degrees). In addition, the pin will be coated with a film of teflon to further aid its disengagement from the drum. One end of the pin will be threaded to provide for axial adjustment in the drum.

The drum will be restrained from rotating in the stowed position by a tapered pin in the support which will mate with a series of holes in the drum end cap.

The outboard ends of the leading edge member contain tapered holes which mate with the tapered plugs on the ends of the movable support extensions.

The installation sequence of the outboard end support will be:

a. The fixed and the movable sections of the support are assembled with the use of a hinge pin and washer spacers. The spacers will limit the vertical play between the two parts to the minimum possible amount consistent with the free rotation of the hinge.

b. Attach the hinge spring.

c. Mount the fixed hinge section on the vehicle mounting structure. Do not tighten bolts.

d. Swing the movable support up to the drum and insert a bolt into the separation nut. The separation nut is mounted on a separate flange on the vehicle mounting structure. Do not tighten bolts.

e. Insert the end of the leading edge member into the taper pin on the movable support extension.

f. Move the support assembly within the clearance provided in the mounting holes until the taper pin in the support lines up with the taper hole in the drum. Tighten all bolts and attach bolt catcher.

g. Shims are provided between the fixed support section and the vehicle mounting surface to provide for the longitudinal alignment of the support and the drum.

h. Insert the taper plug into the drum by using the threaded adjustment on the pin. Lock the pin by using the locknut provided.

i. Rotate the drum in a direction to remove all slack in the solar blanket. Engage the pin in the support with the nearest mating hole in the drum end cap.

j. Make adjustments in the leading edge rod center support as required.

The deployment sequence will be:

a. Signal-to-firing circuit fires separation nut squibs. This disengages the separation nuts (one for each end support of a drum assembly) and ejects the bolts into the bolt catchers. The supports are now free to rotate.

b. The hinge springs act on the movable section of the supports and force the supports to rotate outboard away from the drums.

c. As the supports rotate outboard, the taper pins in the drum and in the leading edge member are removed from their mating holes. The taper ensures that the pins, which describe an arc as they leave their holes, will not bind in the holes.

d. The supports continue to rotate until they are restrained by their built-in stops. The hinge springs will continue to exert a force which will keep the supports fixed against the stops.

e. The end supports are now clear of the drum ends, and the drums are free to rotate about the center support bearings. The leading edge member is now supported only by its center yoke and is free to move when the boom is deployed.

2.3.6 Center Support

THE CENTER SUPPORT, A WELDED ALUMINUM STRUCTURE, IS THE ONLY ATTACHMENT OF THE ARRAY TO THE VEHICLE STRUCTURE IN THE DEPLOYED CONDITION.

The center support is a welded aluminum structure which serves as the primary means of attaching the drums to the vehicle mounting surface. The storage drum is made in two identical halves which are bolted to the right hand and left hand mounting faces of the support. The bottom of the support provides a mounting surface for the boom actuator mechanism which is located between the two drums. The support is attached to the vehicle structure with bolts through holes provided in the support rear mounting surface (See Figure 2-20).

The support structure has been designed to take all the launch loads imposed on the inboard ends of the two drums. Loads on the outboard ends of the drums will be taken by the outboard end supports. In addition, the center support will take all the loads which act along the longitudinal (or rotation) axes of the drums. In orbit, when the outboard end supports have been removed from the drum ends, the drums will be supported as cantilevers from the center support only.

Center Support Details

The support is a welded aluminum structure consisting of a backplate, two flanged vertical side plates, a front horizontal tube, and a central horizontal plate. The complete assembly is 6 inches high by 5 inches wide at the back mounting surface. The top surface of the side plates taper from 6 inches at the back to 5.30 inches at the front. The unit is 5.50 inches long from the back mounting surface to the center of the 2.50-inch-diameter tube.

Four mounting holes are provided on the backplate for mounting to the vehicle. Four holes are provided for mounting the boom actuator. Eight holes in a circular pattern are provided in flanges on each side of the horizontal tube for mounting the two drums.

The support has been designed so that the drum mounting flanges are bolted to the tube mounting flanges, thus forming a continuous structure from one drum to the other. The support structure essentially supports this center tube which, in turn, supports the drums.

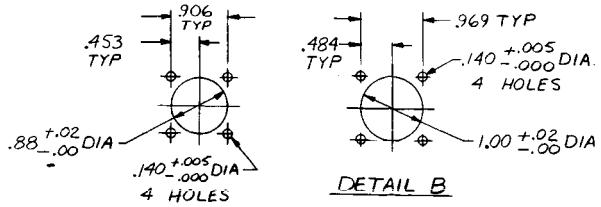

DETAIL A

DETAIL B

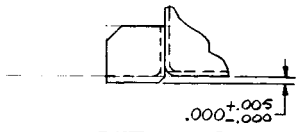

DETAIL C

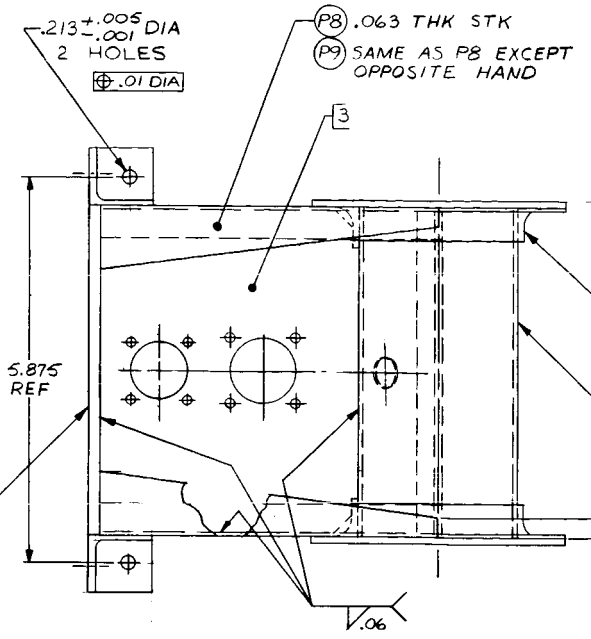

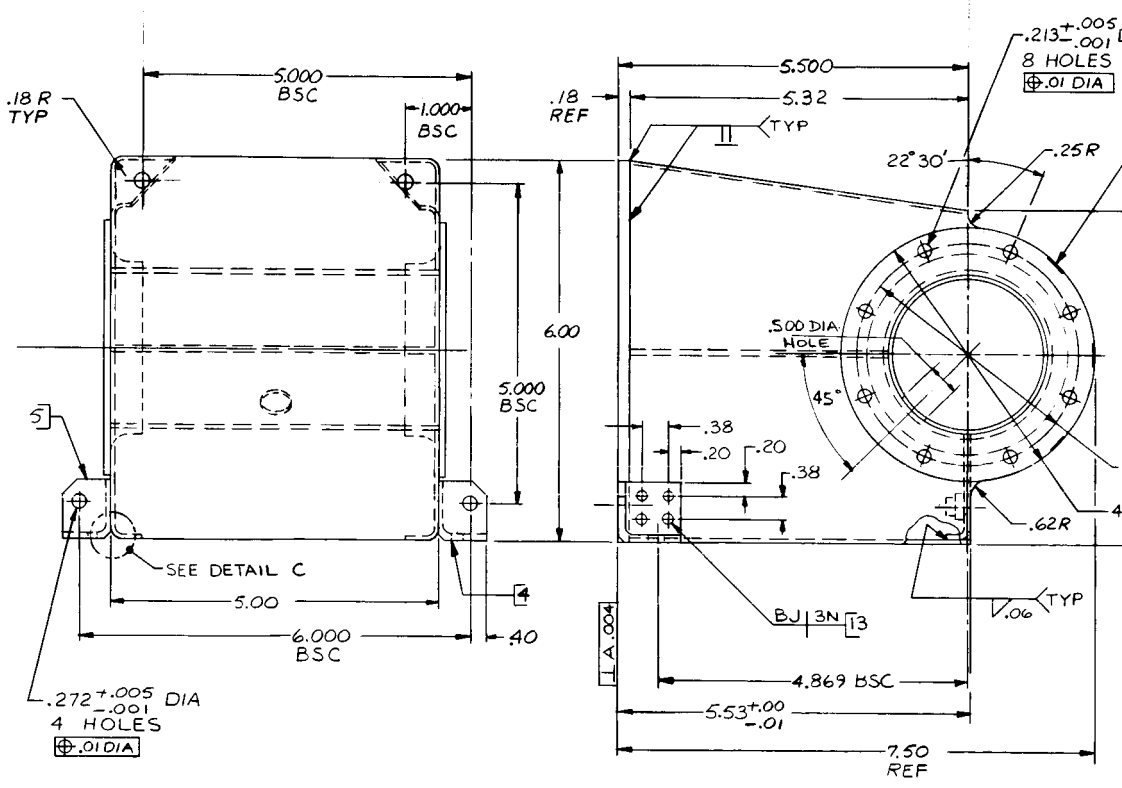

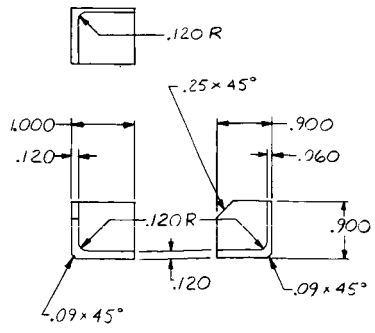

P4
P5 SAME AS P4 SHOWN EXCEPT OPPOSITE HAND

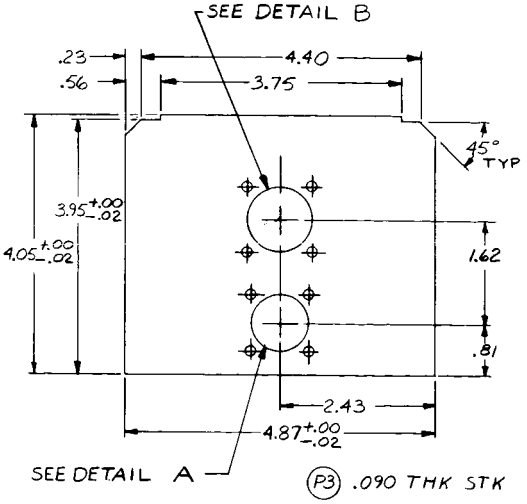

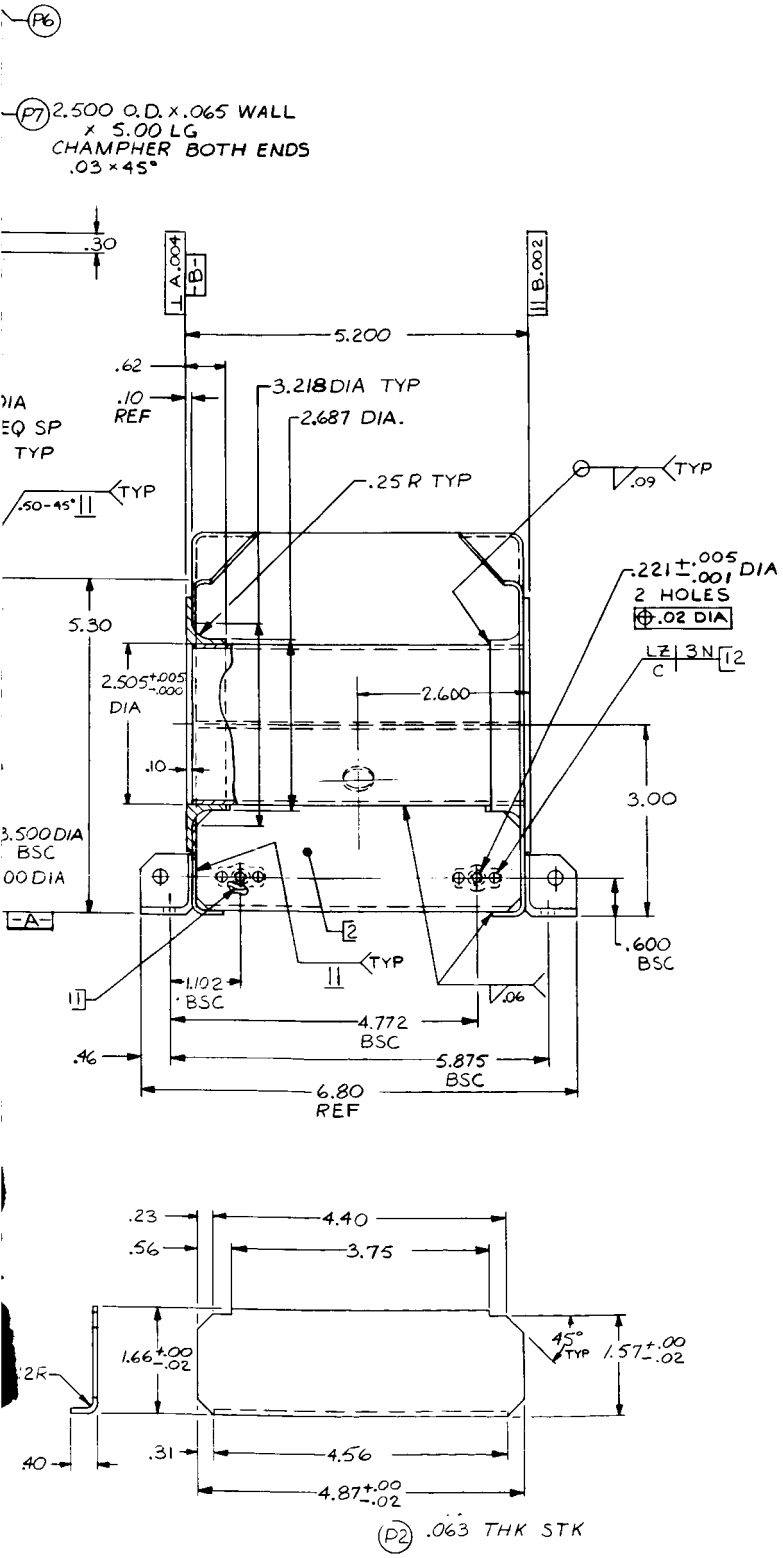

NOTES:

1. INTERPRETATION OF DWG TERMS & TOLERANCES PER 118A1664.
2. INTERPRETATION OF WELD SYMBOLS PER AWS A2.0.
3. RIVET PER 171A4287.
4. ALL BEND RADII TO BE .12 ± .02.
5. FINISH PER 118A1600P133.
6. MARK PART "GE47E214875 " G OR P NUMBER AS APPLICABLE PER 118A1526 CLASS 21.

Figure 2-20. Center Support

The power leads from the solar array pass through the drums and terminate on two connectors located on the central horizontal plate of the support.

2.4 BEARING AND LUBRICATION CONSIDERATIONS

THE SELECTED BEARING FOR THE STORAGE DRUM IS A THIN SECTION, ANGULAR CONTACT, INSTRUMENT BEARING, SIMILAR TO THE TAR SERIES MANUFACTURED BY THE SPLIT BALLBEARING DIVISION OF MPB. THE LUBRICANT SYSTEM RECOMMENDED FOR CONSIDERATION ON THIS PROGRAM IS LUBECO 905, DRY FILM LUBRICANT.

The selected bearing was chosen because of its high load capacity and light weight and because of the successful past use of similar bearings in the Nimbus II satellite solar array drive mechanism. This unit continues to operate perfectly in space after 20 months of flight.

Because the rotating drum, in its operating configuration, will be supported on one end and free on the other end, two preloaded bearings will be used per drum.

Bearing races and balls will be made from 440C stainless steel. It is anticipated that the array may be in its extended position for weeks (or months) at a time, during which time there will be small amplitude oscillations of the bearings. When the array is retracted, the retracting force will be 4 pounds from the spring motor. Thus, it is important to have bearings with the following characteristics:

a. Capability of withstanding the static (nonrotating) radial and thrust loads of launch

b. Retention of lubricating properties in space environment

c. Low starting torque after prolonged idle periods in space

Item a will be accomplished by the selection of the right size bearings for the anticipated loads. Items b and c are related to the lubrication and design of the retaining ring.

Discussion

The present design requirement is for operation at -150°F. The bearing is exposed to the high vacuum of the space environment. This eliminates the possibility of using oil or grease lubricants. There are few oils which will perform satisfactorily at this low temperature and

those that will are too volatile for use in vacuum. This limits the choice to dry lubricants. These are usually categorized into one of two groups:

a. Transfer films: The bearing retainer is made from or coated with a plastic which transfers to the balls and then to the raceways. This provides a readily sheared film between the balls and the races which is then the lubricant. Reinforced Teflon is the most commonly used material.

b. Dry films: This system consists of a solid material which has one readily cleaved plane along which sliding can take place. Molybdenum disulfide is most commonly used. This material is attached to the surface to be lubricated usually with a binder such as sodium silicate or epoxy although systems employing electroplating and in-situ formation of the lubricating material are also being employed.

Materials Recommendation

Two materials have been evaluated in laboratory testing and on flight hardware, and should be considered as possible lubrication systems for the roll-up solar array.

Lubeco 905

This material is a molybdenum disulfide dry film applied by a proprietary electrophoretic process. It is from Lubeco, Incorporated, Compton, California. It has been tested under simulated space conditions by Hughes Aircraft and is rated by them as one of the best dry films. It is the dry film lubricant used on the Surveyor and Lunar Orbiter spacecraft. It has also been tested in the Voyager program discussed below.

The normal thickness of the material is 0.0003 inch, so that allowance should be made for this in specifying bearing internal clearances.

It should be applied to the inner and outer races and to the retainer, but not to the balls. A fully machined bronze retainer should be used.

The bearings should be procured in the unassembled condition and the coating applied. The coated parts should be inspected with a low power microscope up to 40X magnification. After assembly by the manufacturer the bearings should be again inspected.

After assembly, the bearings should be run in to burnish the coating. This should be done first by hand and any debris blown out with clean, dry gas, i.e., not shop air but gas from a dry cylinder or dry system. A millipore or other suitable filter should be employed. This should be done in the controlled environment of a clean room of class 100,000 or better per Federal Standard 209.

After running in by hand, the bearings should be run at 100 rpm for 1 hour and again blown out. This should be repeated if necessary until no dusting occurs.

Reinforced Teflon

Teflon which is reinforced with glass fibers has been tested for use on ball bearings. It is available in two forms. One contains molybdenum disulfide and is sold under the tradenames "Bar Temp" by Barden, Incorporated, a bearing manufacturer, and "Duroid" by Rodgers Corporation, a plastics processor.

In tests at Lockheed Missiles and Space Company, R-3 size bearings (3/16-inch bore, 1/2-inch O.D.) employing Rulon C retainers operated for over 10,000 hours in vacuum at 8000 rpm (References 2-6 and 2-7). Thrust loads were 1/4 to 1 pound per bearing; radial loads were 135 grams per bearing. Pressures were 10^{-7} to 10^{-8} torr. The data is summarized in Table 2-8.

Bearings employing Duroid 5813 retainers and no other lubricant have been successfully tested in vacuum at NASA Goddard (Reference 2-8). Radial loads were from 0.8 ounces to 7.5 pounds; bearing sizes were from R-2 to R-9. In tests at Lockheed under the same conditions as for Rulon C above, Duroid 5813 gave a lifetime of over 5000 hours in one test, but increasing the thrust load reduced the lifetime to less than 100 hours. This data is also included in Table 2-9. Duroid 5813 has also been used in tape recorders installed on spacecraft (Reference 2-9).

Rulon A and Duroid 5813 are both being tested in the Voyager test program described on page 2-72. They have been among the best materials tested.

Table 2-8. Bearings with Self-Lubricating Retainers

Bearing Type	Instrument size ball bearings
Race and Ball Material	440C Stainless steel
Retainer Material	Rulon C
Notes	For low-speed applications, bearing should first be run in at 500 to 1000 RPM at light load (approximately 1/4 lb) for 1 hour to assure transfer of film from retainer. Bearing must be supplied without oil lubrication.

	Load per bearing					
Speed	Radial	Thrust	Temp (^{o}F)	Pressure (torr)	Lifetime	Comments
8000 RPM	137 grams	1/4 lb	125 to 210	4×10^{-7} to 2×10^{-8}	12,600 hr	Reference 2-6. Angular contact bearings R-3 size, two bearings tested. Test discontinued, bearings still operating.
8000 RPM 53 minutes in one direction 7 minutes power off, 53 minutes in opposite direction; repeat.	137 grams	1/4 lb	125 to 180	5×10^{-7} to 6×10^{-8}	8600 hr	Reference 2-7. Angular contact bearing, R-3 size, two bearings tested.
8000 RPM	137 grams	1 lb	145 to 170	4×10^{-6} to 6×10^{-8}	3100 hr	Reference 2-7. Angular contact R-3 bearing, short life is attributed to no thrust load for first 500 hr of testing, two bearings tested.
8000 RPM	136 grams	1/4 lb	90 to 140	760	30,000 hr	Reference 2-7. Still running at end of test, angular contact bearing, R-3 size, two bearings tested.
8000 RPM	136 grams	1/2 lb	130 to 145	1×10^{-7} to 3×10^{-8}	10,770 hr	Reference 2-7. Angular contact bearing R-3 size, two bearings tested.
8000 RPM	138 grams	1 lb	125 to 140	1×10^{-7} to 3×10^{-8}	10,700 hr	Reference 2-7. Test still running when discontinued. Angular contact bearing R-3 size, two bearings tested.
						Material also used in the following flight applications (Reference 2-9) Pegasus 1 & 2 Output shaft bearings

Table 2-9. Bearings with Self-Lubricating Retainers

Bearing Type	Instrument size ball bearings
Race and Ball Material	440C stainless steel
Retainer material	Duroid 5813, 60% Teflon - 40% glass fibers with molybdenum disulfide, from Rodgers Corporation; Bar Temp from Barden Corporation is the same material
Notes	When used at low speed bearings should be first run in at 500-1000 RPM at light load (approximately 1/4 lb) for 1 hour to assure transfer of film from retainer. Purchase without oil lubricant.

	Load per bearing					
Speed	Radial	Thrust	Temp (^{o}F)	Pressure (torr)	Lifetime	Comments
1800 RPM	2.1 oz	Light, not reported	Not reported	5×10^{-8}	1700 hr +	Reference 2-8. Test still running when discontinued; R-2 size-bearing. Two bearings per test.
1800 RPM	10.7 oz	Light, not reported	Not reported	5×10^{-8}	2500 hr +	Reference 2-8. Bearing still running when discontinued; R-3 size bearing. Two bearings per test.
100 RPM	4.5 lb	Light, not reported	Not reported	5×10^{-8}	8200 hr +	Reference 2-8. Test still running; R-4 size bearing. Two bearings per test.
10 RPM	1.5 lb	Light, not reported	Not reported	5×10^{-7}	10,515 hr	Reference 2-8. R-4 size bearing. Two bearings per test.
100 RPM	1.5 lb	Light, not reported	Not reported	5×10^{-8}	8200 hrs +	Reference 2-8. Test still running; B542 tube type bearing. Two bearings per test.
8000 RPM	0.8 oz	Light, not reported	Not reported	5×10^{-7}	4380 hr	Reference 2-8. R-4 size bearing. Two bearings per test.
1 RPM	1.3 lb	1 1/4 lb	Not reported	9×10^{-9}	5800 hr +	Reference 2-8. Test still running. R-6 size bearing. Two bearings per test.
Oscillating 0 - 50^{o} in. 30 sec	7.5 lb	Not reported	Not reported	9×10^{-9}	5800 hr +	Reference 2-8. Test still running; R-9 size bearing. Two bearings per test.
Oscillating 0 - 50^{o} in. 30 sec	1.5 lb	1 1/4 lb	Not reported	9×10^{-9}	5800 hr +	Reference 2-8. Test still running. R-6 size bearing. Two bearings per test.
8000 RPM	137 grams	1 lb	Not reported	10^{-7} 10^{-8} to	28 hr	Reference 2-6. R-3 angular contact bearings; two bearings tested.
8000 RPM	137 grams	1/2 lb	Not reported	10^{-7} 10^{-8} to	62 hr	Reference 2-6. R-3 angular contact bearings; two bearings tested.
8000 RPM	137	1/4 lb	Not reported	10^{-7} 10^{-8} to	5100 hr	Reference 2-6. R-3 angular contact bearings; two bearings tested.
8000 RPM	137	1/4 lb	Not reported	10^{-7} 10^{-8} to	67 hr	Reference 2-6. R-3 angular contact bearings; two bearings tested.
8000 RPM 53 minutes in one direction, 7 minutes power off, 53 minutes in opposite direction, and repeat	137	1/4 lb	Not reported	10^{-7} to 10^{-8}	90 hr	Reference 2-6. R-3 angular contact bearings; two bearings tested.
8000 RPM	137	1/4 lb	Not reported	760	18,800	Reference 2-6. R-3 angular contact bearings; two bearings tested. Reference 2-9. Material also used in the following flight applicative Nimbus Tape recorder bearings.

Although the above bearings were with solid retainers of reinforced Teflon, there should be no problem in using inserts of this material in metal retainers. For the size bearing involved in this application this type is more desirable, since a retainer solely of Teflon this large is difficult to machine and hence is not commonly available and also would be too flexible.

Since these bearings depend on a transfer film, they need to be run in to establish such a film. The tentatively recommended run-in is at 100 rpm with a 2-pound radial load and a 1-pound thrust load for 1 hour, followed by 1 hour at 100 rpm with a 4-pound radial load and a 2-pound thrust load. This is subject to revision based on final decision on determination of preload.

Appropriate GE Experience

As part of the Voyager work, a program testing instrument-size bearings in vacuum is being conducted. The test fixture consists of six shafts mounted on a single rack. Each shaft is driven by its own motor. On the shaft are two pairs of test bearings. One pair supports a 1-1/2 pound weight; the other pair, a 3 pound weight. These provide radial loads which are evenly distributed between the two bearings a pair. Calibrated springs provide a thrust load of 1 pound to the more heavily loaded pair of bearings and 3/4 pound to the more lightly loaded. The shaft is supported on the rack by two bearings. A photograph of this equipment is shown in Figure 2-21.

The bearings are all R-4 size, 1/4-inch bore, 5/8-inch O. D. On each shaft, the same lubricant was used for the four test bearings, and, in so far as possible, for the support. (Due to the insufficient numbers of acceptable test bearings, bearings with Bar Temp/ Duroid 5813 were used for support bearings in some cases.)

A strain gauge system is used for determining torques of each pair of test bearings. Thermocouples in the support bearing housings measure the temperature there.

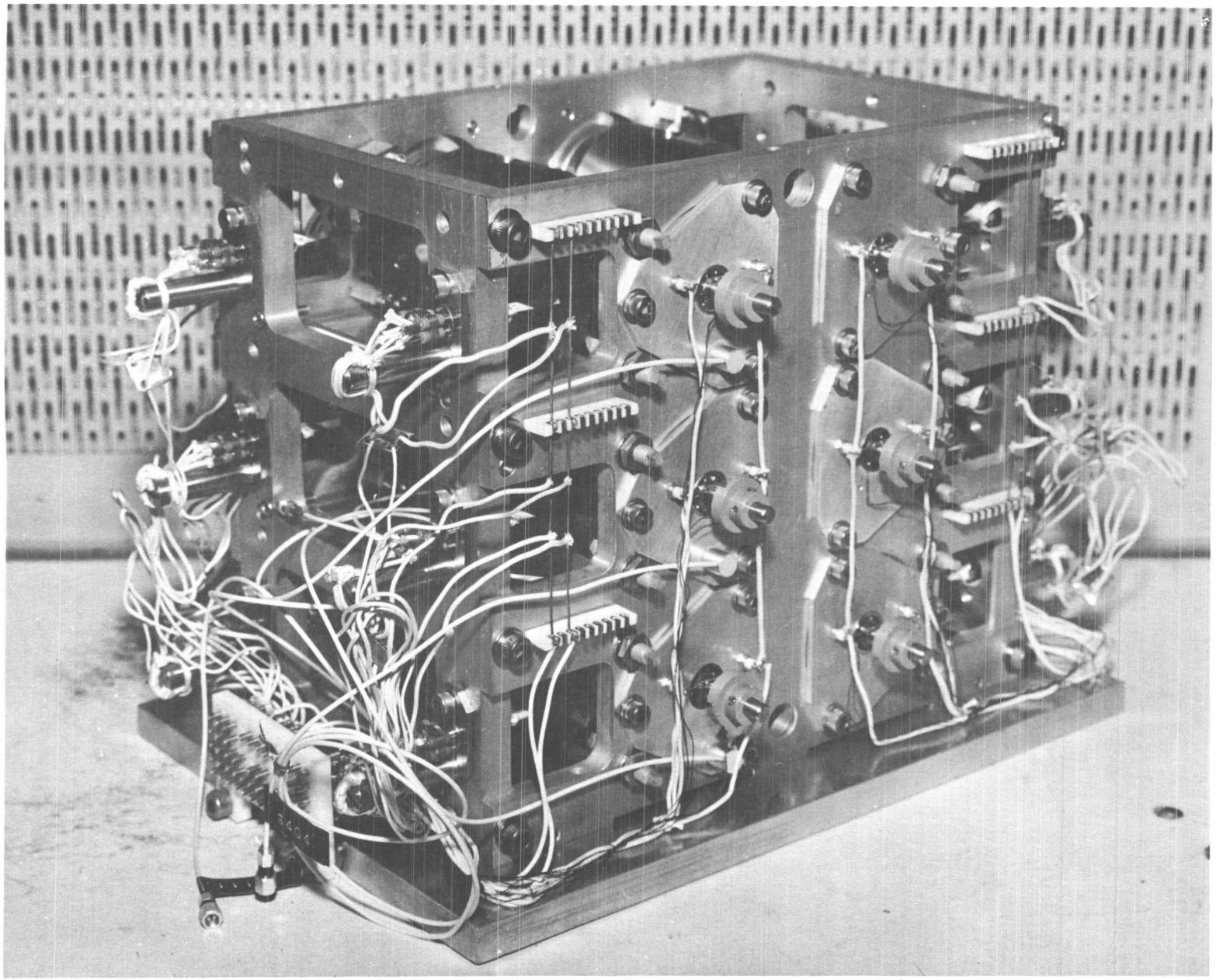

Figure 2-21. Bearing Test Fixture

Two of the above fixtures were fabricated. Each was installed in a separate, new vacuum system.

Test pressures have been 10^{-9} to 10^{-10} torr predominantly with some periods at 10^{-8}.

Test speed has been 480 rpm.

The work has been divided into the following phases:

Phase A 48 hours in vacuum run with reversal every 2 hours.

Phase B The following repeated ten times on each shaft:

a. 4 minutes clockwise operation

b. 2 minutes dwell

c. 4 minutes counterclockwise

d. 2 minutes dwell

e. Repeat

Phase C

a. Dwell 72 hours

b. Operate motors individually until change of torque is less than 10% of average torque

c. Repeat for a total of three times

d. Perform a through c with 48 hour dwells, ?4 hour dwells, 6-hour dwells, and 1-hour dwells

Phase D Operate continuously for 100 hours each week with a reversal after 50 hours. Leave idle on the weekends.

In addition to the above, a brief operation in air was also conducted to verify instrumentation and motor operation.

Of particular interest to this application is the long idle periods. In addition to the ones programmed, the tests were stopped at the end of the year for 288 hours. There were no anomalies in restarting.

Tests in the first fixture are still being run after 86×10^6 revolutions and in the second fixture after 46×10^6 revolutions.

2.5 DEPLOYABLE BOOM STUDIES

This section describes three tests which were performed in an effort to obtain basic engineering information on the Hunter STACER rod and SPAR Aerospace BI-STEM. This information was needed to support the tradeoff studies and analysis which considered the various types of deployable boom systems. These tests included:

a. Hunter STACER Thermal Bending Test

b. Hunter STACER Stiffness Test

c. BI-STEM Static Load Test

2.5.1 Hunter STACER Thermal Bending Test

THE TERMAL BENDING CHARACTERISTICS OF A HUNTER STACER ARE SIMILAR TO A SOLID STAINLESS STEEL TUBE WITH EQUIVALENT DIMENSIONS.

A thermal bending test (in air) was conducted by Hunter Spring Corporation to investigate the hypothesis that the thermally induced deflection of a STACER rod would be less than the corresponding deflections of an equivalent solid 304 stainless steel tube. Thermal bending of the deployed boom is an important design consideration. Figure 2-22 is a sketch of the test setup showing thermocouple location, heating and cooling system positions, and the position of deflection measurements. The test data are summarized in Table 2-10. These data show the thermal bending characteristics of the two types of tubes are similar.

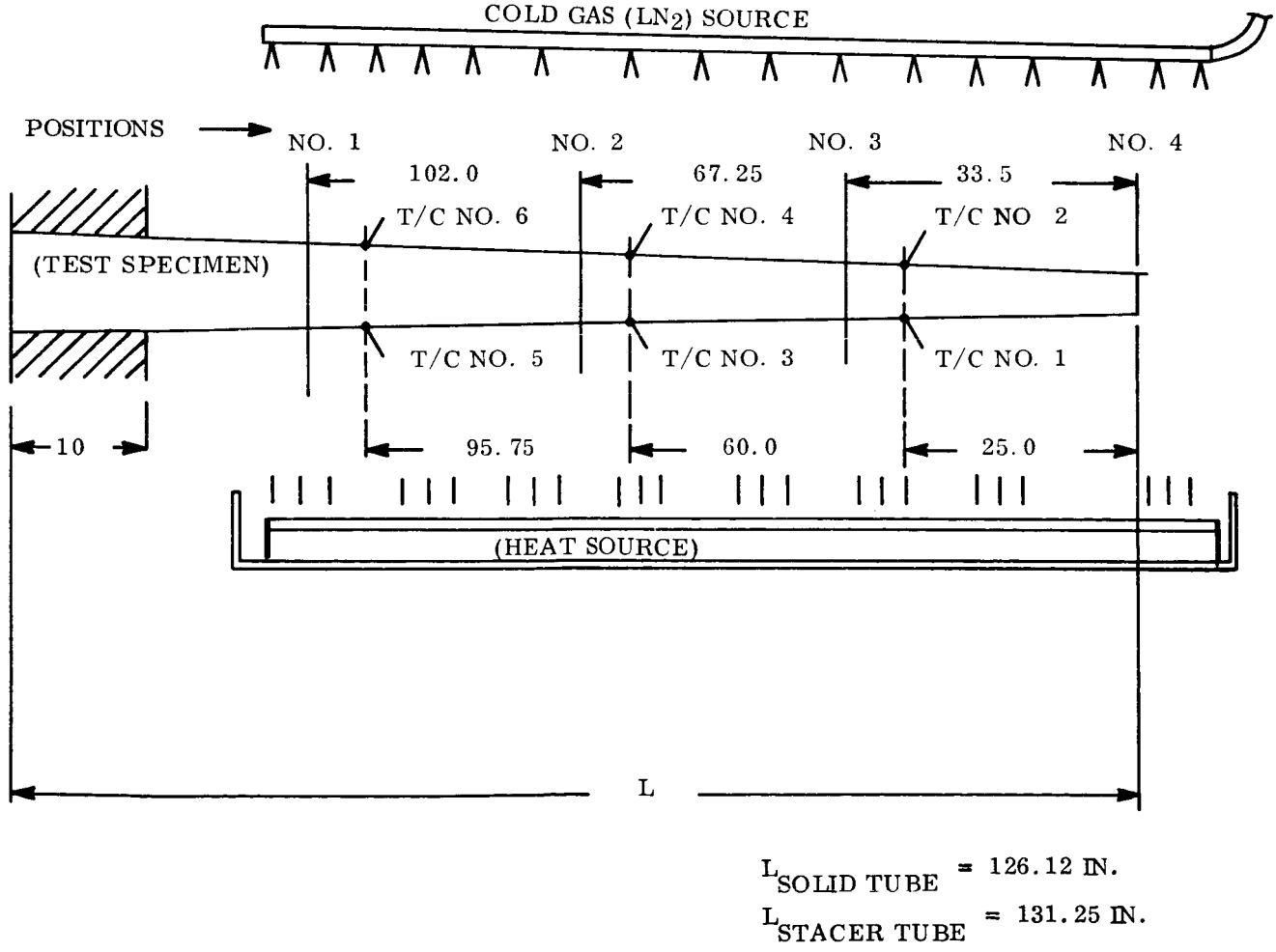

Figure 2-22. Hunter STACER Thermal Bending Test Setup

Table 2-10. Summary of Test Results

Run	Thermocouple (All temperatures in °F) 1	2	3	4	5	6	Deflection Measurement Positions 1	2	3	4	Test Specimen
1	142	68	169	81	179	77	0.0	0.69	1.70	3.75	Solid 304 S/S Tube
2	170	92	169	92	164	97	0.0	0.53	1.50	2.94	1.12 in. Root Dia x 0.020 in. thick
3	152	37	152	51	146	29	0.02	0.75	2.04	4.19	x 0.63 in. Tip Dia x 126.12 in.
4	147	27	140	35	147	36	0.02	0.88	2.33	4.63	Wt = 2.35 lb
1	200	98	184	85	191	89	0.12	0.75	1.80	3.56	Hunter STACER 301 S/S
2	196	98	185	86	191	86	0.12	0.75	1.80	3.56	Tube 0.006 x 6.0
3	206	100	196	88	204	102	0.12	0.69	1.60	3.19	Strip, 1.12 in. Root Dia.
4	206	102	206	91	207	94	0.12	0.69	1.70	3.34	0.50 in. Tip Dia x 131.25 in.
											Wt = 2.05 lb

2.5.2 Hunter STACER Stiffness Test

THE STIFFNESS (EI) OF A HUNTER STACER ROD HAS BEEN EXPERIMENTALLY DETERMINED.

The Hunter STACER rod, a spirally wound tapered unit, is not easily analyzed as a structural element; essentially there is no design data available due to the early development stage of this concept. Therefore, a relatively simple stiffness test was performed on a stainless steel sample to satisfy the need for stiffness characteristics for use in analysis. The test sample was typical of the rods being considered for the roll-up solar array application and was subjected to both a pure end moment and a transverse load. The results obtained, though limited in scope and precision, provide data for comparing the stiffness of the STACER rod with other types rods.

The data shown in Table 2-11 were obtained by a load test on the rod specimen when supported on floats in a water tank. These data consist of deflections measured at points along the rod length for eight loading conditions: five force couples and three lateral forces applied at the member tip. A sketch of the test specimen showing the stations where deflection measurements were made is shown in Figure 2-23. Photographs of the test setup and the method of loading the rod tip are shown as Figures 2-24 and 2-25, respectively.

2.5.2.1 Analysis

It was postulated that deflection of the STACER rod acting as a beam would follow the classical beam equation

$$\frac{d^2y}{dx^2} = \frac{-M}{EI}$$

where M is the bending moment and EI is the member stiffness. The purpose of the experiment was to determine the member stiffness of the test specimen and it should be understood that the member stiffness is not necessarily the product of the modulus of elasticity (E) and the moment of inertial of the cross section (I). Given the equation of the elastic curve under the load, the second derivative can be calculated and the local member stiffness calculated.

Table 2-11. Measured Rod Deflection - Hunter STACER Stiffness Test (Reference Figure 2-23)

No.*	Loading	F (lb)	M (in.-lb)	Deflection												
				1	2	3	4	5	6	7	8	9	10	11	12	TIP
1	Force couple		50.06	0	0.25	0.50	1.00	1.75	2.50	3.50	4.75	6.25	7.75	9.75	12.75	13.00
2	Force couple		75.09	0	0.50	1.25	1.75	2.50	3.75	5.25	7.00	9.25	11.50	13.75	18.00	19.00
3	Force couple		83.44	0	0.50	1.25	2.00	3.25	4.50	6.50	8.25	10.50	13.50	16.50	20.50	21.50
4	Force couple		61.19	0	0.50	1.25	2.00	3.00	4.25	5.75	7.50	9.25	12.00	14.75	18.25	19.00
5	Force couple		36.16	0	0.50	1.00	1.50	2.00	3.00	4.00	5.50	6.50	8.50	10.50	13.25	13.50
6	Lateral force	0.0975	--	0	0	0.50	0.75	1.00	1.50	2.00	2.50	3.25	4.00	4.75	5.50	--
7	Lateral force	0.2075	--	0	0.75	1.00	1.50	2.25	3.00	4.00	5.00	6.50	7.75	9.25	10.75	--
8	Lateral force	0.3780	--	0	0.75	2.00	2.50	4.00	5.50	7.50	9.00	11.50	14.75	16.50	19.50	--

*Tests are listed in the order they were run. Tests 4 and 5 were unloading.

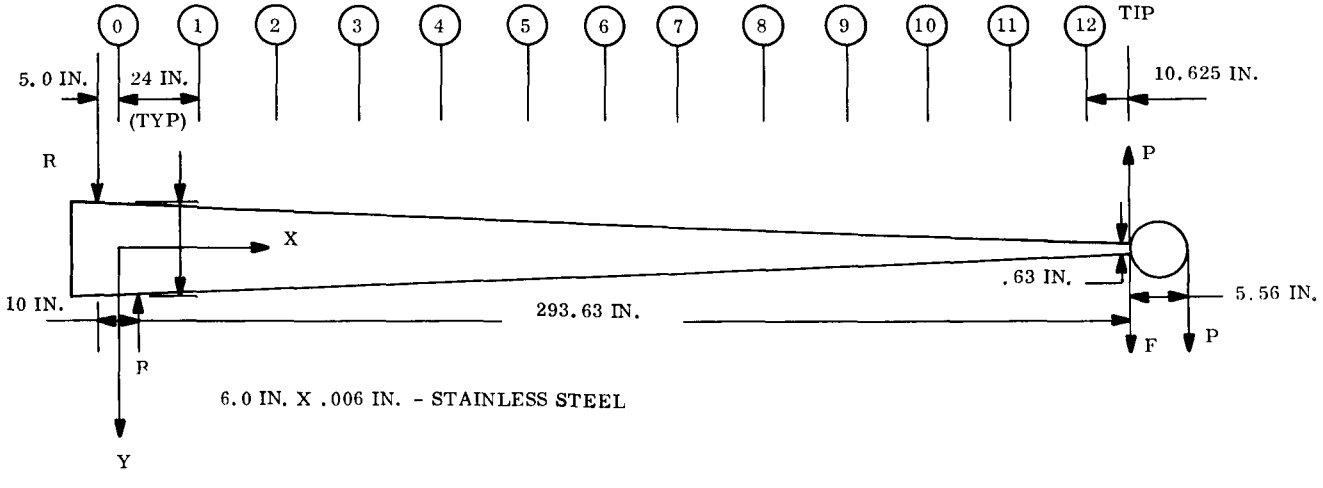

Figure 2-23. Hunter STACER Stiffness Test Specimen

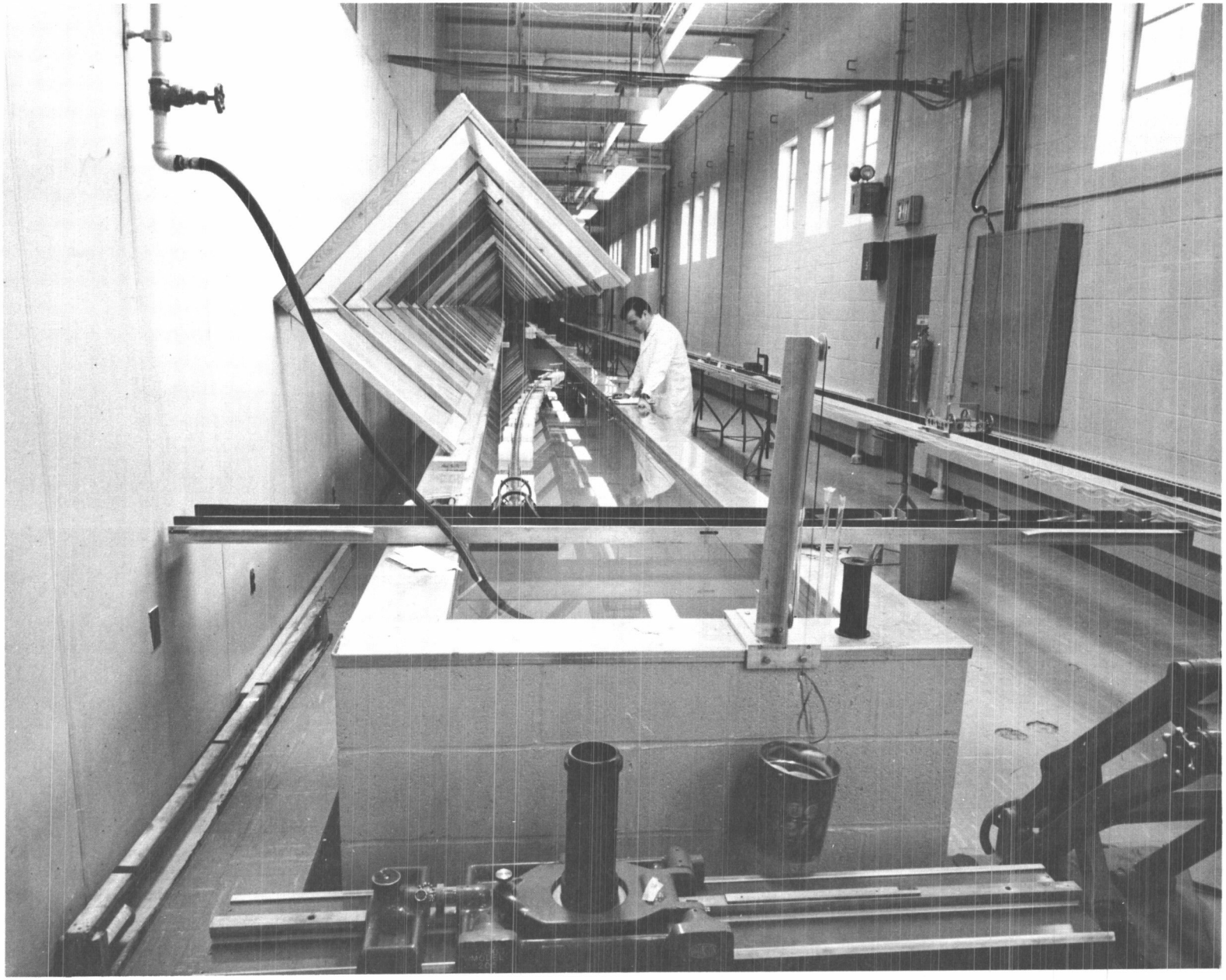

Figure 2-24. Hunter STACER Stiffness Test Setup

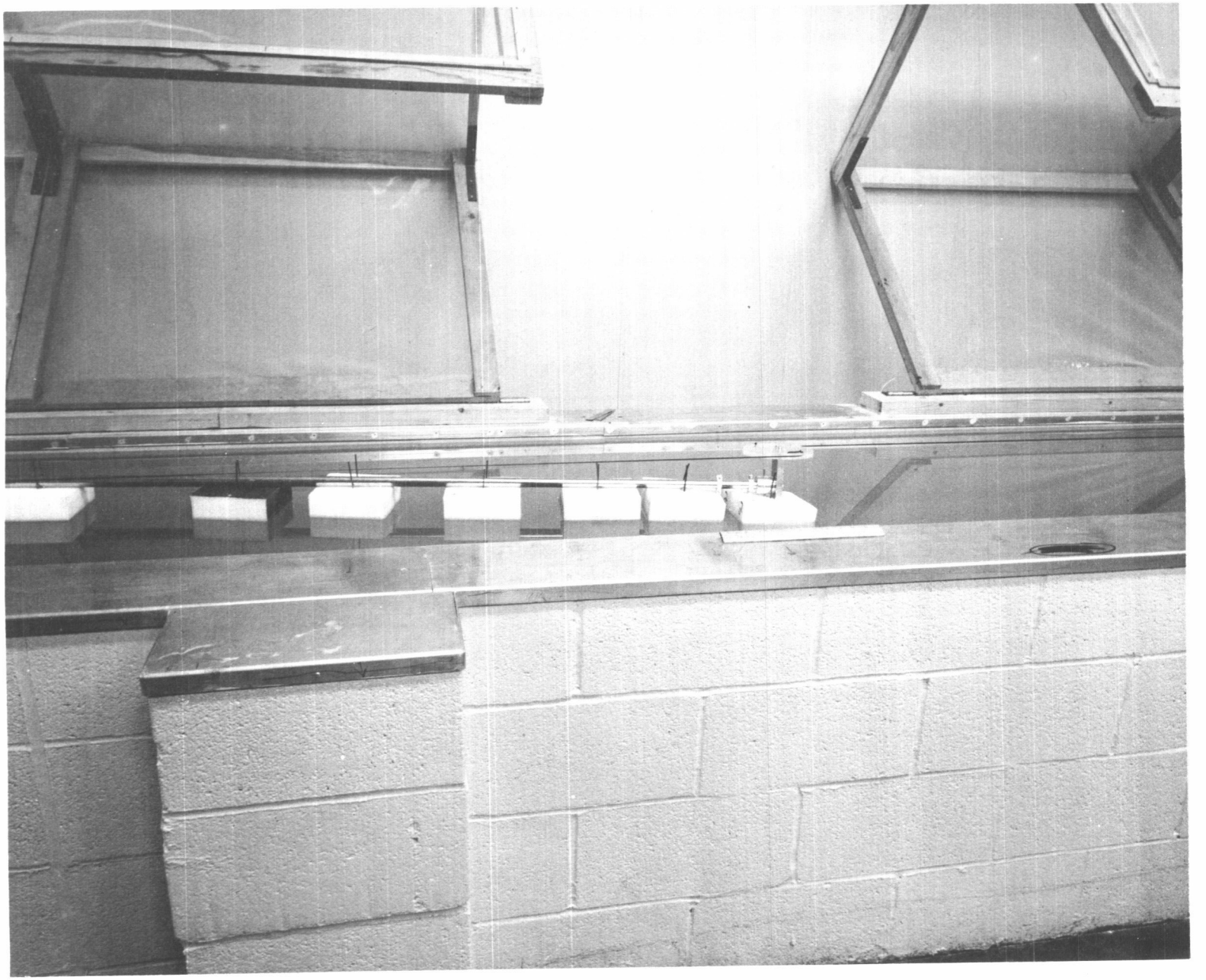

Figure 2-25. Hunter STACER Tip Loading Arrangement

A least squares fit of the polynomial

$$y = a + bx + cx^2 + dx^3$$

to the deflection data was selected as the method for obtaining the elastic curve. Arguments that other functions would be better can be made, but the polynomial served the purpose. This has some justification in that the integration of the deflection equation for constant loads and cross sections yields a polynomial.

It would be convenient if the STACER member stiffness were uniquely determined by the cross section and material. However, because of the way the spirally wrapped tube reacts under loads, it is likely that the member stiffness is a function of local deformation, friction, loading history (hysterisis), and possible other factors.

2.5.2.2 Results

The polynomial curve fits and their associated statistics evaluating the fit are shown on Table 2-12. Also shown is the member stiffness corresponding to these deflection curves.

Figures 2-26 and 2-27, show EI plotted versus length for the eight tests.

Figure 2-28 shows the average stiffness obtained from the eight tests. Table 2-13 lists the average stiffness EI at several locations along the members length along with the sample standard deviation. For purposes of comparison the stiffness (EI) of a constant thickness tapered tube of equivalent weight is shown on Figure 2-28. In this case, a stainless steel tube with 1-3/4 inch and 5/8 inch root and tip diameters and 0.018 inch constant wall thickness will be equal in weight to the STACER rod tested.

2.5.2.3 Discussion of Results

For the magnitude of deflections measured, the curve fits shown in Table 2-12 are reasonably good as illustrated by the mean and variance of the variable n. However, Figures 2-26 and 2-27 and Table 2-13 show considerable variation in the resultant stiffness

Table 2-12. Polynomial Curve Fit

Test	a (1×10^{-2})	b (1×10^{-3})	c (1×10^{-5})	d (1×10^{-7})	E (n)	var (n)	EI (x)
1	-4.731	1.964	7.456	2.317	0.1090	0.02030	$\frac{50.06}{2c + 6dx}$
2	-8.525	8.325	7.562	3.754	0.1475	0.02740	$\frac{75.09}{2c + 6dx}$
3	-7.203	3.867	16.952	2.002	0.0848	0.00286	$\frac{83.44}{2c + 6dx}$
4	-12.036	9.044	10.537	2.781	0.1116	0.01520	$\frac{61.19}{2c + 6dx}$
5	-6.587	7.975	5.606	2.478	0.1302	0.02030	$\frac{36.16}{2c + 6dx}$
6	-3.503	0.328	7.664	-0.369	0.0510	0.00238	$\frac{0.0975\ (298.6 - x)}{2c + 6dx}$
7	-1.717	5.959	1.055	0.158	0.0818	0.02190	$\frac{0.2075\ (298.6 - x)}{2c + 6dx}$
8	-8.516	6.974	23.609	-0.843	0.1512	0.02230	$\frac{0.3780\ (298.6 - x)}{2c + 6dx}$

$y = a + bx + cx^2 + dx^3$

$n = y_c - y_o$

y_o - measured deflection at 14 stations along the length

y_c - curve points at 14 stations along the length

E(n) = Mean of $(y_c - y_o)$ for the 14 stations.

var(n) = Variance of $(y_c - y_o)$

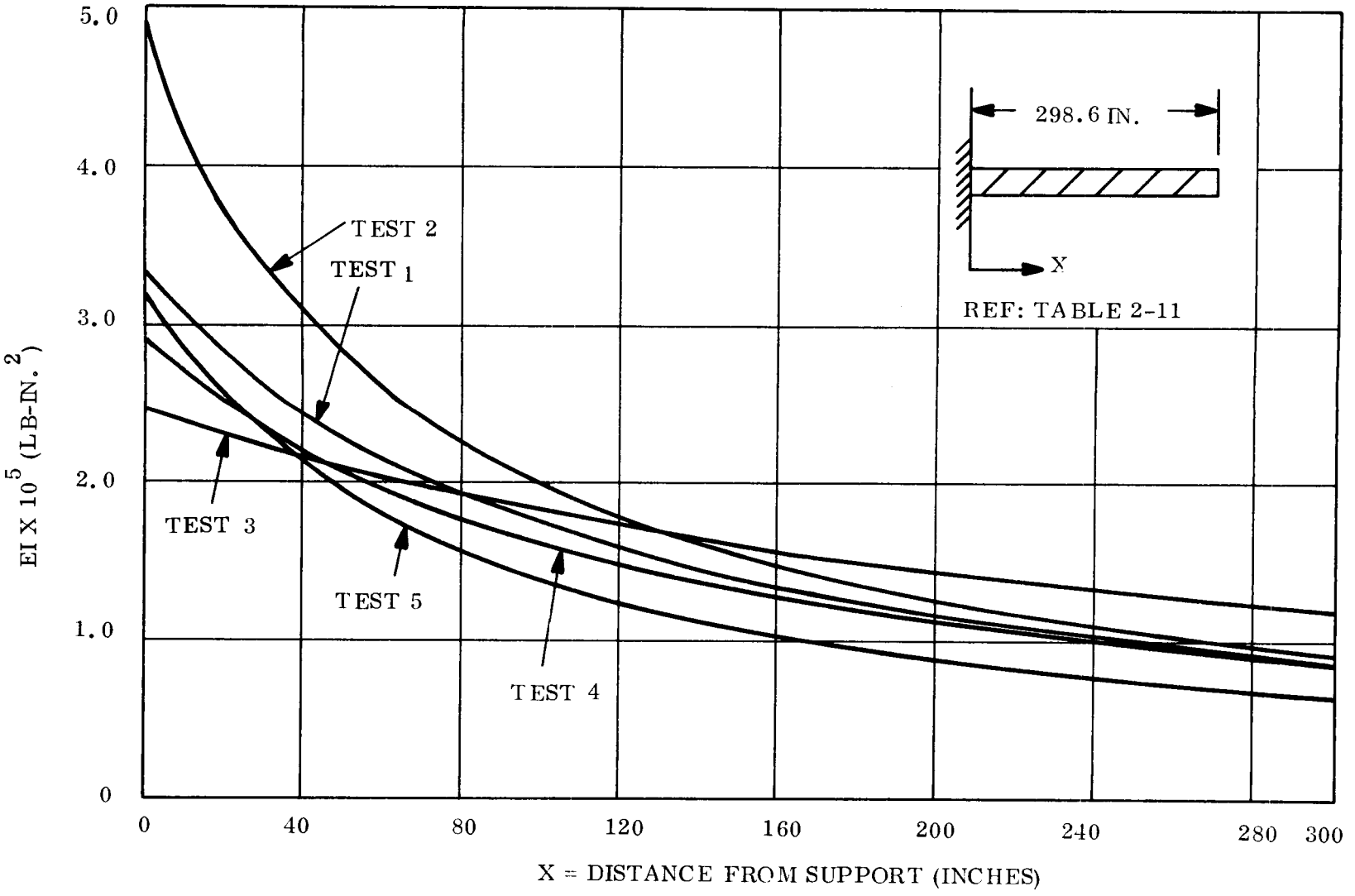

Figure 2-26. Stiffness (EI) Versus Length (Tests 1 through 5)

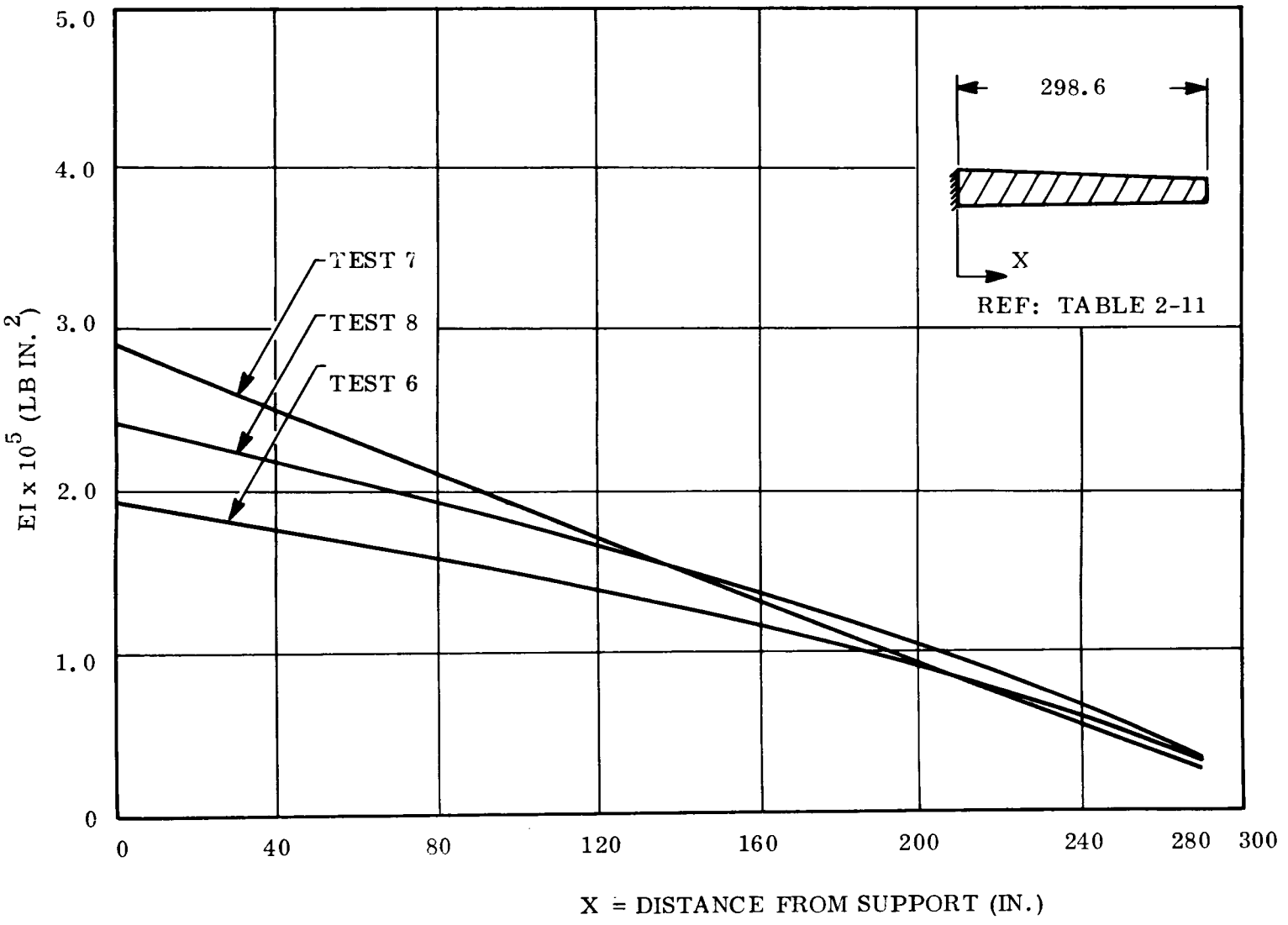

Figure 2-27. Stiffness (EI) Versus Length (Tests 6 through 8)

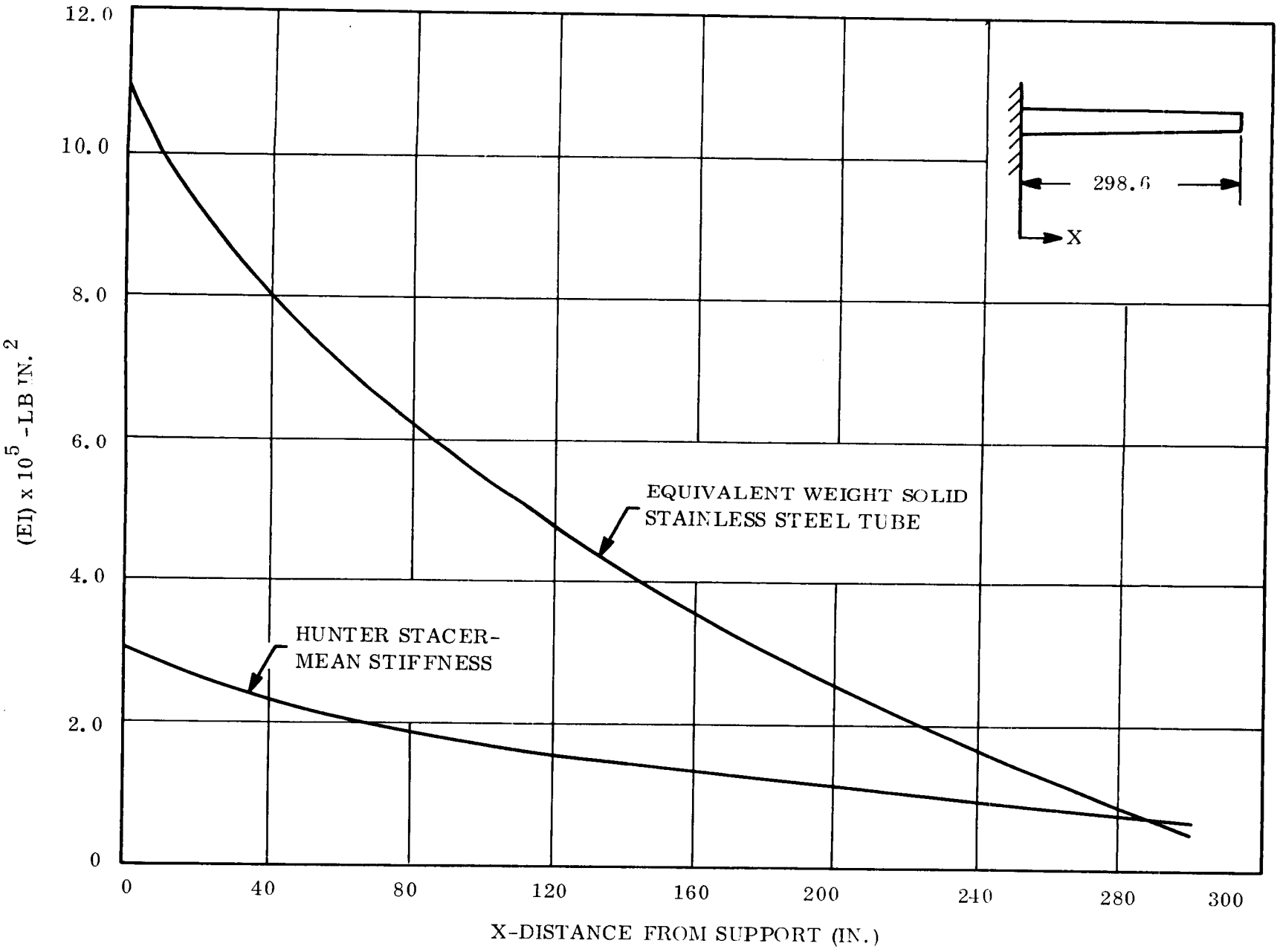

Figure 2-28. Mean Stiffness (EI) Versus Length

Table 2-13. Mean Stiffness and Standard Deviation

Station (in)	Mean Stiffness* (10^5 - lb-in^2)	Standard Deviation (10^5 - lb-in^2)
0	3.016	0.920
30	2.443	0.477
60	2.069	0.269
90	1.790	0.219
120	1.563	0.183
150	1.367	0.169
180	1.191	0.180
210	1.026	0.220
240	0.868	0.289
270	0.713	0.381

*All 8 tests included in mean.

for the rod. Part of this variation may be attributed to the inaccuracies made in making measurements of load and deflection. Some is probably due to the process of taking the second derivative. Thus, it is difficult from the amount of data taken, to separate experimental error from hysteresis and other effects. The mean stiffness for all tests is shown on Figure 2-28.

There seems to be little difference in the results obtained when the member is loaded by lateral forces (Tests 6 to 8) as opposed to bending moments (Tests 1 to 5). Thus, the effects of shear force on the deflection for such a member loaded in this manner may be neglected as in any continuous member of similar dimensions and length.

Figure 2-28 shows the stiffness (EI(x)) of an equal total weight stainless steel tapered tube of the same root and tip diameter as the STACER rod tested. The closed tube has greater stiffness at the root and approximately the same as the STACER at the tip. This result is consistant with the configuration of the rod because its tip has more overlap and interwrap friction. It should be noted, at this point, that the aforementioned equal weight

closed tube is not necessarily the "equivalent structural tube" for purposes of comparison since its weight distribution has been arbitrarily chosen and as such might be dissimilar to a given STACER rod.

From Tests 4 and 5, it is also evident that this member exhibits hysteresis behavior. This might be expected for the STACER since its deflection under load depends to some extent upon friction between wraps of metal.

These data represent the only structural deflection data available for Hunter STACER rods. Though limited in scope, it provides a basis for structural analysis of this type rod. Caution should be used in applying these data to other STACER rod sizes since it is believed that local member stiffness is significantly affected by the helix angle, local friction, and numerous other effects.

2.5.3 BI-STEM Static Load Test

THE SPAR AEROSPACE BI-STEM WILL SUSTAIN THE LOADS IMPOSED BY THE 1 G VERTICAL DEPLOYMENT AS REQUIRED BY THE ENGINEERING DEMONSTRATION MODEL WITHOUT ROD BUCKLING OR DEPLOYER MALFUNCTION.

The objective of this test was to determine experimentally the ability of the "off-the-shelf" BI-STEM to sustain the loads to be imposed in the 1 g demonstration of the solar array as described in Section 2.8. Under these conditions the loads are:

Blanket Tension -- 4.0 lb

Tip Mass Weight -- 1.2 lb

Boom Weight -- 0.2 lb/ft

The maximum length to which these loads apply is 33.5 feet.

The test specimen was a SPAR Aerospace BI-STEM unit No. 5671F1-3, Serial Number SD2, equipped with approximately 40 feet of BI-STEM boom. The boom element details are:

Boom Diameter	--	1.34 inches
Wall Thickness	--	0.007 inch
Material	--	301 S/S
Element Strip Width	--	4.0 inches
No. of Elements/Boom	--	2
Configuration	--	BI-STEM (Front to front underlapped C's)

The unit is powered by a Globe102-A161-11 permanent magnet-type gear-motor with an 80:1 reduction ratio with a series brake. At 27 vdc the motor output torque is 250 oz-in. at 75 rpm.

2.5.3.1 Test Procedure

The test set-up is shown in Figure 2-29. The test facility was a high bay area at the SPAR plant. To gain the maximum deployment height, the unit was mounted 6 feet below the floor level. In spite of this, the maximum possible deployment was 31 feet.

The initial boom deployment axis (as defined by the position of the first 6 feet of boom extension) was accurately aligned with the local vertical by means of a plumb bob. (Note: This step is extremely important in any 1 g demonstrations.) The appropriate tip-mass and blanket tension weights were applied and the boom extended under load. Deflections from the local vertical were measured with a scale. The boom was then retracted under load and the next set of loads was applied.

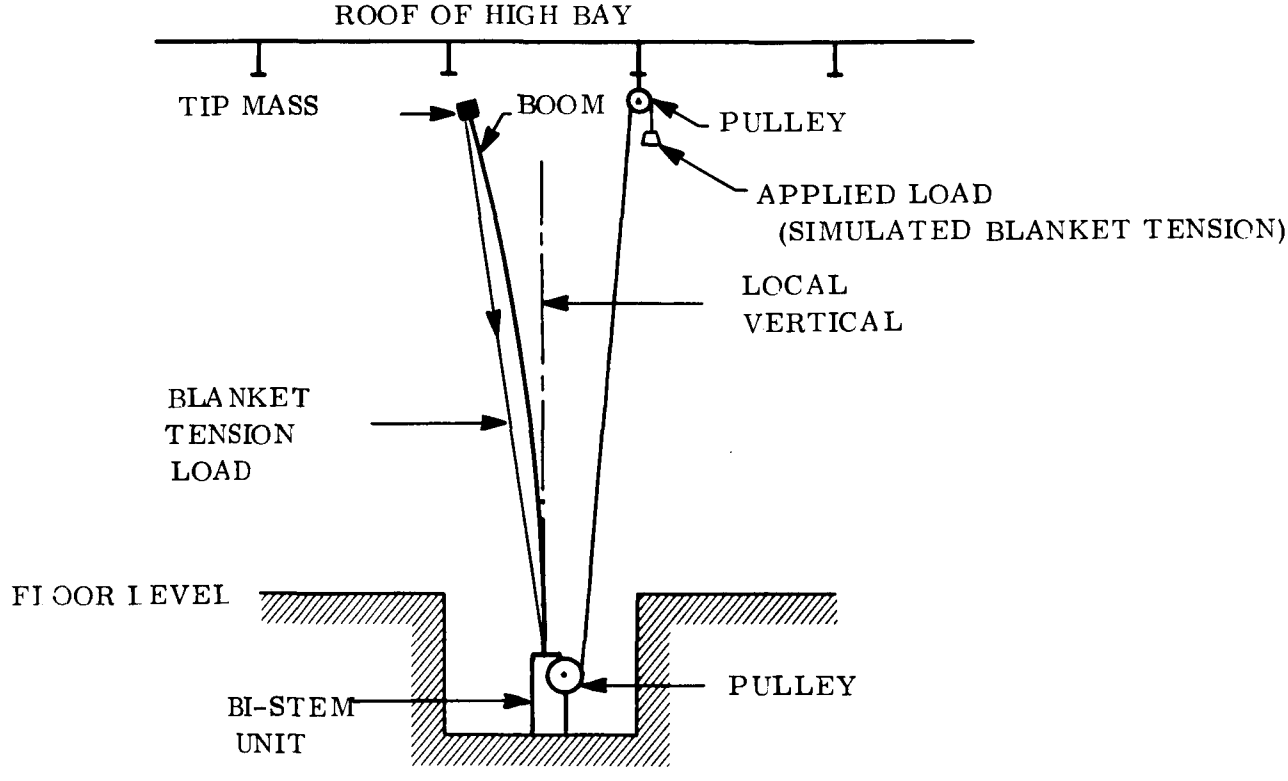

Figure 2-29. BI-STEM Static Load Test Setup

The test results are summarized in Table 2-14. In one test run, the loads were increased above the design values by the ratio of the lengths squared to compensate for the fact that the maximum extended length was limited to 31 feet instead of the design value of 33.5 feet.

Table 2-14. BI-STEM Static Load Test Results

Blanket Tension (lb)	Tip Mass (lb)	Length Along Boom (ft)	Deflection (in.)
0	0	31 (Tip)	4
↓	↓	20	1.75
		14	1
		7.8	0.25
		0	0
0.2	1.2	31 (Tip)	8.50
↓	↓	30	3.75
		14	2.25
		7.8	0.87
		0	0
1.06	1.2	31 (Tip)	8.50
↓	↓	20	4.38
		14	2.50
		7.8	0.75
		0	0
2.0	1.2	31 (Tip)	10.25
↓	↓	20	5
		14	2.75
		7.8	1
		0	0
3.0	1.2	31 (Tip)	10.25
↓	↓	20	5.25
		14	3
		7.8	0.87
		0	0
Design 4.0 Loads	1.2	31 (Tip)	13
↓	↓	20	6.25
		14	3.38
		7.8	1.12
		0	0
Design 4.6 Loads Increased by $\left(\frac{33.5}{31}\right)^2$ ↓	1.4 ↓	31 (Tip)	17
		26	13.25
		20	9
		14	5
		7.8	1.62
		0	0
4.8	1.4	31 (Tip)	18
5.0	1.4	31 (Tip)	18.50

NOTE: In all cases, the boom was loaded by its own weight of approximately 0.2 lb/ft.

2.6 Thermal Analysis

2.6.1 Array Temperature Analysis

THE AVERAGE ARRAY TEMPERATURE AT 1.000 AU IS 123°F (50.5°C). THIS TEMPERATURE CAN BE MAINTAINED WITHOUT RESORTING TO OPTICAL COATINGS ON THE ARRAY BACK SURFACE.

A thermal analyses of the deployed roll-up solar array has been conducted to determine the equilibrium temperatures at 1.000 AU and at 0.733 AU. The geometric relationship of the array and vehicle is shown in Figure 2-30. The cell side of the array is assumed to have an unobstructed view of space. The conversion of solar to electrical energy is taken as 10 watt/ft^2 of array, and the cell packing factor is 0.90. The vehicle wall was assumed to have an emittance of 0.8 and behave as an adiabatic body. The optical properties of the array constituents are summarized in Table 2-15.

Table 2-15. Optical Properties of Array Components

	α_s	ϵ[1]
Solar cell/filter/glass composite	0.71[3]	0.8
2 mil Kapton backed by solar cells	--	0.67[2]
Inactive array surface	0.70	0.65

Notes:

1. α_s = solar absorptance, ϵ = infrared emittance
2. Estimated value based on previous measurements by the General Electric Company on bare Kapton H film
3. Measurements made by the General Electric Company show lower α_s values for N/P then for P/N cells, due to higher reflectance in the near-infrared at the back of the cell. Filter is the blue type, with a cut-on at 0.41 μ.

In order to more accurately assess the vehicle effects upon the array temperature, a radiation network was constructed which considered five bodies rather than simply the vehicle and the array each as a lump. The array was divided into three sections, each 133 inches in length; the vehicle itself was broken up into two halves, each 96 inches in length. The drum was not included because of its generally small influence on the array. Previous studies by the General Electric Company Spacecraft Department have shown that the temperature gradient through the array is small.

A typical equation of the network is shown below, and represents the heat balance per unit area of an array section.

$$S\alpha_s - P = (F_{F-S}\bar{\epsilon}_F + F_{B-S}\bar{\epsilon}_B) B_A + (F_eF)_{B-V_1} (B_A - B_{V_1})$$

$$+ (F_eF)_{B-V_2} (B_A - B_{V_2})$$

where:

S = incident solar flux at 1.000 AU (or 0.733 AU)

α_s = solar absorptance of the array front surface

P = solar energy converted

F = geometric view factor

F_e = emittance factor

B = black body emission

$\bar{\epsilon}$ = average surface infrared emittance

Subscripts

F = front array surface

B = array back surface

V_1 = vehicle section nearest array

V_2 = vehicle section furthest from array

A = array

S = black space

A solution of the five equations of the network resulted in the following temperatures

	1.000 AU	0.733 AU
Array Section Furthest from Vehicle	121°F (49.4°C)	224°F (106.7°C)
Array Section Nearest to Vehicle	125 (51.7)	226 (107.8)
Array Section Located Between the Above	122 (50.0)	225 (107.2)
Vehicle Section Nearest the Array	-82 (-63.3)	-16 (-26.7)
Vehicle Section Furthest from Array	-168 (-111.1)	-116 (-82.2)

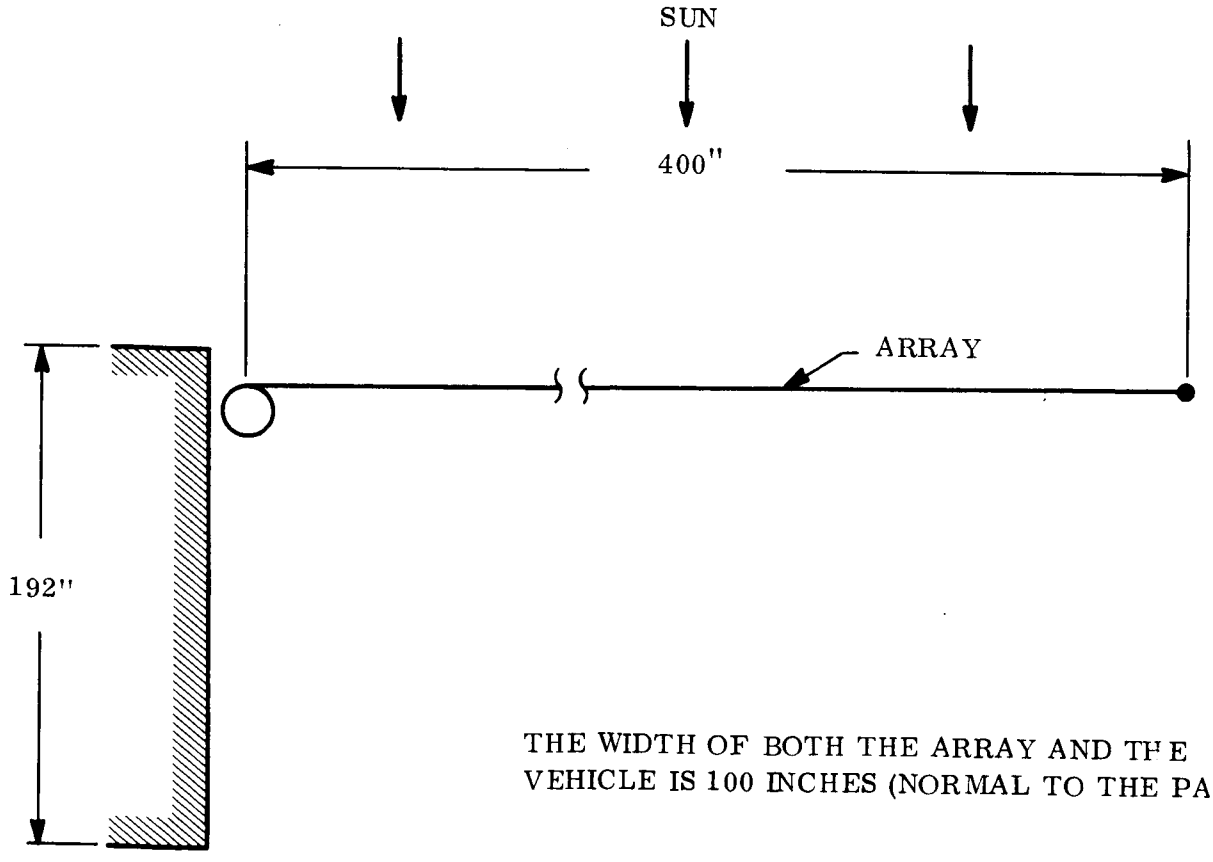

Figure 2-30. Array/Vehicle Geometric Relation

2.6.2 Power Take-off Spiral Analysis

THE MAXIMUM TEMPERATURE OF A POWER TAKEOFF SPIRAL WILL BE 205° F (96.1°C) AT 1.000 AU WHEN TRANSFERRING THE ARRAY MAXIMUM POWER CURRENT (13.8 AMP/SPIRAL).

A thermal analysis of the power takeoff spiral (Configuration 1 of Section 2.2.3) was performed to aid in the tradeoff studies of the various methods of power transfer between the drum and the support structure. The arrangement of the spiral is shown in Figure 2-31. Each of the bodies included in the thermal network was taken as isothermal. Thus, although a portion of the heat generated in the copper spiral is given up by the last wrap (No. 8) to the 2-inch long drum surface, the fin effectiveness of the drum is high enough to assume negligible temperature gradients from the copper facing part of the 8-inch drum to the end of the drum, a distance of 6.5 inches (drum thickness = 0.025 inch). Further, circumferential temperature gradients caused by the sun in the 8-inch drum were not considered ($< 40^{\circ}$ F at 1.0 AU); the temperature of the drum was always treated as a circumferential average.

The spiral wraps, the drum skin, and the outer Kapton layer were assumed closely spaced together, but not touching. The heat transfer between individual layers then followed the laws of radiation for infinite parallel plates. The left edge of the spiral in Figure 2-31 was taken as adiabatic because of the proximity of the second spiral (not shown in the figure). The optical properties of Table 2-16 were used in this analysis.

Before a heat transfer network to determine the spiral temperature was formulated,the sink temperature of the beryllium drum was obtained. The three sources of heat affecting the drum are the sun, the array, and the vehicle wall. Rather than use the average array temperatures reported in Section 2.6.1. new values were obtained for the array sections immediately adjacent to the drum. The vehicle wall temperature was conservatively assured at -80°F (-62°C) and -35°F (-37°C) at 1.000 AU and 0.733 AU, respectively. The resulting average sink temperature for the drum was calculated as -10°F (-23°C) at 1.000 AU, and 60°F (16°C) at 0.733 AU.

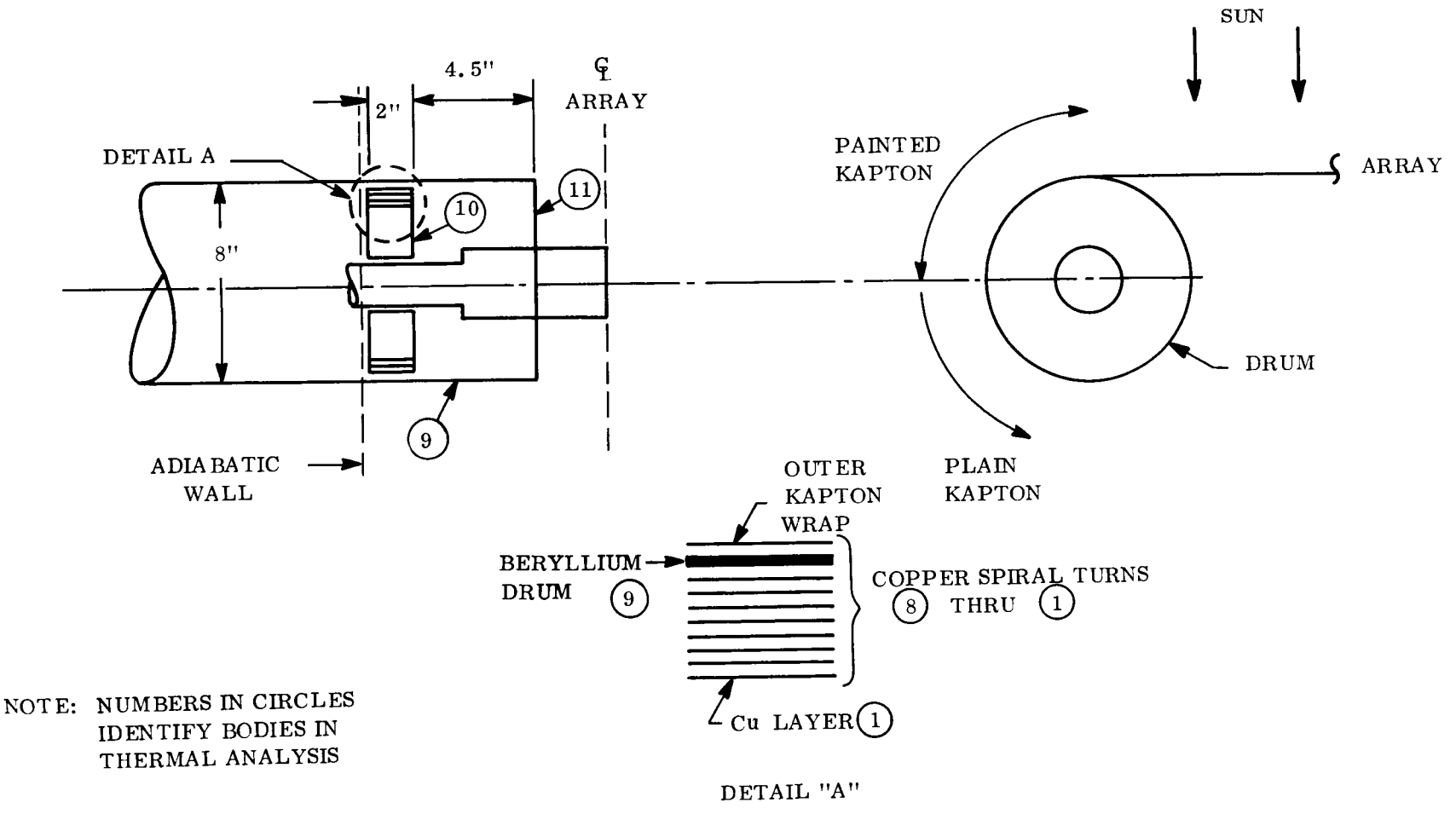

Figure 2-31. Arrangement of Power Takeoff Spiral

Table 2-16. Material and Coating Optical Properties

Item	Properties	Coating
Kapton outer layer, covering the sun exposed 1/4 of the drum, over a length of approximately 15 inches from the end of the drum	$\alpha_s = 0.2,\ \epsilon = 0.8$	White paint or equivalent
Plain Kapton over drum skin	$\epsilon = 0.8$	---
Beryllium drum, both sides	$\epsilon \geq 0.8$	Black paint
Copper spiral, both sides	$\epsilon \geq 0.8$	Black oxide
All equipment inside drum	$\epsilon \geq 0.8$	Black paint
End of 8-inch drum and exposed surface of inner aluminum shaft	$\alpha_s = 0.2,\ \epsilon = 0.8$	White paint or equivalent

A radiation network, including eleven separate bodies, was then formulated to determine the spiral temperature. Heat is lost from the spiral via layer No. 8 to the beryllium skin, and via layer No. 1 to the fiberglass wall normal to the spiral wraps, body No. 10. The heat leak to the inner fiberglass shaft was assumed negligible. The heat transfer network describing heat paths through and from the spiral is shown in Figure 2-32. A solution to the eleven simultaneous equations representing the network resulted in spiral temperatures. The maximum and average spiral temperatures are presented on Figure 2-33 as a function of power dissipation per spiral. The power loss as a function of spiral temperature is determined by the temperature coefficient of resistivity for the copper and is given by the following expression:

$$P_{Loss} = P_o \left[1 + \frac{0.0393}{1.8} (T-68.)\right]$$

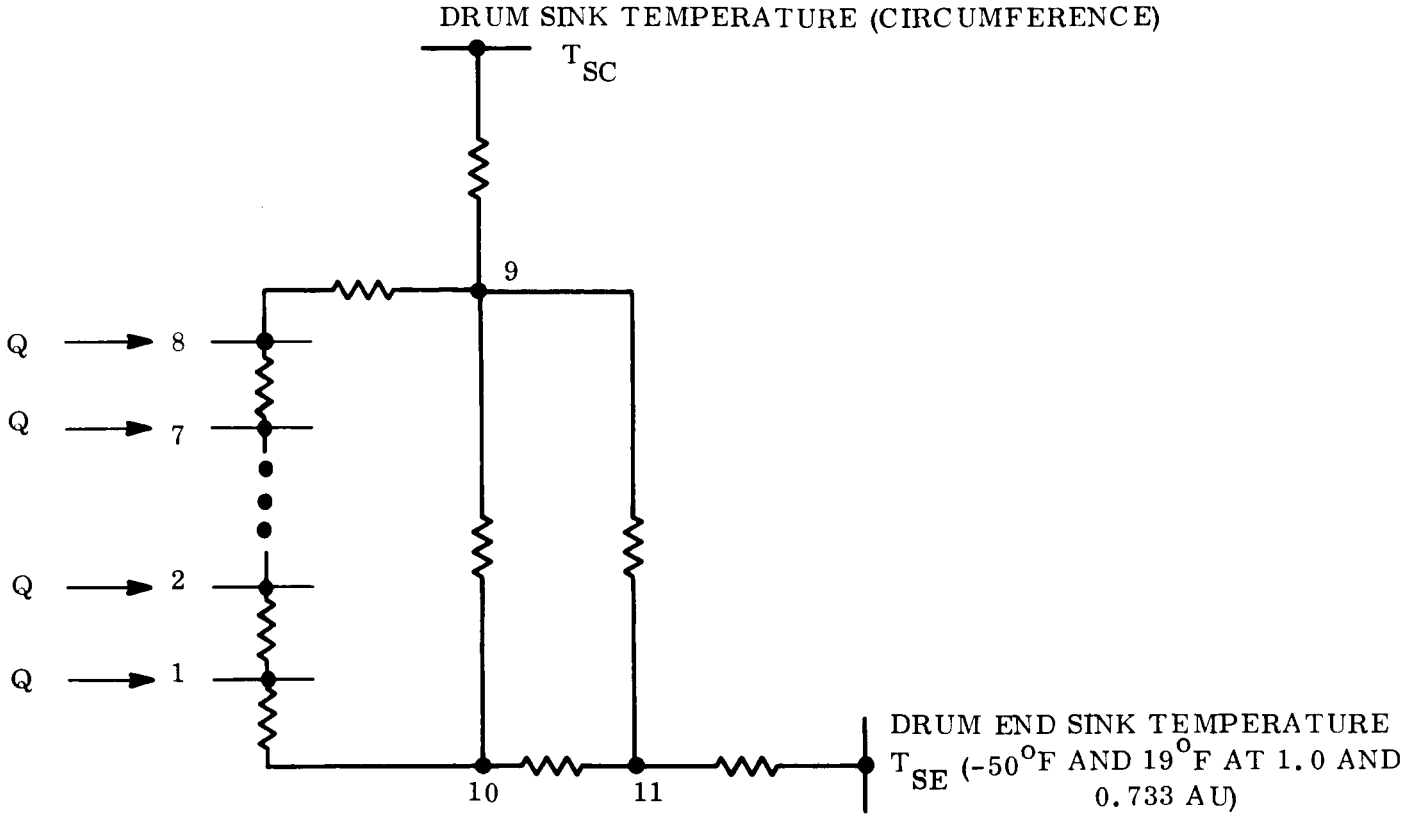

$F_{e\ 9\text{-}T_{SC}} = 0.56$ (INCLUDES KAPTON EFFECTS)

$F_{e\ 9\text{-}10} = F_{e\ 9\text{-}8} = F_{e\ 9\text{-}11} = 0.66$

$F_{e\ 1\text{-}2} = F_{e\ 2\text{-}3} \ldots$ etc. $= 0.66$

$F_{e\ 11\text{-}T_{SE}} = 0.8$

$F_{e\ 10\text{-}1} = 0.66$

$F_{e\ 10\text{-}11} = 0.66$

$F_{1\text{-}2} = F_{2\text{-}3} \ldots$ etc. $= 1.0$

$F_{10\text{-}9} = 0.611$

$F_{10\text{-}11} = 0.23$

$F_{11\text{-}9} = 0.611$

$F_{9\text{-}8} = 0.308$

Q = HEAT GENERATED/Cu WRAP.

Figure 2-32. Thermal Model Network for Power Takeoff Spiral Analysis

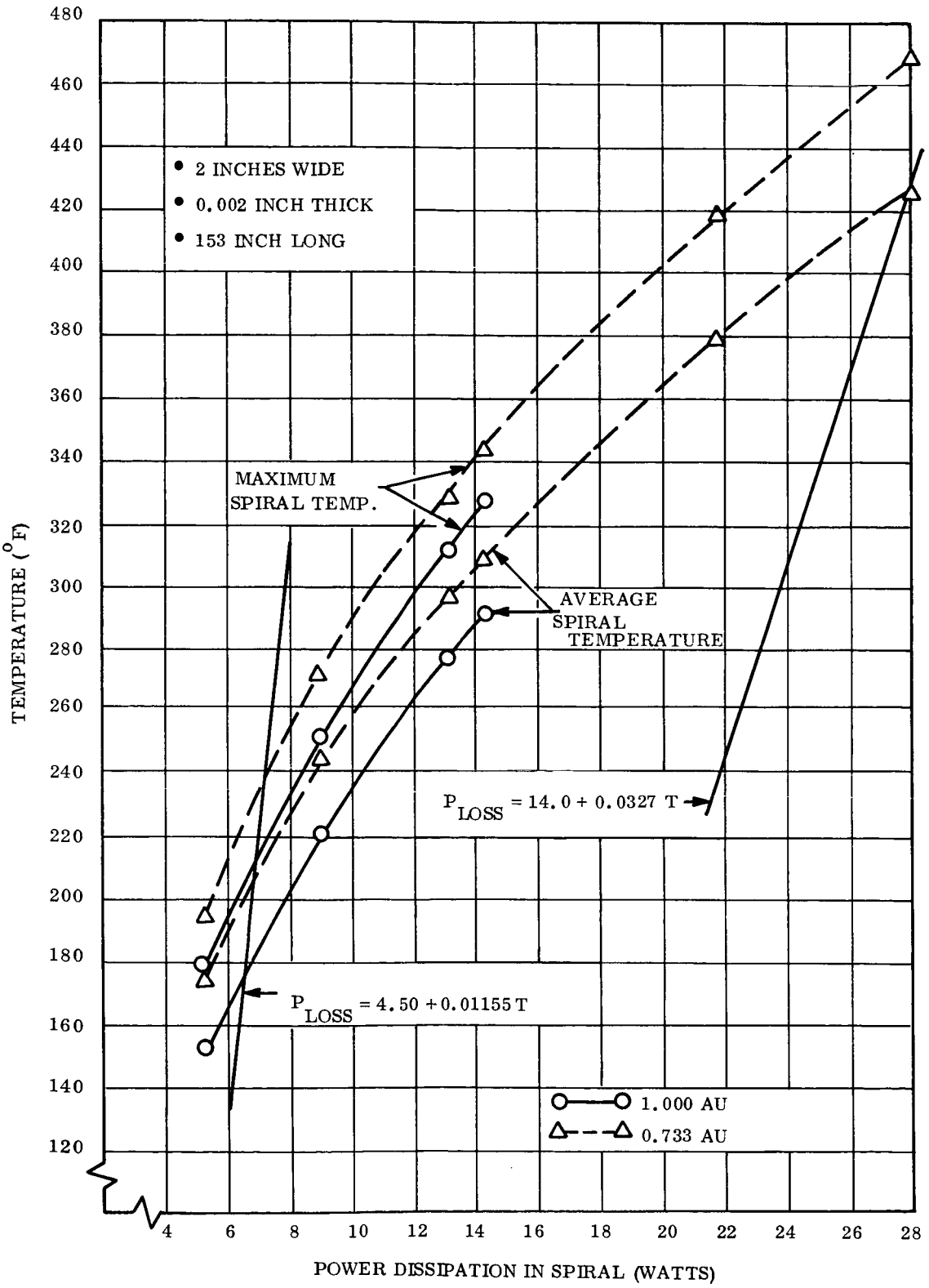

Figure 2-33. Copper Power Takeoff Temperature Versus Power Dissipation

where

P_o = the power dissipation of 68°F

= 5.29 watt (13.8 amp per spiral, max. power current at 1.000 AU)

= 16.2 watt (24.2 amp per spiral, max power current at 0.733 AU)

T = average temperature of the spiral in °F

With the appropriate constants substituted for P_o this equation reduces to:

P_{Loss} = 4.50 + .01155T (at 13.8 amp per spiral)

P_{Loss} = 14.0 + .0327T (at 24.2 amp per spiral)

These equations are plotted on Figure 2-33 so that the equilibrium temperature power dissipation can be determined by the intersection of these linear equations with the solutions for average spiral temperature as obtained from the solution of the heat transfer network. The results of this analysis are shown in Table 2-17.

Table 2-17. Results of Spiral Power Takeoff Thermal Analysis

Distance From Sun	Array Max. Power Current	Max. Spiral Temp. With Max Power Current	Max. Spiral Temp at 27.6 amp	Total Power Dissipation With Max Power Current	Total Power Dissipation With 27.6 amp
(AU)	(amp)	(°F)	(°F)	(Watts)	(Watts)
1.000	27.6	205	---	26	---
0.733	48.4	470	233	112	28

2.7 Solar Cell Module Fabrication

A FIVE CELL SERIES BY FIVE CELL PARALLEL MODULE HAS BEEN FABRICATED USING TECHNIQUES PLANNED FOR THE 30 WATT PER POUND SOLAR ARRAY.

Bonding of the 0.003-inch glass cover slide to the 0.008-inch solar cell is performed in the fixture shown in Figure 2-34. Control of the Sylgard 182 bond thickness to less than 0.001 inch is attained by the spring load on the glass. This load is between 60 and 100 grams because of the individual spring variation and produces uniform squeeze out as determined from measurements of the total unit thickness, which ranges between 0.0102 and 0.0126 inch. These values were measured on a randomly selected sample of 24 assemblies. The thickness of each assembly was measured in five places, and the average thickness was recorded. The average thickness among the 24 samples was 0.0111 inch.

An exploded view of the series interconnection is shown in Figure 2-35. The design of the tab has been modified to include only one loop in the series direction to improve the conductivity, weight, and soldering process efficiency.

The resistance in the series direction of the tab and one solder joint is 0.65 milliohm.

With the extra loop, as shown in Quarterly Report No. 1, (Reference 1-1) the close proximity of the negative and positive joints on the opposite sides of the cell made careful heat sinking necessary when soldering the second joint. This was necessary to avoid loosening of the previous joint. This condition is much improved with the single series loop tab.

Flexibility is still such that a thermal strain of 0.002 inch can be accommodated with less than 0.001 pound resistance force being developed in the solder joints. The joints have been tensile tested to 1.5 pounds without damage to the solder joint, although the tab is completely deformed.

Figures 2-36 and 2-37 show the front and back sides of 5 x 5 cell module.

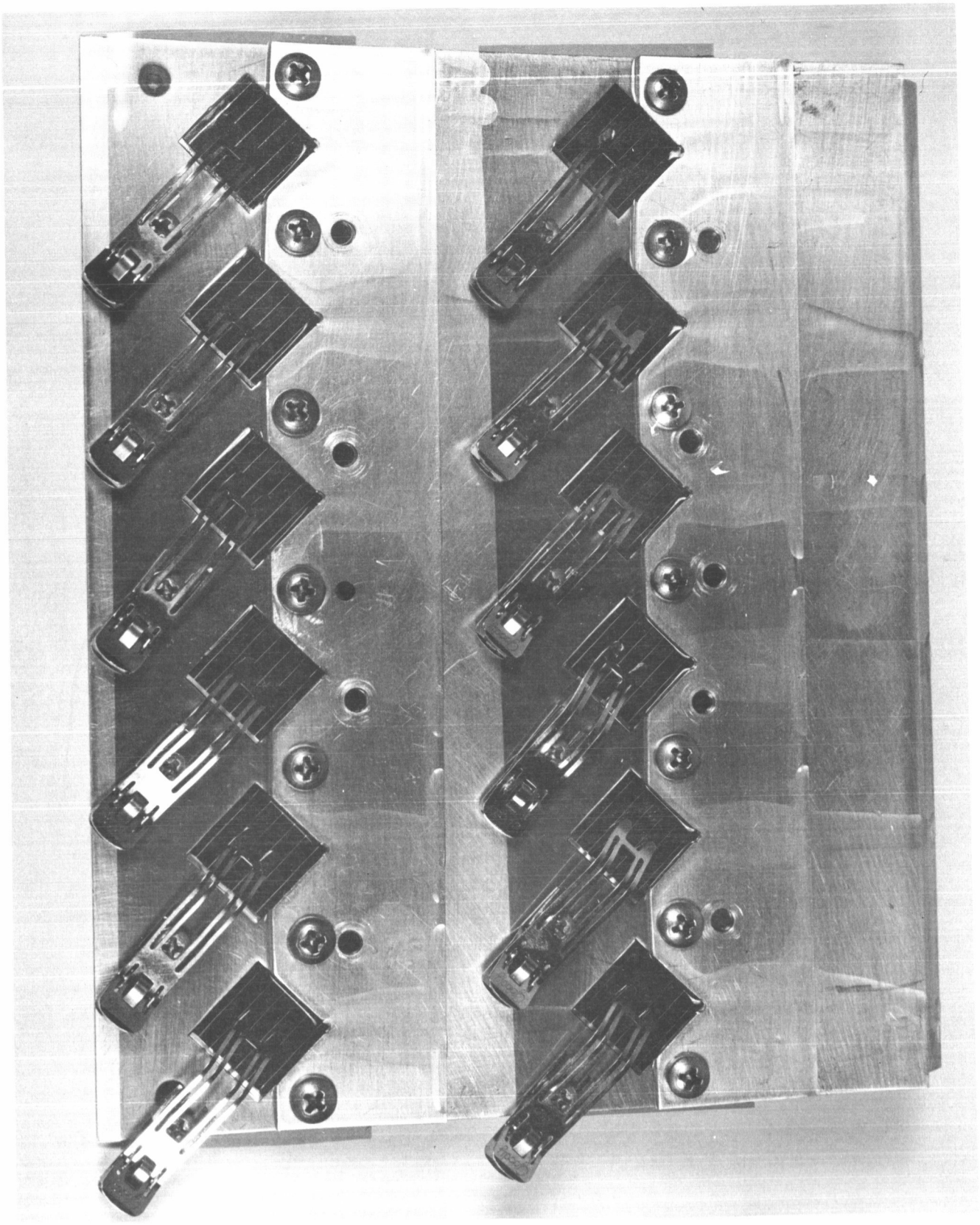

Figure 2-34. Cover Glass Installation Fixture

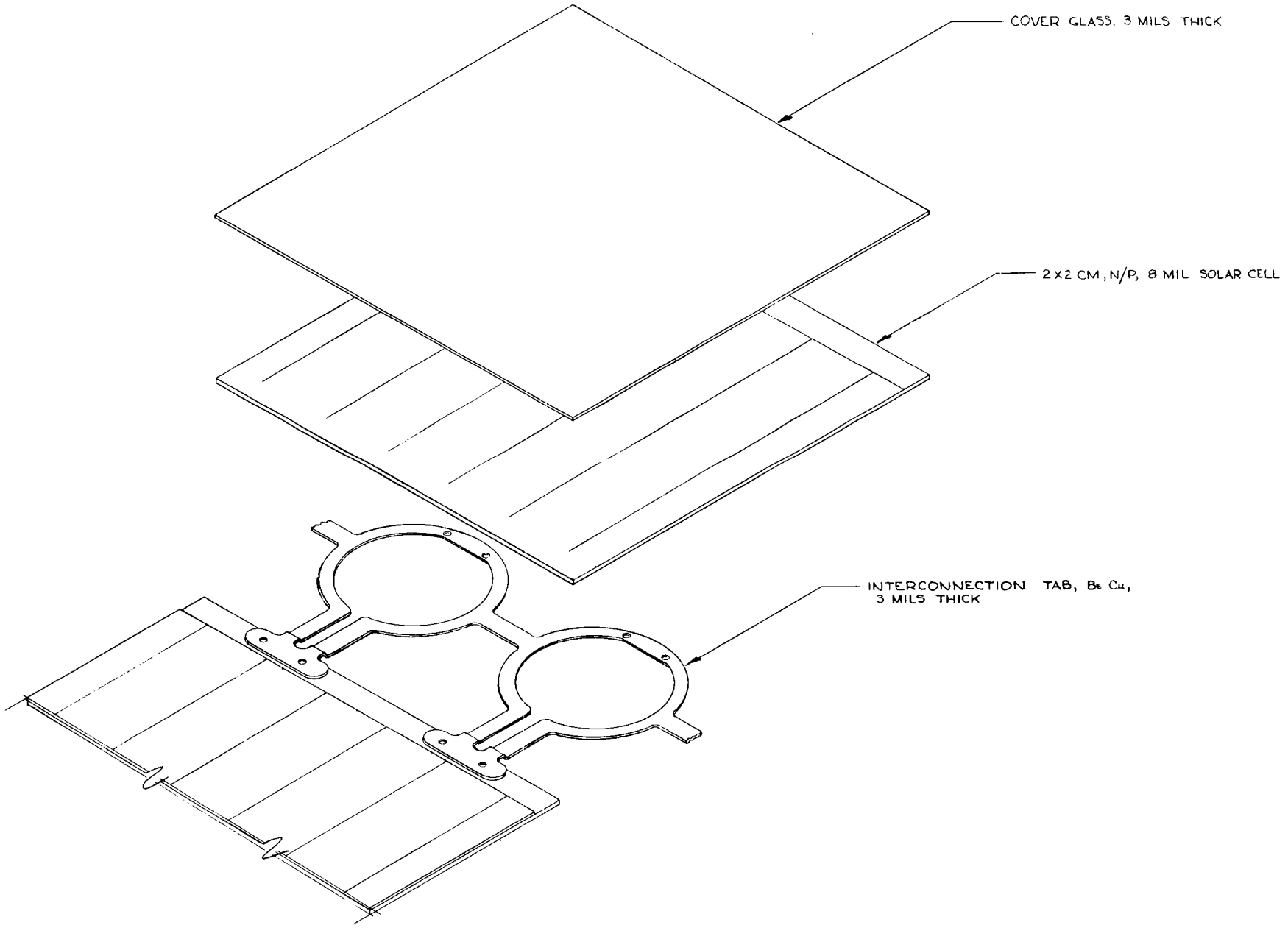

Figure 2-35. Exploded Isometric of Solar Cell/Cover Glass/Tab

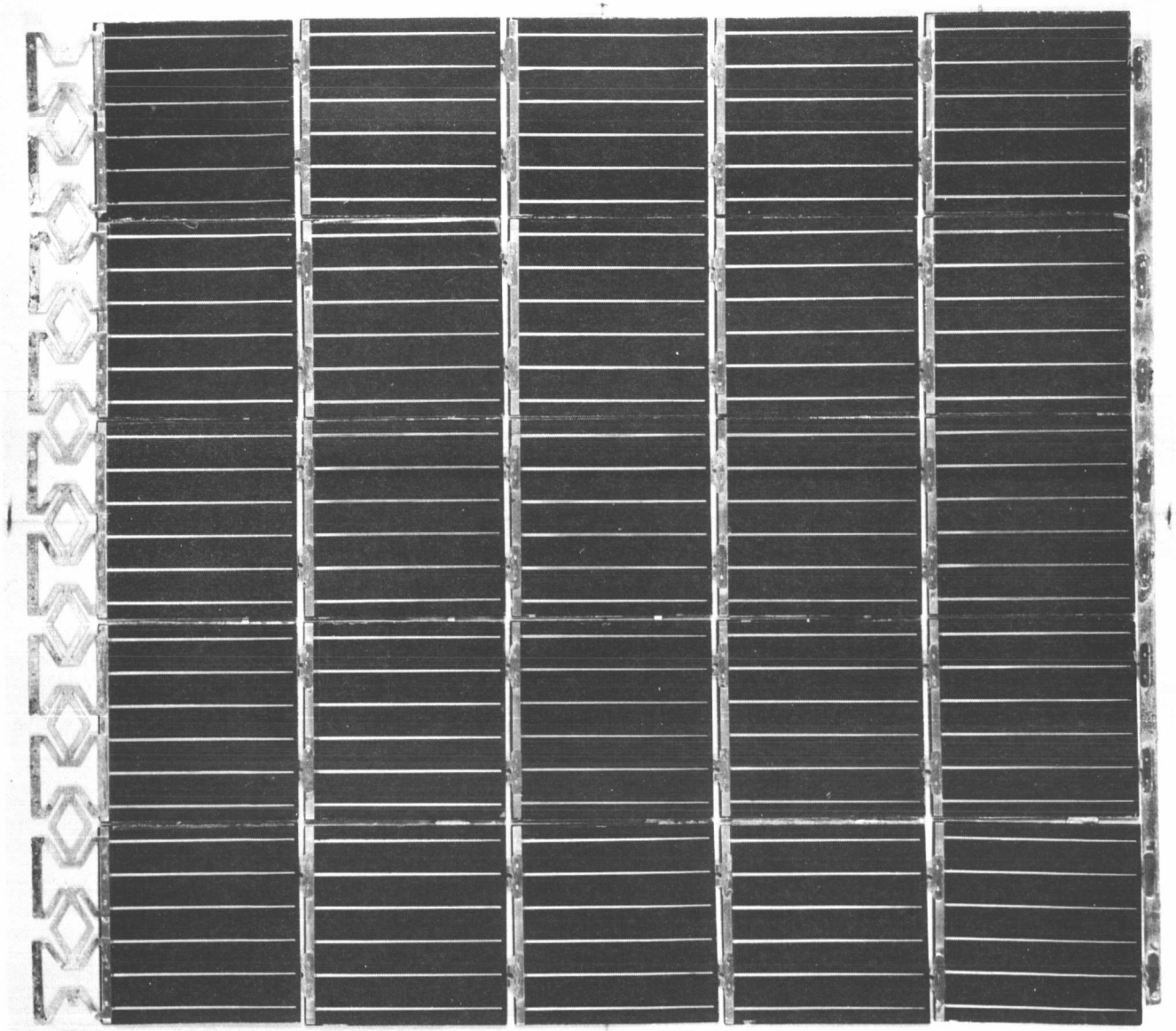

Figure 2-36. 5 x 5 Cell Module - Front Side

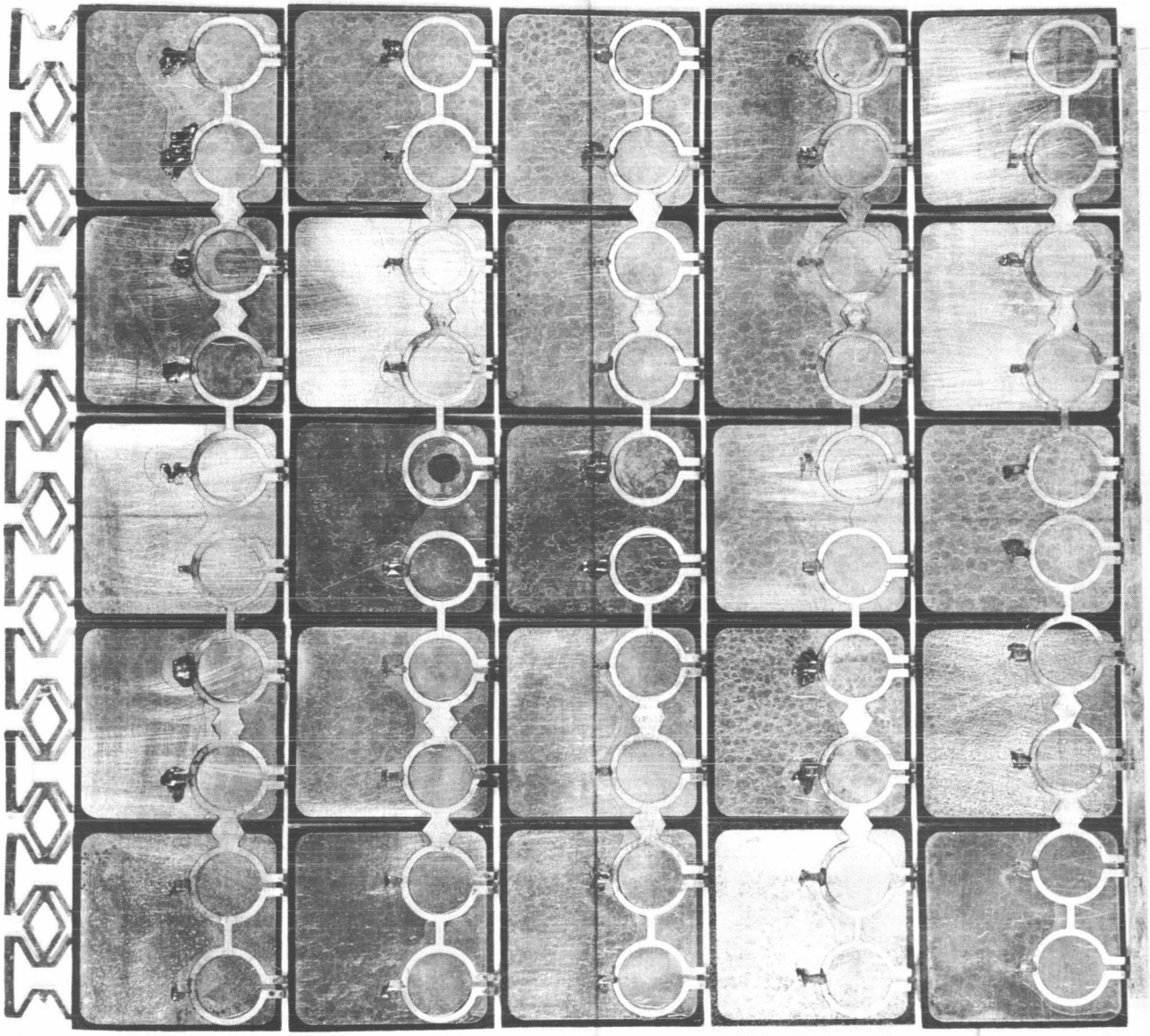

Figure 2-37. 5 x 5 Cell Module - Back Side

2.8 Engineering Demonstration Model

THE ENGINEERING DEMONSTRATION MODEL SHALL PRESENT A CREDITABLE DEMONSTRATION OF THE DEPLOYABILITY OF THE PROPOSED CONCEPT.

The Engineering Demonstration Model is a deliverable end item under the contract. The stated purpose of this model is to demonstrate the deployability of the design concept for the 30 Watt per Pound Roll-up Solar Array. The contract allows a range of requirements that are bounded by the resources available for the model. The force of gravity complicates the design of the model as it is desirable that deployment be accomplished without extensive support equipment. The model will be used for demonstration purposes and will provide an engineering tool for the development of the detailed system design. It is efficient if an element of the model can be used for future test programs to prove the design or provide data for design development.

Based upon the above considerations the primary requirements for the model are to:

a. Present a creditable demonstration of the deployability of the array design in a 1 g field.

b. Be composed of flight design components wherever possible within the constraint of the deployability in a 1 g field.

c. Demonstrate the producibility of the flight solar panel design concept.

d. Demonstrate that the analytical model for the deployed first mode natural frequencies in bending and torsion are accurate.

e. Demonstrate the construction and interconnection of a series string of solar cells which produce the full system voltage.

f. Provide an engineering design tool that feedbacks information into the design of the flight unit.

g. Provide a system that can be used for demonstration purposes that does not require elaborate deployment aids.

h. Provide a test bed for critical elements of the system.

Figure 2-38 shows a pictorial sketch of the proposed Engineering Demonstration Model. This model is essentially the flight solar panel design with the following exceptions:

a. The model has been scaled down in width to match the analytical model used in the dynamics analysis. The inside width of each drum has been reduced from 47.1 inches to 24.0 inches.

b. The array blankets have been replaced with 4.0-inch wide, 1 mil Kapton strips. One series string of solar cells(242 cells in series X 2 cells in parallel) will be installed on each of these strips to demonstrate the construction and interconnection.

c. Flight design materials will be replaced with more conventional materials where it does not compromise the requirements for the model. For example, the boom will not be silver plated, and the bearings will contain conventional oil lubrication.

The two drums are mounted on a test stand which simulates the vehicle interface. This stand is equipped with a level and leveling screws to establish the nominal boom centerline along the the local vertical. The drums and leading edge member are caged as in the flight design except that the capability will exist to replace the electroexplosive devices with solenoid actuated devices. The power supply and controls for the boom actuator will be contained on the test stand. Upon command the uncaging sequence will be initiated and the boom will deploy vertically upward to the fully extended position of 409 inches from the drum centerline. The deployment will stop automatically at the fully extended position. The retraction of the boom will be initiated by reversing the polarity to the motor.

The deployable boom and the drum support system will be a flight-type design. Thus, these elements could be subjected to vibration tests. The solar array blankets will be made of flight-type construction and could be subjected to meaningful thermal vacuum tests. To obtain the vibration characteristics of the solar array blanket, it would be necessary to fabricate a larger unit as the blankets planned for the model are not dynamic equivalents of the flight design.

The model is not capable of being deployed with any significant windage loading. Therefore, the deployment must be accomplished in an enclosed area which is relatively free of air currents. It may be necessary to incorporate simple deployment aids to accomplish the full extension of 33.5 feet.

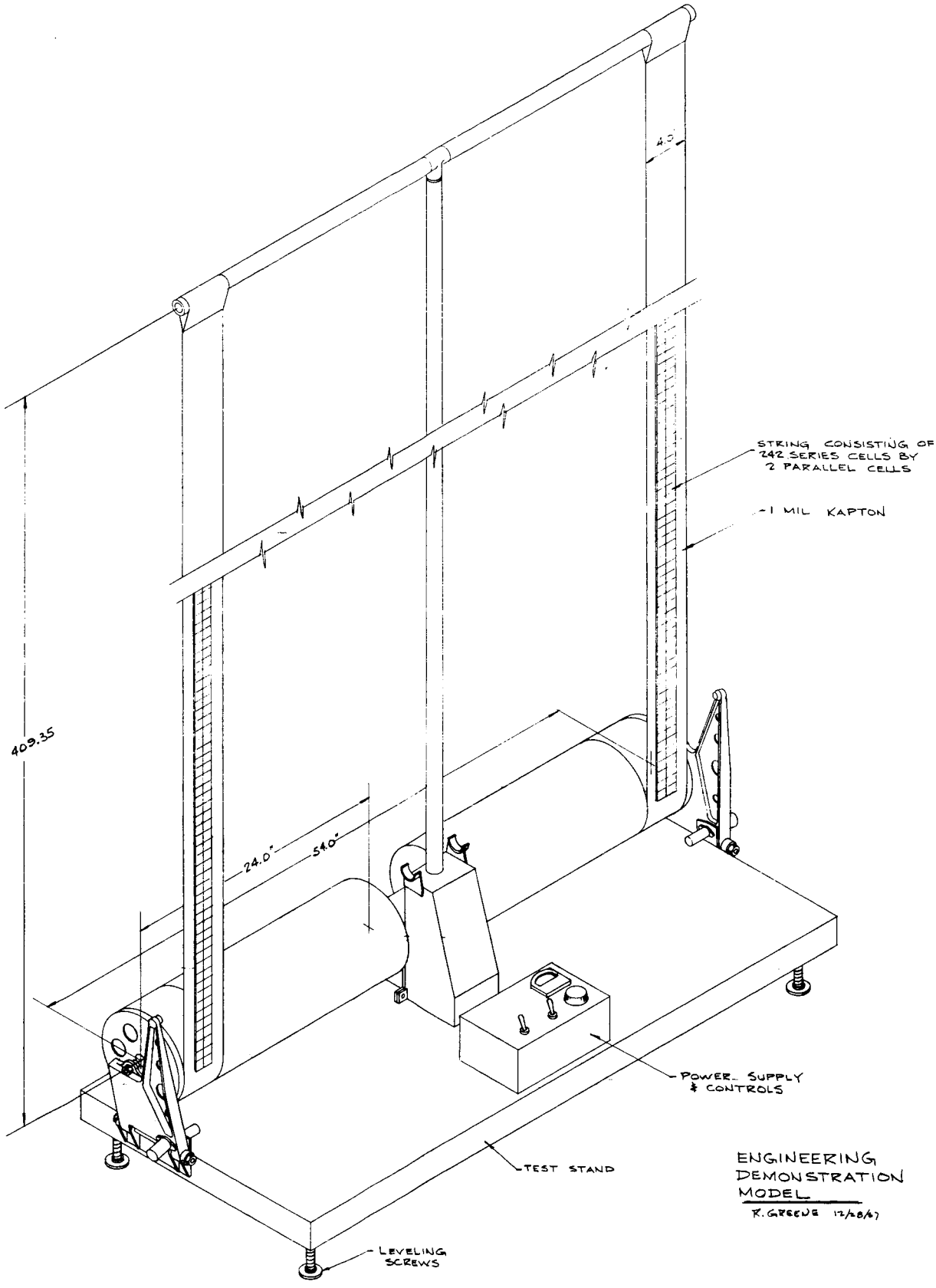

Figure 2-38. Engineering Demonstration Model

2.9 Weight Summary

THE PRELIMINARY DESIGN HAS PROGRESSED TO THE STAGE OF ALLOWING REALISTIC WEIGHTS TO BE CALCULATED. BASED ON THESE WEIGHTS, THE SPECIFIC POWER CAPABILITY OF THE PROPOSED ARRAY IS 33.1 WATT/LB.

The detailed weight breakdown for the proposed 30 watt/lb roll-up solar array is shown in Table 2-18. All the components weights shown in this table have been obtained from calculations based on the preliminary design drawings. The weight of the cover glass, cover glass adhesive and interconnection tabs are based on actual weight measurements. As presently designed, a margin of 7.7 pounds is available for growth during the detailed design of Phase II.

Table 2-18. Weight Summary

Component		Weight (lb)
Array		42.5
Storage Drum		14.9
Shell	5.6	
Outboard end cap	1.5	
Inboard end cap	2.0	
Bearings	1.0	
Neg'ator + mounting hardware	1.3	
Slip rings	0.8	
Support shaft	2.5	
Power feed-throughs	0.2	
Outboard end Support		3.5
Support	2.6	
Separation system	0.9	
Center support		2.1
Leading edge Member		1.0
Tube	0.8	
Center bearing	0.2	
Solar panel actuator		11.0
Thermal control coatings		0.1
Wiring and connectors		0.5
	Subtotal	75.6
Balance remaining for growth		7.7
Specified weight (2500 watts at 30 watt/lb)		83.3

3.0 CONCLUSIONS

Based on the studies completed to date, the following conclusions are presented:

a. It is feasible to design and fabricate a roll-up solar array with a specific power output of 30 watt/lb under the ground rules of the contract.

b. It is both feasible and efficient to design and fabricate the storage drums and leading edge member with beryllium. It is estimated that approximately 3 pounds are saved over an equivalent design utilizing magnesium. Note: 3 pounds is equivalent to 1.2 watts per pound for this system.

c. System tradeoffs and preliminary component designs for a 30 watt per pound system have been completed. Emphasis of the study should shift to the consideration of detailed problems involving fabrication, design details, and acceptance of the design concept by vehicle system engineers and to the design and fabrication of the engineering model.

4.0 RECOMMENDATIONS

It is recommended that early experimental studies be initiated to investigate several potential problem areas which are apparent at this time.

a. How will the array blanket track on the storage drum during retraction?

b. Will the interlayer cushioning be effective with the thinner cell-cover glass combination?

c. Will the array maximum power voltage of 91 volts cause problems in the vacuum thermal environment?

d. Does the analytical dynamics model adequately represent the physical system?

5.0 NEW TECHNOLOGY

No reportable items of new technology have been identified.

6.0 REFERENCES

1-1 Feasibility Study - 30 Watt per Pound Roll-up Solar Array, Quarterly Technical Report No. 1, General Electric Report No. 67SD4403, October 15, 1967.

2-1 Wahl, A. M., Mechanical Springs, McGraw-Hill Book Co., New York, pp. 146-152, 1963.

2-2 Gross, Seigfried, Calculation and Design of Metal Springs, Chapman and Hall Ltd., London, pp. 112-123, 1966.

2-3 JPL Specification SS501407 A

2-4 Florio, F. A. and Jasper, P. E., An Analytical Representation of Temperature Distributions in Gravity Gradient Rods, TIS No. 65SD294, August 6, 1965.

2-5 MacNaughton, J. D., Weyman, H. N., and Groskopfs, E., "The BI-STEM - A New Technique in Unfurlable Structures," presented at the 2nd Aerospace Mechanisms Symposium, May 4-5, 1967.

2-6 Clauss, F. J., Lubrication Evaluation, Lockheed Missile and Space Co., April 1966.

2-7 Young, W. C., Lubrication Evaluation, Lockheed Missile and Space Co., Report A707712, October 1964.

2-8 Evans, Vest and Ward, "Evaluation of Dry Film Lubricating Materials for Spacecraft Applications," Presented at AIAA Sixth Structures and Materials Conference, Palm Springs, California, April 1965.

2-9 Rittenhouse and Singletary, Space Materials Handbook, Supplement I to the Second Edition, NASA SP-3025, pp. S-36-38, 1966.

APPENDIX A

DEPLOYABLE BOOM STRUCTURAL CALCULATIONS

EXTENSION ROD ANALYSIS

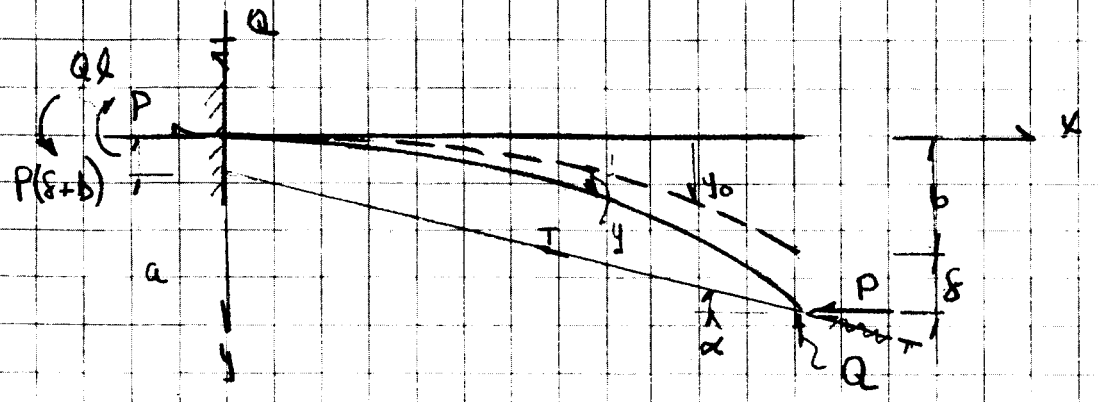

(1) $Q = T \sin\alpha = T\left(\frac{\delta + b - a}{l}\right)$

(2) $P = T\cos\alpha \doteq T$

ASSUME: $y_0 = kx^2 = \frac{b}{l^2}x^2$

(3) $EI\,y'' = -M$ WHERE

(4) $M = P(y + y_0) + Ql - P(\delta + b) - Qx$

(5) $EI\,y'' + Py = -P\frac{b}{l^2}x^2 + Qx - Ql + P(\delta + b)$

(6) LET $k^2 = \frac{P}{EI}$

(7) $y'' + k^2 y = -\frac{k^2 b}{l^2}x^2 + \frac{Q}{EI}x - \frac{Ql}{EI} + k^2(\delta + b)$

(8) $y = A\sin kx + B\cos kx + y_p$

(9) ASSUME $y_p = fx^2 + gx + h$

THEN $y_p' = 2fx + g$

$y_p'' = 2f$

EXTENSION ROD ANALYSIS

$$2f + k^2 f x^2 + k^2 g x + k^2 h = -\frac{k^2 b}{l^2} x^2 + \frac{Q}{EI} x - \frac{Ql}{EI} + k^2(\delta + b)$$

REARRANGING

$$\underset{(1)}{\left[k^2 x^2 f + k^2 x^2 \frac{b}{l^2}\right]} + \underset{(2)}{\left[k^2 x g - \frac{Q}{EI} x\right]} +$$

$$\underset{(3)}{\left[2f + k^2 h + \frac{Ql}{EI} - k^2(\delta + b)\right]} = 0$$

FROM (1)

$$f = -\frac{b}{l^2}$$

FROM (2)

$$g = \frac{Q}{P}$$

FROM (3)

$$-\frac{2b}{l^2} + k^2 h = k^2(\delta + b) - \frac{Ql}{EI}$$

OR

$$h = \delta + b + \frac{2b}{k^2 l^2} - \frac{Ql}{P}$$

THEREFORE (8) BECOMES

$$(10) \quad y = A \sin kx + B \cos kx - \frac{b}{l^2} x^2 + \frac{Q}{P} x + \delta + b + \frac{2b}{k^2 l^2} - \frac{Ql}{P}$$

EXTENSION ROD ANALYSIS

FOR BOUNDARY CONDITIONS:

(11) $y = \dot{y} = 0$ AT $X = 0$

THEN:

$$0 = B + (\delta + b) + \frac{2b}{k^2 l^2} - \frac{Ql}{P}$$

$$B = \left\{ \frac{Ql}{P} - \delta - b - \frac{2b}{k^2 l^2} \right\}$$

$$\dot{y} = kA \cos kx - kB \sin kx - \frac{2b}{l^2} x + \frac{Q}{P}$$

$$0 = kA + \frac{Q}{P}$$

$$A = -\frac{Q}{kP}$$

THEREFORE THE TOTAL SOLUTION IS:

(12) $$y = -\frac{Q}{kP} \sin kx + \left\{ \frac{Ql}{P} - \delta - b - \frac{2b}{k^2 l^2} \right\} \cos kx$$

$$- \frac{b}{l^2} x^2 + \frac{Q}{P} x + \delta + b + \frac{2b}{k^2 l^2} - \frac{Ql}{P}$$

WE ALSO HAVE THE CONDITION $y = \delta$ AT $x = l$

(12a) $$\delta = -\frac{Q}{kP} \sin kl - \delta \cos kl + \left[\frac{Ql}{P} - b - \frac{2b}{k^2 l^2} \right] \cos kl - b$$

$$+ \frac{Q}{P} l + \delta + b + \frac{2b}{k^2 l^2} - Ql/P$$

EXTENSION ROD ANALYSIS

$$(13)\quad \delta = -\frac{Q}{kP}\tan kl + \frac{Ql}{P} - b + \frac{2b}{k^2l^2}\left(\frac{1}{\cos kl} - 1\right)$$

SUBING (1) + (2) INTO (13) GIVES

$$\delta = -\frac{(\delta + b - a)}{kl}\tan kl + \delta + b - a - b + \frac{2b}{k^2l^2}\left(\frac{1-\cos kl}{\cos kl}\right)$$

$$0 = -\delta \tan kl - b\tan kl + a\tan kl - akl \frac{2b}{kl}\left(\frac{1-\cos kl}{\cos kl}\right)$$

$$\delta = b\left\{\frac{2(1-\cos kl)}{(\sin kl)kl} - 1\right\} + a\left(1 - \frac{kl}{\tan kl}\right)$$

$$(14)\quad \delta = b\left\{\frac{2(1-\cos kl) - kl\sin kl}{kl\sin kl}\right\} + a\left\{\frac{\tan kl - kl}{\tan kl}\right\}$$

OR

$$(14a)\quad \delta = \frac{b\{2(1-\cos kl) - kl\sin kl\} + a\{kl\cos kl(\tan kl - kl)\}}{(kl)\sin kl}$$

EXTENSION ROD ANALYSIS

FROM EQUATION (14a) WE SEE THAT THE CRITICAL COLUMN LOAD CORRESPONDS TO $\sin kl = 0$

$$kl = n\pi = \pi$$

$$P_{cr} = \frac{\pi^2 E I}{l^2}$$

THIS IS THE CRITICAL LOAD FOR A PIN-ENDED COLUMN —

WE CAN ALSO SEE THE EFFECT OF a ON THE DEFLECTION — IE. IT WOULD BE ADVANTAGEOUS, IN ORDER TO SATISFY CONDITION 1, TO HAVE A NEGATIVE a.

EXTENSION ROD ANALYSIS

(15) $M = -EI\,y''$

(16) $y'' = \frac{kQ}{P}\sin kx - k^2\left\{\frac{Ql}{P} - \delta - b - \frac{2b}{k^2l^2}\right\}\cos kx - \frac{2b}{l^2}$

FOR MAXIMUM BENDING MOMENT

(17) $\frac{dM}{dx} = 0 = \frac{k^2Q}{P}\cos kx + k^3\left\{\frac{Ql}{P} - \delta - b - \frac{2b}{k^2l^2}\right\}\sin kx$

$$\tan kx = \frac{-\frac{k^2Q}{P}}{k^3\left\{\frac{Ql}{P} - \delta - b - \frac{2b}{k^2l^2}\right\}}$$

(17a) $$= \frac{-\frac{Q}{P}}{k\left\{\frac{Q}{P}l - \delta - b - \frac{2b}{k^2l^2}\right\}}$$

SUBING (1) AND (2) INTO THE ABOVE

$$\tan kx = \frac{-\frac{1}{2}(\delta + b - a)}{k\left\{\delta + b - a - \delta - b - \frac{2b}{k^2l^2}\right\}}$$

(18) $$\tan kx = \frac{\delta + b - a}{kl\left\{a + \frac{2b}{k^2l^2}\right\}}$$

EXTENSION ROD ANALYSIS

COMBINING (14) AND (18)

$$\text{TAN } RX = \frac{b\left\{\frac{2(1-\cos kl)}{kl \sin Rl}\right\} - a\left\{\frac{kl}{\text{TAN } kl}\right\}}{a\,kl + \frac{2b}{kl}}$$

$$\text{TAN } kX = \frac{2b(1-\cos kl) - a(kl)^2 \cos kl}{[a(kl)^2 + 2b]\sin kl}$$

OR

$$[19) \qquad X = \frac{1}{k}\,\text{TAN}^{-1}\left\{\frac{2b(1-\cos kl) - a(kl)^2\cos kl}{[a(kl)^2+2b]\sin kl}\right\}$$

THE APPROPRIATE VALUE OF X ABOVE CAN THEN BE SUBSTITUTED INTO EQ'S (15) AND (16) TO GIVE THE MAXIMUM ROD BENDING MOMENT.

$$(20) \qquad M_{(ROOT)} = Ta$$

EXTENSION ROD ANALYSIS

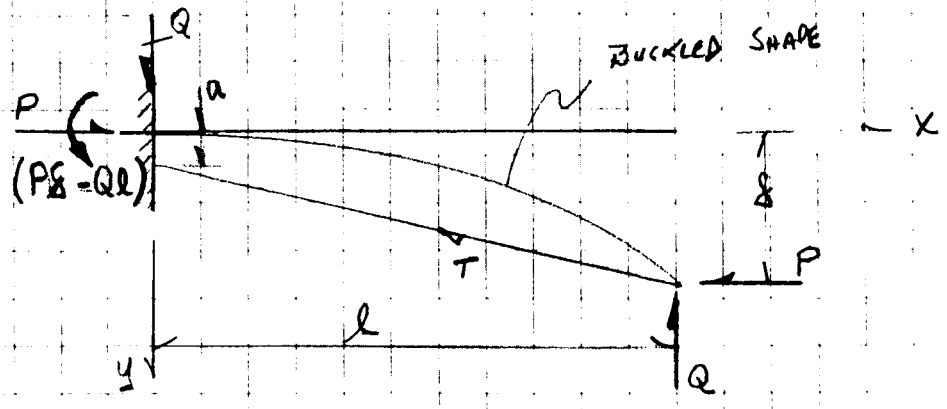

(1) $EI\,y'' = -M = -[(Ql + P\delta) + Py - Qx]$

$$EI\,y'' + Py = Qx - (Ql - P\delta)$$

(2) $$y'' + k^2 y = \frac{Qx}{EI} - \left(\frac{Ql}{EI} - k^2\delta\right)$$

(3) $$y = A\sin kx + B\cos kx + y_c$$

(4) $$y_c = ax + b$$

(4a) $$y_c'' = 0$$

AND $$k^2 ax + k^2 b = \frac{Qx}{EI} - \left(\frac{Ql}{EI} - k^2\delta\right)$$

$$a = \frac{Q}{k^2 EI} = \frac{Q}{P}$$

$$b = -\left(\frac{Ql}{k^2 EI} - \delta\right) = -\left(\frac{Ql}{P} - \delta\right)$$

(14) $$y = A\sin kx + B\cos kx + \frac{Q}{P}x - \frac{Ql}{P} + \delta$$

FOR BOUNDARY CONDITIONS (5)

EXTENSION ROD ANALYSIS

(15) $0 = B - \frac{Ql}{P} + \delta \qquad B = \left(\frac{Ql}{P} - \delta\right)$

(16) $\dot{y} = kA\cos kx - kB\sin kx + \frac{Q}{P}$

$0 = kA + \frac{Q}{P} \qquad A = \frac{-Q}{Pk}$

(17) $y = \frac{-Q}{Pk}\sin kx + \left(\frac{Ql}{P} - \delta\right)\cos kx + \frac{Q}{P}x - \frac{Ql}{P} + \delta$

AT $x = l \qquad y = \delta$

$\delta = \frac{-Q}{Pk}\sin kl + \frac{Ql}{P}\cos kl - \delta\cos kl + \frac{Ql}{P} - \frac{Ql}{P} + \delta$

$\delta = \frac{-Q}{Pk\cos kl}\sin kl + \frac{Ql}{P}$

(18) $\delta = \frac{-Q}{Pk}\left\{\tan kl - kl\right\} \qquad P = T, \quad Q = T\left(\frac{t-a}{l}\right)$

(19) $\delta = a\left\{\frac{\tan kl - kl}{\tan kl}\right\}$

THIS RESULT IS THE SAME AS THAT OF EQUATION FOR $b = 0$

APPENDIX B

COMPONENT SPECIFICATION FOR THE

SOLAR PANEL ACTUATOR

General Electric Company
Missile and Space Division
Spacecraft Department
P.O. Box 8555
Philadelphia, Pennsylvania
19101

Specification SVS-7534
Revision A - 12-29-67

SOLAR PANEL ACTUATOR

Prepared By: _____
D.N. Matteo, Engineer
E/M Control Equipment Engineering

Reviewed By: _____
P. DeMartino, Engineer
Vehicle Structural Analysis

Approved By: _____
E. Buerger, Manager
E/M Control Equipment Engineering

Approved By: _____
K. L. Hanson, Manager
Roll-Up Solar Array Program

Issued By: Print Control & Reproduction Date: December 4, 1967

Revision A Issued By: _____ Date: _____

General Electric Company
Missile and Space Division
Spacecraft Department
P.O. Box 8555
Philadelphia, Pennsylvania 19101

Specification SVS-7534-A
12-29-67

SOLAR PANEL ACTUATOR

1.0 SCOPE

This specification covers design, fabrication and test requirements for a solar panel actuator to be used by the General Electric Company as part of a functional model of a deployable solar array system. The design and assembly of this functional model is a task in the first phase of a program to develop a solar array system to provide an extendible and retractable solar power collection and conversion system for use on earth orbiting, interplanetary, and planet orbiting spacecraft. Accordingly, the design requirements delineated herein reflect the ultimate use in the space application.

The solar panel actuator covered by this document will herein after be referred to as the component.

The component will not be a flight article and, therefore, will not be subjected to the normal qualification and acceptance tests associated with same. Only the tests, inspections, and analyses, specifically delineated in the Quality Assurance Provisions Section will be applied as a measure of acceptability for hardware delivered under a contract or purchase order invoking this specification.

However, certain service conditions and performance requirements are delineated herein for which no specific measures of acceptability are called-out in Section 4.0. These requirements and conditions are included to provide information to the supplier in order that he may advance the design toward the goal of a flight worthy component.

2.0 APPLICABLE DOCUMENTS

2.1 Drawings

GE Source Control Drawing 47E214524

2.2 Specifications

GE Specification 146A9560, preparation for delivery of commercial shipments.

3.0 REQUIREMENTS

3.1 General Requirements

The component is intended for use as an actuation device for a roll-up type solar cell array. It shall consist of two main subdivisions, an extendible and retractable boom and a deployer mechanism. In the launch mode, the entire boom shall be stowed within the deployer mechanism (except as specified elsewhere, herein). Upon command, the deployer mechanism shall extend the boom to the fully extended length or any fraction thereof, while sustaining the loads imposed by the solar array blanket assembly which will be attached to the boom tip. Upon command, the deployer mechanism shall retract the boom to any desired fraction of fully extended length, while sustaining the blanket loads.

3.2 Detail Design Requirements

The requirements delineated herein apply to all components produced in compliance with this specification.

3.2.1 Actuation Capability

With the loads specified in paragraph 3.2.8 applied to the boom tip the component shall be capable of extending to any fraction (including 100 percent) of the fully extended boom length (Paragraph 3.2.2).

The component shall be capable of retracting to any fraction of fully extended boom length (including fully retracted position) under the same loading conditions as described above for extension.

The component shall be capable of extending and retracting under load while being subjected to the solar flux conditions outlined in Paragraph 3.2.8.2, but while in a zero acceleration field.

3.2.2 Fully Extended Length

Fully extended boom length is defined as 33.5 feet ± 2.0 inches, measured from the exit of the deployer mechanism to the end of an attachment plug mounted at the tip of the boom. The component shall function as defined in Paragraph 3.2.1 up to 100 percent of this length, except that the loads of Paragraph 3.2.8 are limited as specified therein.

3.2.3 Total Boom Element Length

The component shall be manufactured with a minimum of 40 feet of boom length. The component shall function as defined in Paragraph 3.2.1 when equipped with this length boom. Prior to delivery GE will specify the length (≤ 40 ft.) at which the boom is to be delivered.

3.2.4 Extension and Retraction Rates

The boom extension and retraction rate shall be 1.5 in./sec ± 1 in./sec.

3.2.5 Component Weight

The maximum total component weight shall be 11.0 pounds including the weight of the boom element.

For the purpose of this requirement, the boom element length shall be that required to extend the boom to the fully extended length (Paragraph 3.2.2).

However, the deployer unit capability, motor size, etc., shall be those required to reliably function with the total boom element length (Paragraph 3.2.3).

NOTE: Minimal component weight is of extreme importance in this application. Accordingly, every effort should be made to reduce the weight as far below the specification weight as possible.

3.2.6 Component Size

With the component in the stowed condition, the component shall fit entirely within the following envelope:

A right, rectangular prism of the dimenions:

5.5 in. x 6.0 in. x 11.0 in.

See GE Dwg. 47E214524 for relationship of this envelope with boom deployment axis and other portions of the component.

3.2.7 Component Mounting

The component mounting provisions shall be per GE Drawing 47E214524.

3.2.8 Loading Conditions

The component (including its extended boom) shall endure each of the following loading conditions without failure, malfunction, or violation of the constraint specified. The loading conditions, lengths, and constraints of this paragraph apply regardless of the actual boom length delivered.

3.2.8.1 Blanket Tension/Gravity

(All loads specified herein are cumulative).

(a) Blanket Tension = 4.0 pounds applied at attachment at the boom tip and directed at a fixed point regardless of boom tip motion (extension, retraction or deflection). This fixed point is defined as the boom exit point on the deployer mechanism. This load will act at any time the boom is extended from its stowed condition and is independent of the length of boom extended, up to 100 percent of fully extended length (Paragraph 3.2.2).

(b) Tip Weight = A mass mounted at the boom tip equal to 1.2 pounds in the 32.2 ft/sec^2 gravity acceleration field. With the boom deployment axis vertically upward this weight will act along the local vertical regardless of the amount of boom extension or deflection.

(c) Boom Weight = The weight of the boom element when deployed vertically upward in the 32.2 ft/sec^2 gravity acceleration field, regardless of deflection and anywhere from zero to 100 percent of fully extended length (Paragraph 3.2.2).

(d) Constraints

With the above loads cumulatively applied, the following constraints apply:

- The boom shall have a positive margin of safety (defined in Section 9.1) with respect to all possible failure modes (critical column load, bending, etc.) without the use of any deployment aids. This constraint applies from stowed position up to 100 percent of fully extended length (Paragraph 3.2.2).

3.2.8.2 Thermal/Blanket Tension (In Orbit Condition)

(All loads specified herein are cumulative.)

(a) Blanket Tension - Same as Paragraph 3.2.8.1 (a).

(b) Solar Flux - All portions of the extended boom will be exposed to solar flux of 260 mw/cm^2 incident on one-half of the boom periphery while the other half is exposed to black space, under hard-vacuum conditions.

(c) Constraints

Under the combined thermal and structural loading conditions of 3.2.8.2 (a) and (b) above and while in a zero "g" acceleration field:

- The boom shall not deflect laterally farther than 50 inches at the tip, at fully extended length (Paragraph 3.2.2).
- The boom shall have a positive margin of safety with respect to all failure modes. (See Note 10.1.)

3.2.9 Straightness and Alignment

3.2.9.1 Boom Deployment Axis

The boom deployment axis will be generally understood to mean the line along which the centroid of the boom tip travels as it is deployed. For the purpose of this specification, this axis will be defined as a straight line perpendicular to the boom mounting plane and passing through the boom centroid at the deployer exit point.

3.2.9.2 Boom Mounting Plane

The boom mounting plane will be defined as a plane generally perpendicular to the 11.0 inch dimension of the component envelope (Paragraph 3.2.6) which plane determines the alignment of the component with its support structure about the two axes mutually perpendicular to the boom deployment axis and each other. The suppliers outline and installation drawing shall define this plane and its precise relationship with actual component mounting surfaces and mounting holes, and will conform to GE Source Control Drawing 47E214524.

3.2.9.3 Boom Alignment and Straightness

When deployed to fully extended length and with the boom deployment axis vertically upward, the boom profile shall be such that its tip falls within a 1 1/2 foot diameter circle centered on the boom deployment axis when deployed vertically upward and when it is entirely unloaded (except for its own weight). These deflections are to be measured relative to the boom deployment axis.

3.2.10 Deployment Motor

The component shall extend and retract the boom by the action of an integrally mounted, DC motor (within the envelope defined in Paragraph 3.2.6).

3.2.10.1 Motor Voltage

The motor shall operate on a voltage of + 27 VDC $\pm$ 4 VDC.

3.2.10.2 Power Required

The total motor current (armature and field) shall not exceed 2.5 amps under normal running conditions (extend or retract). Total motor stall current shall not exceed 6.0 amps.

3.2.10.3 Motor Wiring

The motor may be a shunt, a series wound, or a permanent magnet DC type. In any case, wiring shall be such that the reversal of polarity of power applied to a single pair of wires or the changing of the wire to which one polarity is applied (external to the component) shall reverse the direction of boom deployment.

3.2.10.4 Limit Switches

The component shall be equipped with two limit switches, one which is mechanically actuated at fully extended length and

one which is mechanically actuated when the boom is totally stowed within the component. The wiring of all switches is to be brought out of the component separate from the motor wiring.

3.2.10.5 Connectors

No connectors are required. Six foot long, No. 22 AWG, Teflon coated wire flying leads will be provided on all wires requiring external connection.

3.2.11 Caging

All tip mounted masses will be externally caged by other components in the system. The boom tip will be restrained against extension or retraction motions during the launch phases by this external caging. Accordingly, no tip-mass caging requirements apply to the component.

3.2.12 Tip Attachment

In order to facilitate the attachment of solar array hardware to the boom tip, a tip plug will be required. This tip plug shall be equipped with internally threaded holes per GE Drawing 47E214524. This tip plug and its attachment to the boom element shall be capable of transmitting all loads specified in Paragraph 3.2.8 to the boom with a large margin of safety.

3.2.13 Telemetry

Other than the limit switches specified in Paragraph 3.2.10.4 (which may be used for both telemetry and power cut-off), no telemetry will be required.

3.2.14 Attachment to Forward End of Deployer

The component shall be equipped with six internally threaded holes at the boom exit end of the deployer as defined on GE Drawing 47E214524. GE will attach rigid brackets to each of the two patterns

of three holes. The component shall be capable of sustaining without failure or subsequent malfunction a 25 pound static load applied in any direction to each of these rigid brackets at the point defined as the "load application point" on GE Drawing 47E214524.

3.3 Service Conditions

The service conditions delineated in this section are intended as a guide in addressing the component design to future flight applications. These service conditions do not form part of the specified requirements on the component except where they are specifically invoked in Section 4.0.

3.3.1 Operating Conditions

3.3.1.1 Radiation

Total accumulative radiation dosage shall be 10^7 rads.

3.3.1.2 Temperature (Steady State)

$-50^{\circ}C$ to $+60^{\circ}C$

3.3.1.3 Pressure

760 mm Hg

to

10^{-10} mm Hg

3.3.1.4 Thermal Shock

Transient thermal shock from $-100^{\circ}C$ to $+75^{\circ}C$ at rates not less than $30^{\circ}C$ per minute, acting only on extended boom.

3.3.2 Nonoperating Conditions

3.3.2.1 Temperature (Steady State)

$-50^{\circ}C$ to $+60^{\circ}C$

3.3.2.2 Humidity

$93\% \pm 3\%$ at $+30^{\circ}C \pm 2^{\circ}C$

3.3.2.3 Pressure

760 mm Hg

to

10^{-10} mm Hg

3.3.2.4 Vibration

In the stowed condition, with the boom tip externally restrained against extend or retract motion and attached to a rigid fixture at the mounting points delineated in GE Drawing 47E214524, the applicable vibration environment is:

Sinusoidal
(ALONG 3 MUTUALLY PERPENDICULAR AXES)

Frequency (cps)	Acceleration (g's, 0 to peak)	Sweep Rate
0 - 13	limited to 0.5 inch double amplitude	2 octaves per minute
13 - 25	4.0 g	
25 - 250	8.0 g	
250 - 400	12.5 g	
400 - 2000	4.0 g	

Random Gaussian
(ALONG 3 MUTUALLY PERPENDICULAR AXES)

Frequency (cps)	Duration	PSD Level (g^2/cps)
25 to 200	3 minutes	roll off at 6 db/octave
200 to 600		0.10
600 to 2000		6 db/octave

3.3.2.5 Acceleration

± 13 g ± 0.7 g at CG along three mutually perpendicular axes and varying across the component by not more than 1.3 g from the specified 13 g, when mounted per GE Drawing 47E214524.

3.4 Workmanship

The component shall be constructed in a thoroughly workmanlike manner. Particular attention shall be paid to neatness and thoroughness of soldering, wiring, marking, plating, painting, riveting, machine screw assemblage, welding, brazing, and freedom of parts from burrs.

3.5 Life

The deployer mechanism shall be capable of 150 cycles of full extensions and full retractions with no deleterious effects on performance or structural integrity. The boom element shall be capable of 50 such cycles.

4.0 QUALITY ASSURANCE PROVISIONS

Consistent with the philosophy that this item is not a flight component, the only measures of acceptability will be those specified in Paragraphs 4.1, 4.2, 4.3 and Note 10.2.

4.1 Examination of Product

4.1.2 Visual and Mechanical Inspection

The component shall be visually and mechanically inspected to determine that materials, finishes, design, workmanship, construction, weight, dimensions, and markings conform to the applicable drawings and to the requirements of this specification.

4.1.3 Circuit Isolation, Continuity and DC Resistance

The component shall be checked for conformity with the electrical requirements of the applicable drawing and this specification when measured with a voltmeter and/or ohmmeter.

4.2 Straightness and Alignment

The component shall be checked for conformity with the requirements of Paragraph 3.2.9.3 by vertical deployment in a one "g" field as specified in that paragraph.

4.3 Functional and Static Load Test

The component shall be tested to demonstrate all the requirements of Paragraph 3.2 except that the requirements of Paragraph 3.2.8.2 will be demonstrated by analysis in lieu of test as defined in Note 10.1.

5.0 PREPARATION FOR DELIVERY

The component shall be prepared for delivery in accordance with GE Specification 146A9560.

6.0 DRAWINGS

The supplier shall deliver with the component a complete set of production drawings defining the component in its most up-to-date configuration. In addition, the supplier shall supply such drawings as will be from time-to-time (prior to delivery) required by GE to define the design and interface details of that component.

7.0 DESIGN REVIEW

GE reserves the right to review the design details from time to time as the design progresses. These reviews will take the form of informal sessions wherein GE engineers are acquainted with the manner in which the requirements of this specification are being met. These sessions will also be used to identify areas where mutual benefit can be derived by analytical support being applied by GE.

8.0 ACCESS TO ANALYSIS

GE shall have access to all analysis performed in configuring the component to meet this specification.

9.0 DEFINITIONS

9.1 Margin of Safety (MS)

For purposes of the specification margin of safety is defined as:

$$MS = \frac{\text{Allowable Load (Stress)}}{\text{Applied Load (Stress)}} - 1$$

The component shall not yield (or suffer permanent set) under design limit load nor suffer ultimate failure under ultimate load.

Ultimate Load = 1.25 Design Limit Load

All static loads specified herein are design limit loads.

NOTE: Column instability is defined as ultimate failure.

10.0 NOTES

10.1 GE assumes responsibility for showing analytical proof of meeting the constraints of Section 3.2.8.2 provided that:

- The component satisfies the requirements of Sections 3.2.8.1 and 3.2.9.3, and
- The configuration of boom is such that its most pessimistic thermal bending performance can be approximated by a 1.4 inch diameter, 0.007 inch wall, seamless, stainless steel tube coated on its OD with a thermal control coating with a solar absorptivity of 0.15 or less.

Any thermal control coatings of the actual boom required to match this approximation need not be applied to the boom element supplied with the component. However, a 4-foot (minimum) sample of the thermally coated boom element shall be delivered to GE on or before the delivery date of the component.

10.2 A structural analysis to determine the susceptibility of the component to the vibration environment of Section 3.3.2.4 is to be performed and delivered on or before the component delivery date. The purpose of this analysis is to identify areas of the component where future design changes might be required to allow flight components to survive the environment specified.